ALTERATION OF INTRACELLULAR CALCIUM RELEASE MEDIATED BY CD38 UNDER CHRONIC HYPOXIA IN PULMONARY ARTERIAL SMOOTH MUSCLE CELL

by

Suengwon Lee

A dissertation submitted to Johns Hopkins University in conformity with the requirements for the degree of Doctor of Philosophy

Baltimore, MD
March 2014

© 2013 Suengwon Lee
All rights reserved.

Abstract

Prolonged exposure to hypoxia due to high altitude or pulmonary diseases like chronic obstructive pulmonary disease causes chronic hypoxia-induced pulmonary hypertension (CHPH), which results in right heart hypertrophy, worsens the prognosis of the underlying pulmonary diseases, and even death. Chronic hypoxia (CH) impacts various targets in the pulmonary vasculature such as pulmonary artery (PA), leading to complex physiologic responses during the development of CHPH. It is well established that CH alters calcium (Ca^{2+}) homeostasis in pulmonary arterial smooth muscle cells (PASMCs) due to the enhancement of extracellular Ca^{2+} influx as the result of changes in the expression and activities of various membrane channels, transporters, and exchangers. However, the evidence for alterations of intracellular Ca^{2+} release in PASMCs caused by CH is scanty to date.

CD38 is a multifunctional enzyme that synthesizes the endogenous Ca^{2+} mobilizing messengers cyclic adenosine diphosphate-ribose (cADPR) and nicotinic acid adenine dinucleotide phosphate (NAADP), which are potent regulators of Ca^{2+} release via ryanodine receptor (RyR)-gated sarcoplasmic reticulum and NAADP-sensitive endolysosomal Ca^{2+} stores, respectively. CD38 is thought to play important roles in $[Ca^{2+}]_i$ regulation via Ca^{2+} release, contributing to diverse physiologic responses in many different cell types. However, its functions and regulatory mechanisms in PASMCs are still unclear. In particular, there is no systematic study on the mechanism of agonist-induced activation of CD38 in PASMCs. Furthermore, the effect of CH on CD38-dependent Ca^{2+} release in PASMCs has not been examined. The objective of this thesis research is to examine systematically the mechanism of agonist-induced CD38 activation

and the CH-induced alteration of CD38 expression and activity in PASMCs, as to provide novel insight into the contribution of CD38 in the development of CHPH.

The first part of this thesis research determined the expression of CD38, and its roles in angiotension II (Ang II)-induced vasoconstriction in PAs, and Ang II-induced Ca^{2+} release (AICR) in PASMCs. Examination of the expression profile of CD38 in various rat arteries indicates a relatively high level of CD38 expression in PA smooth muscle and PASMCs. Application of Ang II to PASMCs elicited Ca^{2+} response composed of both extracellular Ca^{2+} influx and intracellular Ca^{2+} release AICR activated in the absence of extracellular Ca^{2+} was significantly reduced by pharmacological or by siRNA inhibition of CD38, implying that CD38 mediates AICR in PASMCs. AICR was suppressed by the cADPR antagonist cADPR 8-Br-cADPR or the inhibition of the RyR-gated Ca^{2+} released with ryanodine. It was also suppressed by the NAADP-antagonist Ned-19 or the disruption of endolysosomal Ca^{2+} stores by the vacuolar H^{+}-ATPase inhibitor bafilomycin A1. Suppression of AICR by the inhibition of cADPR- and NAADP-dependent pathways was non-additive, indicating inter-dependence between RyR- and NAADP-gated Ca^{2+} release in PASMCs. Furthermore, AICR was inhibited by the protein kinase C (PKC) inhibitor staurosporine, the non-specific NADPH oxidase (NOX) inhibitor apocynin and DPI, the NOX2 specific inhibitor gp91ds-tat, and the reactive oxygen (ROS) species scavenger TEMPOL. These results provide direct evidence that Ang II activates CD38-dependent Ca^{2+} release via the PKC-NOX2-ROS pathway in PASMCs.

The second part of the research characterized the CH-induced alterations in the expression and functions of CD38 in PASMCs. The expression of CD38 protein and

mRNA were both significantly upregulated in the PA smooth muscle of CH rats. The upregulation of CD38 in PA of CH rats was time-dependent, observed after 3–7 days of hypoxic exposure and declining after 3 weeks of CH. NADase activity of CD38 in PA smooth muscle was significantly increased, whereas the activity in whole lung was decreased after 1-week hypoxia, suggesting specific CD38 upregulation in hypoxic PA. AICR was significantly increased in PASMCs of CH rat. The CH-induced enhancement in AICR was completely vanished by the inhibition of CD38, indicating that CH triggers augmentation of CD38 activity in PASMCs. The CH-induced upregulation of CD38 expression and activity were due to the direct effect of hypoxia on PASMCs. *In vitro* exposure of PASMCs from normoxic rats to hypoxia caused significant increase in CD38 expression and enhancement in AICR, which was abolished by the inhibition of CD38 activity. Moreover, the CH-induced upregulation of CD38 expression in PASMCs was inhibited by calcineurin/NFAT inhibitors, indicating that CH induces CD38 upregulation in PASMC mediated by the calcineurin/NFAT-pathway. Furthermore, the NAADP-dependent Ca^{2+} channel TPC1 and TPC2 was increased in CH rat PA. Hence, these results suggest that CH increases the expression and activity of CD38 and the CD38-dependent Ca^{2+} release in PASMCs.

Collectively, the results indicate the CH-induced enhancement of CD38 expression and activity in PASMCs may contribute to the alteration of Ca^{2+} homeostasis in PASMCs. It also implies that CD38 could be a possible therapeutic target for the treatment of this dreadful disease.

Thesis Advisor:

Dr. James S.K. Sham

Thesis Committee Members:

Dr. Bradley Undem

Dr. Steven An

Dr. Janice Evans

Dr. Machiko Shirahata

Dr. Anthony K.L. Leung

Acknowledgement

First, I would like to express my sincerest gratitude to my advisor, Dr. James S.K. Sham, for his great supervision and encouragement. He has supported me continuously throughout the research project whilst allowing me to test the hypothesis with continuous teaching and guidance, without which this dissertation would not have been possible. In addition, I'd also like to thank my thesis committee members, Drs. Bradley Undem, Machiko Shirahata, Steven An, Janice Evans, and Anthony K.L. Leung for their insightful advice that help me to overcome all the obstacles I encountered in this project.

I am grateful to the former and current lab members, Dr. Xiao-Ru Yang, Dr. Hui Sun, Dr. Amanda H. Lin, Dr. Krishna Subedhi, Dr. Huang Chun, Dr. Sheng-Ying Chung, Omkar Paudel, Yong-Liang Jiang, Yang Xia, Jinxing Hu, and Zhen Zhen Fu. Each has provided excellent advice and guidance as research colleagues and also as good friends. I also thank the administrative staff of the Program in Respiratory Biology and Lung Disease and Department of Environmental Health Science for their support in my daily work, especially Mary Thomas, Ruth Quinn, Patty Poole, and Courtney Mish.

Additionally, it is my pleasure to express my gratitude to my friends, Dr. Jin Y Ro at University of Maryland, Dr. Kideok Jin in NIA, Dr. Chang-Hun Lee from DGIST in South Korea, Ted Taek-Ryul Kim, Hangeul Kim, Imsik Choi, Tae-June Bang, Suk-Jin Lee, Seung-Ho Ryu, and all people who let me have memorable experience at Johns Hopkins University. I also owe gratitude to Baltimore Life Science Association for providing wonderful opportunities to share my academic knowledge and develop my scientific network with many brilliant scientists. Especially, I would like to emphasize gratefulness my classmates in Respiratory Biology and Lung Disease program, Letitia

Weigand, Luis Pichard, Blake Bennett, and Tina-Marie Lieu. It will be impossible to forget what we experienced and shared during the program in JHSPH.

I would also like to convey a special acknowledgement to my parents Sa Lee and Chang-soon Choi, my wife Soona Shin, and my brother Hyoung-Won Lee, for their love and confidence in me. Nothing can be compared with the solace and comfort of my family.

Finally, I want to thank everyone who contributed to this work, and I apologize that I could not mention them all one by one. I thank those who are now reading this dissertation, for your interest in my study makes my work worthwhile.

Above all, this volume is dedicated to God, who loves and creates me,

my father and mother, who guided my life,

and my wife and best friend Soona with my love.

Contents

List of Tables

List of Figures

Chapter 1

Chapter 3

Chapter 4

Chapter 5

Abbreviation

AngII, angiotensin II

AICR, angiotensin II-induced Ca^{2+} release

APC, apocynin

Baf A1, bafilomycin A1

cADPR, cyclic adenosine diphosphate ribose

CH, chronic hypoxia

Cyc A, cyclosporin A

DPI, diphenyleneiodonium

IP_3R, inositol trisphosphate receptor

NA, nicotinamide

NAD, nicotinamide adenine dinucleotide

NAADP, nicotinic acid adenine dinucleotide phosphate

NOX, NADPH oxidase

NFAT, nuclear factor of activated T-cells

PA, pulmonary artery

PASMC, pulmonary arterial smooth muscle cell

PH, pulmonary hypertension

PKC, protein kinase C

ROS, reactive oxygen species

Rya, ryanodine

RyR, ryanodine receptor

TPC, two-pore channel

CHAPTER 1

BACKGROUND AND INTRODUCTION:

OVERVIEW OF CALCIUM REGULATION

I. Overview of Ca^{2+}

A. Ca^{2+} homeostasis

Ca^{2+} plays a pivotal role in the regulation of a wide spectrum of physiological functions including cell proliferation, differentiation, membrane trafficking, secretion, apoptosis, regulation of endo- and exocytosis, enzyme activity, fertilization, innate immunity, gene transcription, progression of cell cycle, and cell contraction [1,2,3,4,5,6,7,8]. Resting intracellular Ca^{2+} concentration ($[Ca^{2+}]_i$) is tightly regulated and maintained at approximately 100 nM in skeletal muscle, cardiac muscle, and vascular smooth muscle [9,10,11], whereas the concentration of extracellular Ca^{2+} is approximately 1.1 to 1.5 mM [12]. This huge gradient is maintained by energy-consuming pumps and ion exchangers on the innately ion-impermeable lipid-bilayer plasma membrane and intracellular organelle membrane [13]. Because of this Ca^{2+} gradient across the membrane, the regulation of $[Ca^{2+}]_i$ depends on many different types of extracellular Ca^{2+} influx and intracellular Ca^{2+} release pathways, as well as Ca^{2+} removal and uptake pathways [14]. Further, the intracellular Ca^{2+} signals are compartmentalized into local and global Ca^{2+} signals with specific spatial/temporal properties to regulate the effectors in various subcellular compartments and activate different Ca^{2+}-dependent physiological processes.

B. Ca^{2+} mobilization

There are two major mechanisms for increasing $[Ca^{2+}]_i$ levels: Ca^{2+} entry from extracellular fluid and intracellular Ca^{2+} release from a variety of cellular organelles such as endoplasmic or sarcoplasmic reticulum (ER/SR), endolysosomes, mitochondria, and

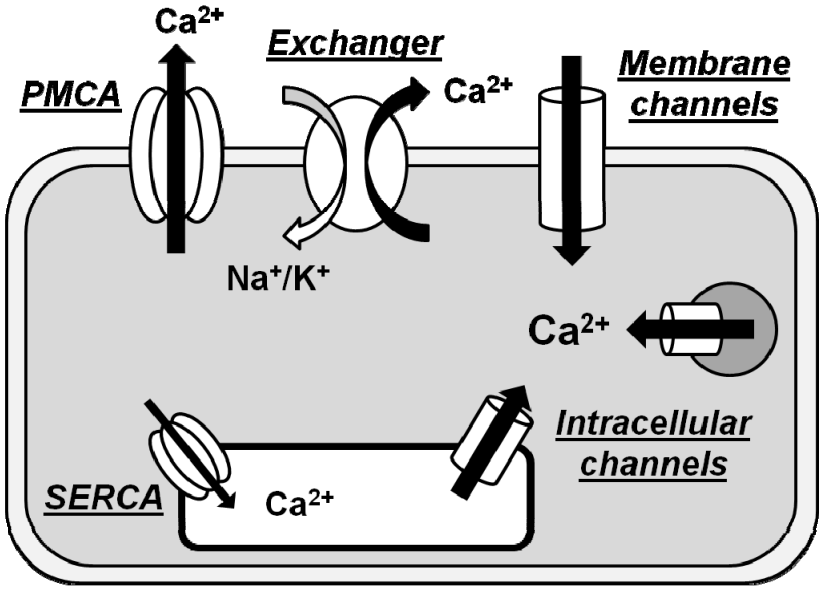

Figure 2.1. Overview of Ca^{2+} mobilization in cell Ca^{2+} homeostasis is maintained by ATPases (PMCA and SERCA) and exchangers in plasma or organelle membrane. Ca^{2+} mobilization is gradient-driven across the cellular and organelle membrane via Ca^{2+} permeable channel on membrane. (Abbreviation: PMCA, plasma membrane Ca^{2+} ATPase; SERCA, sarcoplasmic/endoplasmic reticulum Ca^{2+} ATPase)

the nuclear envelope [7,15,16,17]. The opening of Ca^{2+}-permeating channels in the plasma membrane and the organelle membranes leads to gradient-driven Ca^{2+} mobilization into the cytoplasm. Subsequently, cytoplasmic Ca^{2+} is rapidly removed or taken up via different types of exchangers and energy-consuming ATPases on the plasma or organelle membranes to restore resting $[Ca^{2+}]_i$ [7]. The general overview of the intracellular Ca^{2+} regulatory mechanism is described in Fig. 1.

In smooth muscle cells, elevation of $[Ca^{2+}]_i$ is essential for cell contraction. Ca^{2+} binds to calmodulin to form Ca^{2+}-calmodulin complex, leading to the activation of myosin light chain kinase. Myosin light chain kinase facilitates actin-myosin cross-bridge

formation by phosphorylation of serine residue in myosin light chain, leading to the contraction of smooth muscle cells [18,19,20]. Thus, the regulatory mechanism of $[Ca^{2+}]_i$ is crucial to the physiological functioning of the vasculature. In this chapter, two regulatory mechanisms of Ca^{2+} mobilization—(a) Ca^{2+} influx from extracellular space and (b) Ca^{2+} release from intracellular Ca^{2+} stores to cytoplasm—will be reviewed focusing on Ca^{2+}-permeable channels with an emphasize on pulmonary arterial smooth muscle cells (PASMCs).

1. Ca^{2+} influx pathways in PASMCs

Activation of Ca^{2+}-permeable channels on the plasma membrane allows Ca^{2+} influx due to the large Ca^{2+} gradient (high Ca^{2+} outside and low Ca^{2+} inside). A variety of Ca^{2+}-permeable channels exist in the cell membrane. They can be categorized as either voltage-dependent or voltage-gated Ca^{2+} channels (VDCCs/VGCCs) or voltage independent Ca^{2+} channels [21,22]. Furthermore, channels for other ions, such as K^+ and Cl^-, are required for maintaining and modulating Ca^{2+} mobilization.

a. Voltage-dependent (gated) Ca^{2+} channels (VDCCs/VGCCs)

The open-state and closed-state of VDCCs are dependent on the voltage gradient across the plasma membrane, which is referred as membrane potential. At the resting membrane potential, VDCCs in PASMCs are mainly in the closed-state, and exhibit minimal spontaneous activity [23]. Membrane depolarization activates VDCCs and Ca^{2+} influx, leading to various vascular response including pulmonary vasoconstrictions [24,25] and myogenic tones [26,27]. Beside the open/closed-state, VDCC can transition

from the open-state to the inactivated-state (different from closed-state), which occurs slowly in a voltage and time-dependent manner [28].

Based on the voltage dependence, VDCCs in PASMCs are classified into two subtypes, the high-voltage activated L-type Ca^{2+} channel, and the low voltage-activated T-type Ca^{2+} channel. L-type Ca^{2+} channels are activated at a threshold potential of approximately -40 to -50 mV and T-type VDCCs are activated at a lower membrane potential of -60 to -70 mV [29,30]. L-type Ca^{2+} channels have a relatively slower inactivation compared to the T-type Ca^{2+} channels, and contribute to high-K^+-induced contraction [29,30,31], and hypoxic pulmonary vasoconstriction [32,33]. Although it had been little known about T-type Ca^{2+} channels in PASMCs, recent studies suggested that it may control proliferation [30,34] and contribute to the development of lung disease such as chronic hypoxia-induced pulmonary hypertension (PH) [35].

b. Voltage-independent Ca^{2+} channels

(1) Transient receptor potential channels

Transient receptor potential (TRP) channels are voltage-independent cation channels, which play important roles for Ca^{2+} entry, particularly in vascular smooth muscle cells. TRP channels are consisted 7 subfamilies, namely canonical (TRPC), vanilloid-related (TRPV), melastatin-related (TRPM), ankyrin (TRPA), polycystin-related (TRPP), mucolipin-related (TRPML) and no mechanoreceptor potential C (TRPN or nompC) subfamilies [21,36]. All TRP channels have a structural similarity for six transmembrane domains, a pore-forming loop between the fifth and sixth transmembrane domain with highly conserved TRP domains. TRP channels operate as specific Ca^{2+}

pathways responsive to a variety of stimuli such as depletion of Ca^{2+} store, ligand-receptor activation, and mechanical stress by formation of homogenic or heterogenic tetrameric structure [21]. TRPC, TRPV, and TRPM channels have been identified in pulmonary arterial smooth muscle and several members of TRP subfamilies such as TRPC 1/6 and TRPV4 are crucially associated with the enhancement of myogenic tone and agonist-induced vasoreactivity in pulmonary vasculature under prolonged hypoxic exposure [21,37,38].

The physiologic functions of TRP channels vary depending on the specific subtypes in PASMCs. In particular, TRPC1/4 plays a role in Ca^{2+} influx as a store-operated Ca^{2+} channel and TRPC3/6 as a receptor-operated Ca^{2+} channel [21]. TRPV4 is the most abundant member of TRPV subfamily and one of the mechanosensitive Ca^{2+} channels, which is activated by mechanical stress such as stretch, and plays a crucial role for the development of elevated pulmonary arterial pressure in response to prolonged hypoxic exposure [39].

(2) Receptor-operated Ca^{2+} entry

Receptor-operated Ca^{2+} entry (ROCE) occurs via Ca^{2+} permeating channels, which are activated as the result of the binding of agonists to their receptor. Activation of ROCE does not require membrane depolarization. ROCE can be activated via G-protein-coupled receptors (GPCRs), receptor tyrosine kinases (RTK) and guanylyl cyclases as well as the direct interaction with signaling molecules such as trimeric G proteins and polyunsaturated fatty acids (i.e. arachidonic acid) [40,41]. Activation of receptors such as GPCRs increases the synthesis of the second messengers including inositol-1,4,5-

triphosphate (IP_3), and diacylglycerol (DAG), by phospholipase C (PLC). Indeed, it has been reported that various TRP channels play a pivotal roles in ROCE as the channels activated by those signaling molecules. Particularly, previous studies have indicated that several members of TRPC subfamily such as TRPC3/6 in PASMCs might play the role of ROCE, contributing to increase in $[Ca^{2+}]_i$ [21,42,43].

Ca^{2+}-sensing receptor (CaSR) is a unique type of GPCRs coupled with PLC, contributing to Ca^{2+} mobilization in PASMCs [44]. Particularly, CaSR is another novel candidate in the progression of pathophysiologic states such as PH development by modulating Ca^{2+} entry [44,45]. Yamamura et al. demonstrated that the elevation of extracellular Ca^{2+}-induced resting $[Ca^{2+}]_i$ in PASMCs from idiopathic PH patient was prevented by the antagonist of the CaSRs [45]. Moreover, the expression of CaSRs in PA from monocrotaline (MCT)-induced pulmonary arterial hypertension animal was significantly upregulated compared to control, resulting in the excessive proliferation of PASMCs [45].

(3) Store-operated Ca^{2+} entry

Depletion of Ca^{2+} in ER/SR triggers Ca^{2+} influx to replenish the Ca^{2+} stores and preserve the functions of ER/SR [46]. This mechanism of Ca^{2+} entry is called "capacitative Ca^{2+} entry" or "store-operated Ca^{2+} entry (SOCE)" [46,47]. Traditionally, it is known that SOCE is initiated typically by Ca^{2+} release through IP_3 receptors (IP_3Rs) activated by IP_3 as the result of GPCR and RTK activation, resulting in store-operated inward current (I_{SOC}) or Ca^{2+}-release-activated Ca^{2+} current (I_{CRAC}) [48]. Thus, "Ca^{2+}

sensors" in ER/SR is required for the coupling of Ca^{2+} depletion with SOCC in membrane.

There is strong evidence that SOCE is modulated by the ER/SR-resident Ca^{2+} sensor stromal interaction molecule (STIM) proteins, STIM1 and STIM2 isoforms, which have different Ca^{2+} sensitivity. STIM is a ER/SR membrane-spanning protein, composed of ER/SR lumen segment, containing Ca^{2+}-sensitive EF hand near N-terminus, and cytoplasm segment containing ezrin/radixin/moesin (ERM) domains in C-terminus [49]. Particularly, STIM1 is expressed as a dimer stabilized by ERM domain in basal state, while the Ca^{2+} store depletion in ER/SR lumen, sensed by EF hand, causes the oligomerization of STIM1 molecules. The formation of STIM1 multimer results in the translocation of STIM1 and coveys the information of Ca^{2+} depletion to store-operated Ca^{2+} channels in cell membrane, mediated by complex domains in C-terminus [49,50]. Furthermore, studies also characterized that STIM2 has lower sensitivity to ER/SR $[Ca^{2+}]_i$ than STIM1, and acts as another Ca^{2+} sensor capable of detecting a small decrease in ER/SR $[Ca^{2+}]_i$, triggering SOCE [51].

Over the past decade, many studies addressed that TRPC channels, such as TRPC1/4, are a crucial candidate for SOCE particularly in PASMCs [52,53]. Particularly, TRPC1-mediated SOCE is activated by the formation of a complex with STIM1 in PASMCs [54]. This typical Ca^{2+} current generated by TRPC1-STIM1 interaction is namely I_{SOC} [55]. In addition, there is a novel aspect of SOCE mediated by the complex of STIM with Orai1, a pore subunit of Ca^{2+} release-activated Ca^{2+} channels (CRACs) in plasma membrane [55,56]. The mechanism has been shown that the complex of ERM domains in oligomerized STIM1 stimulate the dimerization of Orai1 dimers to form

tetrameric Orai1 channels, leading to generating inward Ca^{2+} current, called I_{CRAC} [57]. Although Orai and TRPCs clearly function independently, evidence also elucidated that Orai-activating region of ERM domains in STIM1 has a capacity for binding to TRPC channels, suggesting the interaction between Orai1-STIM-TRPC for inward Ca^{2+} current [58]. Overall, those results implicate that functional activity of Orai1 and TRPC is regulated by STIM1 with both dependent and independent manner, contributing to generation of inward Ca^{2+} current for SOCE.

(4) Other types of Ca^{2+} channels in plasma membrane

There are other types of Ca^{2+} permeable cation channels in cell membrane of PASMCs. Ligand-gated ion channels are transmembrane proteins which are activated by binding of specific ligands such as adenosine triphosphate (ATP) to P2X purinergic receptors [59], and urokinase plasminogen activator to N-methyl-d-aspartate receptor-1 [60]. Another type of Ca^{2+} permeable channels called cyclic nucleotide-gated ion channels are also found in vascular smooth muscle [61,62,63]. They are activated by cyclic nucleotides such as cAMP and cGMP. However, their expression in PASMCs has not been clearly examined yet.

c. Ion channels that modulate Ca^{2+} entry

(1) K^+ channels

K^+ channels are composed of pore-forming subunits (α-subunits) and accessory subunits (β-subunits) depending on their functional and structural diversity [64]. In PASMCs, there are at least three major groups of K^+ channels characterized by several

biophysical and pharmacological properties: voltage-dependent K^+ (K_V) channels, Ca^{2+}-activated K^+ (K_{Ca}), and ATP-sensitive K^+ channels, contributing to changes in membrane potentials. [64,65,66,67]. It is clear that K_V channels and K_{Ca} channels play important roles in modulating Ca^{2+} influx via voltage-gated Ca^{2+} channels in PASMCs [66].

K_V channels in PASMCs play an important role in regulating membrane resting potential [66]. The α subunits of the K_V channels have six transmembrane domains and pore-formation regions and are encoded by the K_V gene family, which comprises at least 36 members grouped into 12 subfamilies (K_V1–K_V12) [68]. A reduction of K_V channel activity causes membrane depolarization and the activation of VDCCs, leading to the elevation of $[Ca^{2+}]_i$ in PASMCs and eventually pulmonary vasoconstriction. In contrast, activation of K_V channels results in hyperpolarization and inhibition of Ca^{2+} influx via VDCCs [66,69,70].

K_{Ca} channels operate as a "negative feedback pathway" for the regulation of membrane potential and vasoconstriction [66,71]. K_{Ca} channels can be classified into three subtypes based on their biophysical properties: large-conductance and voltage-dependent Ca^{2+}-activated K^+ (BK_{Ca}) channels, intermediate-conductance Ca^{2+}-activated K^+ channels, and small-conductance Ca^{2+}-activated K^+ (SK_{Ca}) channels [72]. A rise in $[Ca^{2+}]_i$ activates K_{Ca} channels, resulting in K^+ efflux, outward current, hyperpolarization, and deactivation of VDCCs [66,72]. It has been shown that local Ca^{2+}-release events through ryanodine receptors (RyRs), called "Ca^{2+} sparks," evoke hyperpolarization and vasorelaxation in systemic vascular smooth muscles while Ca^{2+} sparks in PASMCs cause membrane depolarization vasoconstriction, implying that the coupling of RyR to K_{Ca} channels in PASMCs may be different from other systemic myocytes [73].

(2) Ca^{2+}-activated Cl^- channels

Ca^{2+}-activated Cl^- channels (CaCCs) are activated by $[Ca^{2+}]_i$ at the range of 0.2–5 μM, leading to an inward Cl^- current in various cell types including PASMCs [74,75]. In general, elevated $[Ca^{2+}]_i$ triggers activation of CaCCs, resulting in membrane depolarization and the subsequent activation of VDCCs to further increase depolarization and Ca^{2+} influx [74]. In particular, CaCC in PA smooth muscle is a major physiological target of Ca^{2+} sparks causing depolarization while other systemic vascular smooth muscle is associated with K_{Ca} channels leading to hyperpolarization [76]. Recent studies demonstrated that TMEM16A, a member of the TMEM16 family, is the main component of CaCC subunits in PASMCs [75,77,78]. Recently, Sun et al. demonstrated that prolonged hypoxia causes upregulation of TMEM16A and an increase in Cl^- current through CaCCs in PASMCs [75], which is associated with elevated agonist-induced vasoreactivity in PA [79]. These results suggest that CaCCs play a potent role in Ca^{2+} homeostasis and physiological response in PASMCs [75].

2. Ca^{2+} release from intracellular Ca^{2+} stores in PASMCs

There are three major intracellular Ca^{2+} stores, namely the IP_3R-gated and RyR-gated Ca^{2+} stores in the ER/SR, and the nicotinic acid adenine dinucleotide phosphate (NAADP) receptor-gated stores in the endolysosomes [43,80,81,82]. Ca^{2+} release from these stores are triggered by specific Ca^{2+} second messengers, namely IP_3, cyclic adenosine diphosphate-ribose (cADPR), and NAADP, respectively. These Ca^{2+}-release channels may interact with each other through "cross-talk" mechanisms. In particular,

activation of Ca^{2+}-release channels may result in depletion of Ca^{2+} stores in the ER/SR and may trigger SOCE.

a. IP_3R-gated Ca^{2+} release

One of the most well characterized Ca^{2+} release mechanisms is IP_3-dependent Ca^{2+} release. Ligand binding to GPCRs and RTKs activates PLC to convert phophatidylinositol 4, 5-bisphosphate (PIP_2) to IP_3 and DAG. IP_3 activates IP_3Rs on the ER/SR, resulting in Ca^{2+} release whereas DAG activates other pathways such as PKC signaling pathways resulting in diverse cellular activity [43,83]. Various types of agonists such as endothelin-1 (ET-1), angiotensin II (Ang II), acetylcholine, 5-HT, thromboxane, and growth factors stimulate the production of IP_3 and activate to Ca^{2+} release via the IP_3R-gated channel in the ER/SR [83].

There are three mammalian IP_3R isoforms, IP_3R1 to 3 [83,84,85]. IP_3R1 is the major isoform in systemic vascular smooth muscle cells, and all three isoforms are expressed in PASMCs [73,86]. IP_3Rs have many regulatory sites, which interact with Ca^{2+}, ATP, and protein kinases, leading to modulation of channel function [87,88,89,90]. In particular, Ca^{2+} regulates the channel opening of IP_3R in a biphasic manner, facilitating the channel opening at low Ca^{2+} (<300 nM) and inhibiting it at high Ca^{2+} (>300 nM), thereby leading to positive and negative feedback regulation of IP_3R-gated Ca^{2+} release [89].

In general, IP_3R-gated Ca^{2+} release is responsible for agonist-induced Ca^{2+} release and evokes "Ca^{2+} waves" and elevation of global $[Ca^{2+}]_i$, triggering vasoconstriction in vascular smooth muscle [73,91]. It has also been demonstrated that local Ca^{2+} events

from IP_3Rs, called "Ca^{2+} puffs," elicit spontaneous outward currents (STOCs) by activation of BK_{Ca} and SK_{ca}, leading to hyperpolarization and a decrease in Ca^{2+} influx through VDCCs/VGCCs in smooth muscle cells [92]. Moreover, agonist-induced Ca^{2+} release through IP_3R increases the occurrence of Ca^{2+} sparks mediated by RyR-gated Ca^{2+} release, implying cross-talk between IP_3R- and RyR-gated Ca^{2+} release in PASMCs [73].

b. RyR-gated Ca^{2+} release

There are three different RyR subtypes; RyR1 was originally cloned from skeletal muscle, RyR2 was identified in cardiac muscle, and RyR3 was originally described in the brain. RyRs are tetrameric channels composed of four RyR monomers of each subtype and are distributed in many other tissues including vascular smooth muscles [82,93]. RyR1 is activated mainly by a voltage-dependent mechanism with dihydropyridine receptors (i.e. L-type VDCCs) as the voltage sensor [94]. RyR2 and RyR3 are activated by Ca^{2+} entry or release through the Ca^{2+}-induced Ca^{2+} release mechanism [4,95,96,97]. In addition, the activity of RyRs is regulated by many regulatory proteins and molecules including FK506 binding proteins (FKBPs), calmodulin, Ca^{2+}-calmodulin-dependent kinase, PKA, triadin, junctin, and calsequestrin [82,88,98]. There is also clear evidence that the second messenger, cADPR, activates RyR2, leading to Ca^{2+} release in vascular myocytes including PASMCs [99,100,101]. The detailed mechanism and characteristics of cADPR are described in the section on cADPR and CD38.

RyR-gated Ca^{2+} release may operate as a frequency-dependent negative modulator of membrane potential [102,103]. There is clear evidence that RyR1 and RyR2

play important role in excitation-contraction coupling in skeletal (mechanical coupling) [104,105] and cardiac muscle (Ca^{2+}-induced Ca^{2+} release), respectively [106]. In systemic vascular myocytes, RyR1 and RyR2 are required for the generation of Ca^{2+} sparks, and RyR3 is involved in the agonist-induced elevation of global $[Ca^{2+}]_i$ [93,107,108]. Ca^{2+} sparks are RyR-gated local Ca^{2+} release events. The elevation of these local Ca^{2+} signals in systemic myocytes leads to vasodilation and hyperpolarization via activation of K_{Ca} channels [102]. In contrast, Ca^{2+} sparks in distal PASMCs cause membrane depolarization [73,109,110]. In rat PASMCs, RyR2 is the most abundant of the three subtypes, and RyRs are differentially localized in the subsarcolemmal (RyR1/RyR2) and perinuclear regions (RyR3). Agonist-induced Ca^{2+} sparks in peripheral and perinuclear regions exhibit different spatiotemporal properties in PASMCs [93].

c. NAADP-gated Ca^{2+} stores

Recent evidence indicates that Ca^{2+} stores are not limited to the ER/SR but are also present in other organelles such as endolysosomes [81,111,112]. In endolysosomes, vacuolar-type H^+-ATPases generate H^+ gradient across the organelle membrane. This gradient allows Ca^{2+} entry into endolysosomes via H^+-Ca^{2+} exchangers [113]. Ca^{2+} release from the endolysosomal store is mediated by NAADP-sensitive channels [114,115,116]. NAADP is generated from inactive nicotinamide adenine dinucleotide phosphate (NADP) by the enzymatic activity of CD38 [116]. It was reported that NAADP-sensitive Ca^{2+} release channels on endolysosomes are encoded by two-pore channels (TPCs) [117]. Mainly, there are two subtypes of TPCs: TPC1 and TPC2. TPC1s are widely expressed in all stages of endolysosomes, and TPC2s are expressed

predominantly in late endosomes and lysosomes [118]. Western blot detected both TPC1 and TPC2 in rat PA smooth muscle [114]. In particular, the mRNA level of TPC1 was approximately five times higher than that of TPC2 [114].

Functional studies in systemic vascular smooth muscle showed that NAADP-gated Ca^{2+} release contributes to vasoconstriction induced by ET-1 and norepinephrine [119,120]. In PASMCs, NAADP triggers a Ca^{2+} burst (a spatially restricted Ca^{2+} release) and global Ca^{2+} waves, which are inhibited by depletion of endolysosomal Ca^{2+} stores and inhibition of RyRs, implying that NAADP-gated Ca^{2+} release is coupled to RyRs through Ca^{2+}-induced Ca^{2+} release [114,121]. Moreover, integrin-specific ligands (GRGDSP) also trigger NAADP- and RyR-gated Ca^{2+} release in PASMCs [122]. These results suggest that cross talks between NAADP-gated and other Ca^{2+} release channels (e.g., RyR and IP_3R) may play crucial roles in agonist-induced Ca^{2+} signaling though complex interactions in PASMCs.

II. CD38 as a master Ca^{2+} regulator

CD38 is a membrane glycoprotein discovered as a surface marker of lymphocytes [123,124]. It was subsequently reported that CD38 is a ubiquitous multifunctional ectoenzyme responsible for the synthesis of the second messengers cADPR and NAADP [125,126]. In this section, the multifunctionality of CD38 and its products cADPR and NAADP is reviewed. The crystal structure of cADPR and NAADP is shown in Figure 1.2 [115].

A. Generation of cADPR and NAADP by CD38

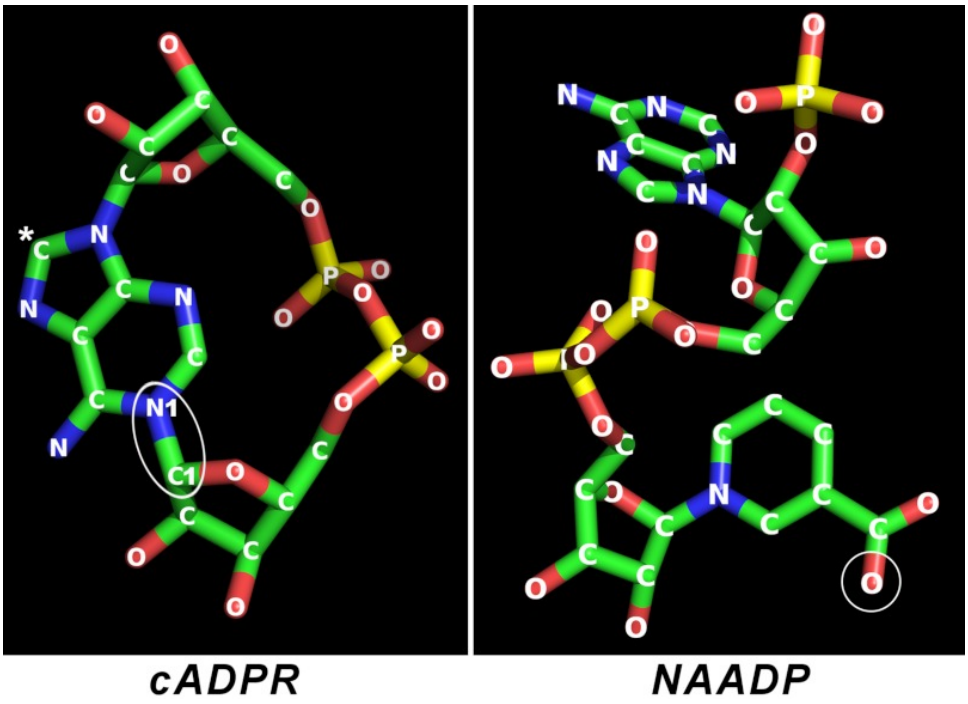

Figure 1.2. Cristal structure of cADPR and NAADP *Left*: The C8 of cADPR is indicated by a white asterisk. Attachment of a bromo (8-bromo-cADPR) or an amino (8-NH2-cADPR) group at this position converts the compound to a specific antagonist of cADPR. *Right*: The structure of NAADP is identical to that of its parent NADP, except that the amide nitrogen of the nicotinamide group of NADP is changed to oxygen as indicated by the circle. Blue, nitrogen; red, oxygen; yellow, phosphorus; green, carbon. The image and legend are cited from the following reference [115].

In 1987, Lee et al. showed that a metabolite of nicotinamide adenine dinucleotide (NAD^+) in sea urchin egg increases Ca^{2+} release from the intracellular Ca^{2+} store with a potency comparable to IP_3 [127,128]. They subsequently identified that the metabolite is cADPR [129,130,131], which is the endogenous messenger for the activation of RyR-gated Ca^{2+} stores [132,133]. cADPR exerts its action by binding to FKBP12/12.6, an accessory protein that stabilizes RyR1/3 and RyR2, respectively, causing its dissociation from RyRs to initiate Ca^{2+} release [134,135]. Furthermore, cADPR may increase the

activity of SERCA in removing cytosol Ca^{2+} and refilling the ER/SR [136]. These studies clearly suggested that cADPR is an important regulator of intracellular Ca^{2+} stores and release.

The enzyme that catalyzes the formation of cADPR from NAD^+ was first identified in *Aplysia Californica* and is known as ADP-ribosyl cyclase [137]. Subsequent studies found that 86 of the 285 amino acids in ADP-ribosyl cyclase from *Aplysia Californica* are identical to the human lymphocyte surface antigen CD38, which is an approximately 45 kDa transmembrane type II glycoprotein ubiquitously distributed in mammalian tissues [138,139,140,141,142,143,144]. CD38 was first identified as a T and B lymphocyte-specific surface antigen and is expressed at the late stage of maturation [123,145]. Subsequently, it was reported that CD38 also converts NAD^+ and cADPR to ADP-ribose (ADPR), indicating that it is a multifunctional enzyme that uses more than one substrate [146,147,148]. The multifunctionality of CD38 is dependent on pH. A neutral pH favors cylcase activity for converting NAD^+ to cADPR [149]. Under an acidic environment, CD38 catalyzes a base-exchange reaction for β-$NADP^+$ and nicotinic acid to generate NAADP [149,150].

As mentioned above, NAADP is a highly potent Ca^{2+}-mobilizing agent, which triggers Ca^{2+} release from thapsigargin-insensitive lysosome-related acidic organelles that are fundamentally different from the IP_3- or cADPR-dependent stores [112,150,151]. In addition, CD38 also hydrolyzes NAADP to ADP-ribose-2'-phosphate (ADPRP) at an acidic pH [144]. The pH dependency of CD38 is dictated by Glu-146 and Asp-155 in the active site of CD38. Under neutral pH, these "acidic residues" are negatively charged and repel the negatively charged nicotinic acid, leading to the selection of substrate and its

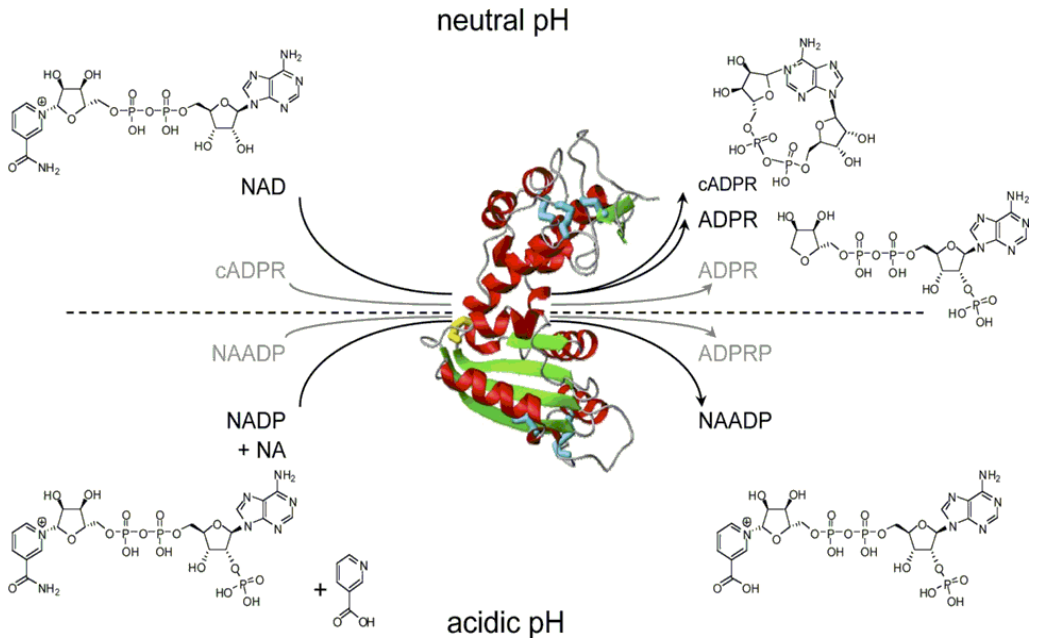

Figure 1.3. Schematic diagram of multifunctionality of CD38 The multifunctionality of CD38 activity is dependent on circumstant pH; enhanced cyclase activity in neutral pH and catalase activity in acidic pH. The product of cyclase and catalase (cADPR and NAADP, respectively) is also hydrolyzed into ADPR and ADPPR, respectively, by CD38. Abbreviations used: cyclic ADP-ribose, cADPR; ADP-ribose, ADPR; nicotinic acid adenine dinucleotide phosphate, NAADP; nicotinic acid, NA; ADP-ribose-2'-phosphate, ADPRP. This image is cited from the following reference [126].

consequent metabolite [152]. A schematic overview of CD38 enzyme activity is shown in Figure 1.3 [126].

Moreover, CD38 is a key enzyme for NAD^+ degradation in mammalian cells [125]. Research provided strong evidence that nicotinamide phosphoriboxyltransferase (NAMPT; the same with visfatin or PBDF) plays a key role in de novo synthesis of NAD^+ [153,154]. However, little is known about the degradation of cellular NAD^+ levels

except regarding CD38 as a glycohydrolase [155]. The catalytic site of CD38 is located on the extracellular domain of the cell; yet the topological model for determining cADPR internalization is still unclear [156]. A recent study provided evidence that CD38 can be a type II or type III protein. In the latter case, the enzyme-catalytic domain is oriented toward the cytoplasm such that it is more efficient in generating intracellular cADPR than type II CD38. These results strongly suggest that flipping the catalytic sites of CD38 is an important regulatory mechanism for mediating Ca^{2+} release [157]. A schematic overview of CD38-dependent Ca^{2+} release mechanism is shown in Figure 1.4

B. CD38 and TRPM2

CD38 may modulate other channels in addition to RyR- and NAADP-gated Ca^{2+} stores, such as TRPM2 [158]. TRPM, which is named after the tumor suppressor melastatin, has eight mammalian subtypes, TRPM1 to 8, and plays an important role in Ca^{2+} mobilization in different cell types [159,160]. TRPM2, previously called LTRPC2, is known as a "chanzyme" (channel enzyme) due to the presence of an enzymatic domain in its C terminus [158]. The C terminus of TRPM2 has a regulatory binding motif (a Nudix-like domain) that is targeted by ADPR [160,161]. Since CD38 generates ADPR through hydrolysis of NAD^+ and cADPR at neutral pH, TRPM2-gated Ca^{2+} mobilization is influenced by the enzyme activity of CD38. TRPM2 is expressed in the plasma membrane, contributing to Ca^{2+} influx, but is also found in the lysosomal membrane, implying that it may operate as a Ca^{2+} release channel [161].

ADPR triggers the activation of TRPM2, contributing to the elevation of $[Ca^{2+}]_i$ in various cell types such as pancreas β cells (release) [161], immunocytes (influx)

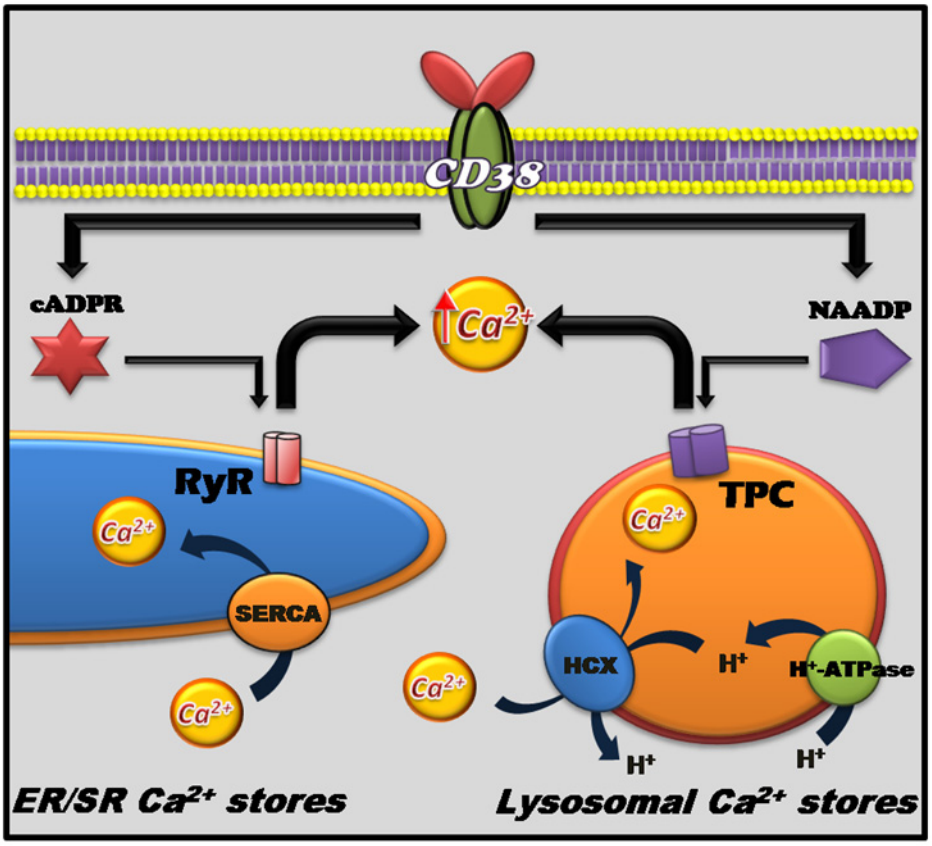

Figure 1.4. Schematic diagram of CD38-dependent Ca^{2+} release CD38 synthesizes two messenger molecules, cADPR and NAADP, which activate RyR in ER/SR and the NAADP-dependent Ca^{2+} channel two-pore channel (TPC) in endolysosme, respectively.

[162,163], and insulinoma cell lines (influx) [164]. In vasculature, TRPM2 plays a pivotal role in cell death depending on oxidative and nitrosative stress, as well as interaction with silent information regulator 2 [159]. Nonetheless, this information suggests that CD38 contributes to diverse cell physiology through the generation of different second messengers for Ca^{2+} mobilization in PASMCs. However, to date, the term for the activation of CD38 generally refers to the enhancement of cyclase and

catalase activity in synthesizing cADPR and NAADP, respectively, rather than of the hydrolase activity for the generation of ADPR.

C. Physiological function of CD38

Because CD38 was first discovered as a surface marker for lymphocyte differentiation, the investigation was initially focused on its physiological function as an antigen for proliferation to apoptosis of T and B cells, as well as hematopoietic cells [123,165,166]. However, it is now clearly established that the enzymatic activity of CD38 plays an important physiologic function along with NAD^+ consumption and cADPR/NAADP synthesis, contributing to intracellular Ca^{2+} mobilization in a variety of cells such as cardiomyocytes [167,168], neuronal cells [169,170], osteoblasts [171], hepatic stallate cells [172], pancreatic acinar and β cells [173,174], airway smooth muscle cells [141,175], renal arterial smooth muscle cells [120], and PASMCs [176,177].

CD38 knockout (KO) mice exhibit phenotypic defects including depressed insulin secretion due to impairment in pancreas acinar and β cells [173,178] and increased susceptibility to bacterial infection due to disruption in the chemotaxis of neutrophils [179]. In addition, recent population studies provided evidence that the functional defect of CD38 is correlated with HIV infection, leukemia, myeloma, solid tumors, type II diabetes mellitus, asthma, bone metabolism, and autism spectrum disorder [180,181,182,183,184]. However, while the cADPR level decreases in many tissues in CD38 KO mice, the levels in the heart and brain are not significantly different than those of the wild type. This implies that other types of ADP-ribosyl cyclase, in addition to CD38, may be present [179,185].

D. Regulation of CD38 in vascular smooth muscle

CD38 is widely distributed in many different types of vascular smooth muscle. Its expression has been reported in the aorta, coronary artery, and PA [122,186,187,188]. Furthermore, studies also have found ADP-ribosyl cyclase activity in the aorta, coronary artery, renal artery, and PA. Direct application of cADPR to vascular microsomes causes intracellular Ca^{2+} release [186,187,189,190,191]. Activation of the cyclase has been implicated in vascular responses induced by norepinephrine, ET-1, Ang II, agonists of M1-muscurinic receptors, and reactive oxygen species [192,193,194,195,196]. A study demonstrated that Ang II and NE-induced elevation of $[Ca^{2+}]_i$ in renal afferent arterioles *in vitro* and renal vasoconstriction *in vivo* were attenuated by more than 50% through pharmacological inhibition of CD38 or RyRs [197]. Moreover, vascular response to agonists including Ang II, NE, and ET-1 decreased in the aorta and renal artery of CD38 KO mice [186,197].

Similar to cADPR, application of NAADP promotes vascular smooth muscle micosomal Ca^{2+} release [198,199]. ET-1 and NE also stimulate production of NAADP in coronary arterial myocytes and renal afferent arterioles triggering Ca^{2+} mobilization from the lysosomal Ca^{2+} store [119,120]. In addition, a study using CD38 KO mice showed that activation of the death receptor Fas stimulated lysosome-dependent Ca^{2+} release though NAADP [111].

E. Regulation of CD38 in PASMCs

Expression of CD38 and the activity of ADP-ribosyl cyclase have been reported in PASMCs [122,191]. However, there is little information on the regulatory mechanism of CD38 including agonist-induced Ca^{2+} mobilization mediated by CD38 activation in PASMCs. A study examining ET-1-induced elevation of Ca^{2+} sparks and Ca^{2+} bursts mediated by RyR- and NAADP-gated Ca^{2+} release, respectively, showed that ET-1 activates the cyclase and catalase activity of CD38 [114]. It was also reported that the specific integrin-ligand GRGDSP stimulates the production of cADPR in PASMCs and activates RyR- and NAADP-gate Ca^{2+} release [122]. Indeed, NAADP induces spatially restricted Ca^{2+} bursts, which initiates global Ca^{2+} waves [121,200]. It was postulated that the lysosome-related Ca^{2+} stores and RyR-gated Ca^{2+} stores are co-localized to form a highly specialized "trigger zone" for NAADP-dependent Ca^{2+} signaling such that the NAADP-induced Ca^{2+} signal is amplified by RyRs.

One of the unique features of Ca^{2+} mobilization in PASMCs is hypoxia-induced Ca^{2+} response mediated by RyR-gated Ca^{2+} release, contributing to hypoxic pulmonary vasoconstriction in response to acute hypoxic exposure [201,202,203]. To date, there are at least two hypotheses for the mechanism of hypoxia-induced activation of RyRs, which are related to cADPR and reactive oxygen species (ROSs), respectively. One of the hypotheses proposed that the reduction in the ratio of β-NAD^+ to β-$NADP^+$ by hypoxia stimulates the activation of RyRs, leading to an increase in $[Ca^{2+}]_i$. Increased β-$NADP^+$ inhibits hydrolase activity of CD38, contributing to accumulation of cADPR, which triggers RyR-gated Ca^{2+} release from SR [176]. This hypothesis suggests that CD38 plays an important role for redox sensing in PASMCs under acute exposure to hypoxia.

However, the information has been limited to acute hypoxia, and the possible alteration of CD38 under prolonged exposure to hypoxia in PASMC is completely unknown.

Indeed, the regulatory mechanism of CD38 and CD38-dependent Ca^{2+} release mechanism as well as CD38-mediated physiologic response in PASMC are very scanty. Because of the lack of information, this thesis research focused on the regulatory mechanism of CD38 expression and activity as a potent modulator of Ca^{2+} release in PASMC.

CHAPTER 2

BACKGROUND AND INTRODUCTION: PULMONARY HYPERTENSION AND ALTERATION OF CALCIUM REGULATION

Chapter 1 reviewed the physiology and the regulatory mechanism of intracellular Ca^{2+} with emphasis on pulmonary arterial smooth muscle cell (PASMC). In this chapter, it is followed by a overview on pulmonary hypertension (PH) and its association with the alteration of Ca^{2+} homeostasis in PASMC. Review on this chapter further focuses on a novel mechanism of intracellular Ca^{2+} release mediated by the CD38-dependent Ca^{2+} pathways, which may contribute to the regulation and dysregulation of Ca^{2+} homeostasis in PASMC particularly under chronic hypoxic (CH) exposure that may cause chronic hypoxia-induced pulmonary hypertension (CHPH).

I. Pulmonary hypertension

A. Overview of pulmonary hypertension

PH in humans is defined as a mean pulmonary arterial pressure (PAP) higher than 25 mm Hg at rest or 30 mm Hg during physical activity as well as increased pulmonary vascular resistance higher than 240 dynes/sec/cm^{-5} [204]. According to the recently updated clinical classification of PH by the Fourth World Symposium in Dana Point 2008, PH is categorized into five groups: (a) pulmonary arterial hypertension, (b) PH with left heart disease, (c) PH associated with lung disease and/or hypoxemia, (d) PH due to chronic thrombotic and/or embolic disease (CTEPH), and (e) PH due to miscellaneous factors [205,206,207]. PH is associated with multiple risk factors including gender, family history, disease, toxins, behavior patterns, and environment [205]. Although the mechanism varies depending on the type of PH, the elevation of PAP is clearly associated with increased pulmonary vascular resistance due to the alteration of structure and contractility in vasculature, eventually leading to right heart failure [208]. In particular,

Table 2.1. Revised WHO classification of PH (reprinted from ACCF/AHA 2009 Expert Consensus Document on Pulmonary Hypertension [208])

1. Pulmonary arterial hypertension (PAH)
1.1. Idiopathic (IPAH)
1.2. Familial (FPAH)
1.3. Associated with (APAH):
1.3.1. Connective tissue disorder
1.3.2. Congenital systemic-to-pulmonary shunts
1.3.3. Portal hypertension
1.3.4. HIV infection
1.3.5. Drugs and toxins
1.3.6. Other (thyroid disorders, glycogen storage disease, Gaucher's disease, hereditary hemorrhagic telangiectasia, hemoglobinopathies, chronic myeloproliferative disorders, splenectomy)
1.4. Associated with significant venous or capillary involvement
1.4.1. Pulmonary veno-occlusive disease (PVOD)
1.4.2. Pulmonary capillary hemangiomatosis (PCH)
1.5. Persistent pulmonary hypertension of the newborn
2. Pulmonary hypertension with left heart disease
2.1. Left-sided atrial or ventricular heart disease
2.2. Left-sided valvular heart disease
3. Pulmonary hypertension associated with lung diseases and/or hypoxemia
3.1. Chronic obstructive pulmonary disease
3.2. Interstitial lung disease
3.3. Sleep disordered breathing
3.4. Alveolar hypoventilation disorders
3.5. Chronic exposure to high altitude
3.6. Developmental abnormalities
4. Pulmonary hypertension due to chronic thrombotic and/or embolic disease (CTEPH)
4.1. Thromboembolic obstruction of proximal pulmonary arteries
4.2. Thromboembolic obstruction of distal pulmonary arteries
4.3. Nonthrombotic pulmonary embolism (tumor, parasites, foreign material)
5. Miscellaneous
Sarcoidosis, histiocytosis X, lymphangiomatosis, compression of pulmonary vessels (adenopathy, tumor, fibrosing mediastinitis)

exposure to chronic hypoxia due to high altitude or airway/alveolar disease such as chronic obstructive pulmonary disease and fibrosis causes CHPH [206]. This dissertation focuses on CHPH in order to understand the possible mechanism linked to the underlying Ca^{2+} mechanism in PASMCs.

B. Hypoxia-induced pulmonary hypertension

As described above, acute exposure to hypoxia causes hypoxic pulmonary vasoconstriction (HPV) in PA [202]. HPV is a unique feature in PAs that shunts the blood to the O_2-rich regions of the lungs to match the ventilation-perfusion ratio [176,209,210]. However, prolonged exposure to hypoxia causes PH, which is characterized by increased vasomotor tone; enhanced vasoreactivity to agonists including ET-1, Ang II, and serotonin (5-HT); and remodeling of pulmonary vasculature [75,211,212,213], eventually leading to right heart failure and worsening the prognosis of the underlying disease [207].

The pathogenesis of CHPH involves multiple factors with a wide spectrum of mechanisms in PASMCs. Heterozygous mice of hypoxia-inducible factor-1 (HIF-1), an O_2-sensitive transcription factor, demonstrated a delayed development of CHPH [214]. Inhibition of the translocation of nuclear factor of activated T-cells (NFAT) activated by Ca^{2+}-calcineurin attenuates CHPH and decreases $[Ca^{2+}]_i$ proliferation in PASMCs [215,216,217]. Abnormal regulation of endothelium-derived factors, including enhanced ET-1 and reduced nitric oxide production, also contribute to the development of CHPH [218,219]. Moreover, the vasoactive agonists that activate Rho A/Rho kinase signaling—such as ET-1, thromboxane A2, norepinephrine, histamine, and serotonin (5-HT)—all contribute to development of CHPH [220,221,222,223,224,225]. Accordingly, elevation of Rho kinase activity alters cytoskeleton properties including increased stress fiber formation [226] and myofilament Ca^{2+} sensitivity in PASMCs [227]. Excessive ROS generation mediated by NADPH oxidase [228,229] and xanthine oxidase [230,231] are also involved in the development of CHPH. Furthermore, alterations of extracellular

matrix deposition and production, including collagen production and enhanced serine elastase activity, are associated with the development of CHPH [232,233].

II. Alteration of Ca^{2+} homeostasis in PASMCs

Substantial evidence indicates that CH causes intrinsic changes in ionic balance and Ca^{2+} homeostasis in PASMCs, leading to membrane depolarization, elevation of resting $[Ca^{2+}]_i$, and changes in electrophysiological and Ca^{2+} responses to vasoconstrictors and vasodilators [234,235,236,237,238]. These functional changes in PASMCs involve alterations in multiple Ca^{2+} pathways and are crucial for the development of CHPH [69,239]. An increase in $[Ca^{2+}]_i$ stimulates gene transcription through activation of Ca^{2+}-regulated transcription factors such as NFAT, a process known as excitation-transcription coupling, which is essential for vascular remodeling and smooth muscle proliferation [240,241]. Elevated $[Ca^{2+}]_i$ also promotes Ca^{2+} binding to calmodulin and activates Ca^{2+}-calmodulin-dependent myosin light chain kinase and actin-myosin interactions to enhance vasoconstriction. As mentioned, enhanced agonist-induced Ca^{2+} influx [242] and enhanced myofilament Ca^{2+} sensitivity depending on Rho kinase pathways operate synergistically to promote vasoconstriction [227].

A. Hypoxic-induced alteration of Ca^{2+} influx

1. K^+ channel dependence

CH alters Ca^{2+} influx through multiple mechanisms in PASMCs. It has been clearly demonstrated that hypoxia suppresses K^+ currents [69]. The activity of K_V channels ($K_{V1.5}$ and $K_{V2.1}$) in PASMCs significantly decreases under CH exposure and is

associated with the downregulation of K_V channel expression [70,234,235,236,237,243,244,245,246,247]. Since the K_V channel is the major conductance controlling the resting membrane potential [70,238,248], the downregulation of K_V channels causes membrane depolarization and subsequent activation of the VDCCs, leading to Ca^{2+} influx and increase in $[Ca^{2+}]_i$ [234,249]. It is interesting to note that the heterogeneity of K_V channel expression in proximal and distal PA may lead to differential responses to CH in terms of vascular remodeling, cell proliferation, and apoptosis [250]

It is unclear, however, which other types of K^+ channels are involved in the response to CH in PASMC. Large-conductance K_{Ca} (BK_{Ca}) channels, which are inactive at resting membrane potential, apparently do not play a primary role in the development of CHPH [251,252,253]. The general consensus on the role of BK_{Ca} is that the elevation of $[Ca^{2+}]_i$ activates BK_{Ca}, limiting the extent of depolarization as a form of regulatory feedback to VDCC-gated Ca^{2+} entry in PASMCs. Likewise, although it was reported that a fall in ATP during hypoxia triggers ATP-sensitive K^+ channels, which are regulated by the ADP/ATP ratio, the activity was not directly required for the alteration of K^+ entry [254]. The activity of the channels is dependent on ATP content, which decreases during hypoxic exposure. ATP-sensitive K^+ channels may be involved in the vasorelaxation phase of HPV [251,254]. Nielsen et al. showed that the expression of polyunsaturated fatty acid-activated two-pore domain K^+ channel (K_{2P}) is altered in hypoxia, contributing to endothelium hyperpolarization and pulmonary artery relaxation in hypoxic PH [255].

2. TRP channels

CH can also modulate Ca^{2+} influx through non-voltage-dependent and nonselective cation channels such as TRP channels, which are known to have diverse physiological functions in vascular smooth muscles [21,256]. In particular, previous studies demonstrated that CH upregulates the store-operated TRPC1 and receptor-operated TRPC6 expression in PAs and enhances both SOCE and ROCE in PASMCs [238]. Differential inhibition of those two pathways using a pharmacological blocker indicated that the SOCE is responsible for elevated resting $[Ca^{2+}]_i$ in PASMCs and resting vasotone in PAs from CH animals. A subsequent study also demonstrated that the upregulation of TRPC1 and TRPC6 is the direct effect of hypoxia on PASMCs and requires the full expression HIF-1α [257]. Sildenafil, a specific phosphodiesterase-5 inhibitor, which is known to attenuate CHPH [258], significantly reduces basal $[Ca^{2+}]_i$ and SOCEs mediated by decreased expression of TRPC1 an TRPC6 [259,260,261]. Also, sodium tanshinone IIA sulfonate inhibited the CH-induced upregulation of TRPC1/6 in PASMCs, contributing to attenuating basal $[Ca^{2+}]_i$ and cell proliferation [262].

In particular, recent studies also provided evidence that TRPC1 and TRPC6 differentially contribute to the full development of CHPH. The regulatory mechanism of HPV by acute exposure to hypoxia was absent in TRPC6 KO mice while TRPC6 KO mice were not protected from CHPH, including vascular remodeling and right heart hypertrophy [263]. In contrast, TRPC1 KO mice was failed to experience pulmonary vascular remodeling underlying the development of CHPH [264]. In particular, CH-induced enhancement of the vasomotor tone of PA was blunted in TRPC1 KO mice but not in TRPC6 KO mice CHPH, whereas CH-induced augmentation of vasoreactivity to 5-HT decreased in both TRPC1 and TRPC6 KO mice PAs [38]. These results strongly

indicate that TRPC1 and TRPC6 in PA differentially contribute to the development of CHPH with discrete, time-dependent roles when exposed to hypoxia.

In the monocrotaline (MCT)-induced pulmonary arterial hypertension model (MCT causes pulmonary endothelial damage and PA remodeling) results in increased SOCE mediated by the upregulation of TRPC1 and TRPC4, leading to the enhancement of vasoreactivity to ET-1 in PASMCs [265]. Further studies demonstrated that the absence and inactivation of TRPC4 attenuated the severity of lesion formation in PA and right heart failure, indicating that TRPC4 is critically associated with the development of pulmonary arterial hypertension [265,266].

An increasing number of studies have also implicated the roles of other TRP channels in CHPH development. A recent study demonstrated that TRPV, a mechano-sensitive vanilloid TRP channel, is the only CH-induced upregulated channel among the members of the TRPV and TRPM subfamilies. Since pharmacological activation of TRPV1 and TRPV4 can trigger an increase in the migration of PASMCs, its upregulation may contribute to PH development [39,267]. In particular, the development of CHPH was significantly attenuated in TRPV4 KO mice [37,39]. TRPV4 gene deletion also decrease 5-HT-induced $[Ca^{2+}]_i$ and reduce vasoreactivity to 5-HT compared to the wild type under CH exposure [37,39].

It was also reported that a TRPV4-mediated increase in $[Ca^{2+}]_i$ was significantly attenuated by the inhibition of RyR2, and both TRPV4 and RyR2 expression are enhanced in CH rats. This suggests complex interplay between TRPV4 and RyR2 may also contribute to the development of CHPH [268]. Moreover, the expression of TRPM8 is significantly declined in the PAs of both CHPH and MCT-induced PH. It is associated

with decreased TRPM8 menthol-induced vasorelaxation in PH rats, indicating that the downregulation of TRPM8 may associate with increased vasoreactivity in PH [269].

3. Ca^{2+} channels

It is unequivocal that VDCC-gated Ca^{2+} influx increases with membrane depolarization mediated by K^+ channels in PASMCs during CHPH [270,271]. Pharmacological inhibition of L-type Ca^{2+} channels ($Ca_v1.2$), such as nifedipine or verpamil, partially attenuated CHPH [35,272,273,274,275], implying that the activity of $Ca_v1.2$ may be enhanced in PAs under CH exposure [35,276]. In addition, evidence also demonstrates that the expression of VDCCs in PASMCs is upregulated in response to CH. Wan et al. demonstrated that both $Ca_v1.2$ (L-type) and $Ca_v3.2$ (T-type) are specifically upregulated in PA but not in systemic vasculature under CH exposure, suggesting that upregulation of both L- and T-type VDCCs may play a role in CHPH development [35].

However, it was reported that an ET-1-induced change in $[Ca^{2+}]_i$ in PASMCs is altered and mediated by VDCC independent from the alteration of membrane potential after CH exposure. Meanwhile, ET-1 neither triggers Ca^{2+} release nor alters membrane potential mediated by the inhibition of K^+ channels following CH exposure [236,274]. Subsequent studies demonstrated that ET-1 initiates a Ca^{2+} influx through VDCCs in PASMCs from CH rats, mediated by activation of PKC, Rho kinase, and tyrosine kinases [277].

4. Other channels

The Ca^{2+}-dependent channels of PASMCs are also affected in CHPH. Although K_{Ca} channels may not contribute to the process of CHPH development, Sun et al. recently demonstrated that CH enhances the activity of CaCCs in PASMCs through upregulation of TMEM16A, a member of the TMEM16 family, contributing to increased agonist-induced pulmonary vasoconstriction via the activation of VDCC-gated Ca^{2+} influx [75]. In addition, the acid-sensing ion channel 1 (ASIC1), another novel channel, may modulate other mechanisms of Ca^{2+} entry, contributing to CHPH. In particular, Jernigan et al. showed that ASIC1 may contribute to SOCE in pulmonary vascular smooth muscle [278]. A subsequent study also demonstrated that elevation of SOCE in PA from CH rats was prevented by the inhibition of ASIC1, leading to the speculation that the CH-induced enhancement of SOCE is mediated in part by ASIC1 in PASMCs and contributes to the development of CHPH [279,280].

B. Hypoxic-induced alteration of intracellular Ca^{2+} release

Despite the well-established investigation of the extracellular Ca^{2+} influx, the information on the alteration of intracellular Ca^{2+} release mechanisms in PASMCs during CH is scant. Bonnet et al. found that in the early stage (1–2 weeks) of CH, the main PA rings in rats exhibited spontaneous and rhythmic contractions, spike-like membrane depolarization, and elevation in resting $[Ca^{2+}]_i$. The spontaneous rhythmic contraction was inhibited by disabling Ca^{2+} release from SR using ryanodine, tetracaine, or CPA [281]. This spontaneous rhythmic contraction of the main PA diminished after 3–4 weeks of CH when vascular remodeling and PH was fully established, suggesting that there is a time-dependent alteration of the Ca^{2+} release mechanism from SR stores under CH.

Increasing evidence indicates that CH increases the level of intracellular ROS originating from mitochondria and NADPH oxidase in PASMCs [282,283]. Accordingly, the elevation of ROS is responsible for hypoxic-induced elevation of $[Ca^{2+}]_i$ mediated by Ca^{2+} release [284]. In particular, the CH-induced generation of ROS triggers dissociation of the complex of RyR2 and FK506 binding protein 12.6 (FKBP12.6) [285]. As mentioned above, FKBP12.6 dissociation can be regulated by cADPR [286]. Yet, the regulation of cADPR synthesis in PASMCs by CH has not been established. Moreover, exogenous application of ROS also activates Ca^{2+} release via both IP_3R- and RyR-gated Ca^{2+} stores in PASMCs [287]. These results imply that CH may enhance generation of ROS, triggering the activation of RyR- and IP_3R-gated Ca^{2+} release in PASMCs.

C. Regulation of CD38 by hypoxia in PASMCs

Recent studies demonstrated that CD38 appears to play an important role in acute HPV. The hypoxic response in PAs or PASMCs has been shown to be consistently suppressed by the inhibition of RyRs [177,191,201,288,289]. Studies of rabbit and rat PAs showed that acute exposure to hypoxia promotes the accumulation of cADPR to elicit Ca^{2+} release from RyR-gated Ca^{2+} stores to initiate vasoconstriction in PAs [177,191]. Particularly, Wilson et al. demonstrated that (a) acute hypoxia reduces the ratio of β-NAD^+ to β-$NADH^+$ in PA, (b) β-$NADH^+$ inhibits the hydrolase activity of CD38, and (c) accumulation of cADPR leads to HPV mediated by RyR-gated Ca^{2+} release. Based on these observations, acute hypoxia may have a direct influence on CD38-dependent mechanisms, and CD38 may act as a redox sensor in PASMCs [191].

Nevertheless, although there is still controversy about the role of CD38 as a redox sensor in HPV [290], there is no systematic research on the role of CD38 in the regulation of intracellular Ca^{2+} mobilization, in particular Ca^{2+} release, in PASMCs. Furthermore, it is completely unknown whether CH regulates the expression and activity of CD38, as well as cADPR and NAADP-dependent Ca^{2+} release, in PASMCs.

III. Statement of thesis objective

Ca^{2+} is an indispensible element that plays a pivotal role in maintaining normal cell function. The regulatory mechanism of intracellular Ca^{2+} is a complex response to chemical and physical stimulus in PASMCs. Profound changes in $[Ca^{2+}]_i$ homeostasis occur due to CH, but the mechanisms for these changes are still not fully understood. In particular, the functional alterations in intracellular Ca^{2+} release processes in PASMCs have been barely investigated. Thus, *the overall aim of this thesis research is to investigate the novel mechanism of CD38-dependent Ca^{2+} release and the changes in its enzymatic activity and expression in PASMCs under exposure to CH.*

To investigate the objectives, *the first aim of this dissertation is to determine the underlying mechanism of agonist-induced CD38 activation using Ang II as the activator of intracellular Ca^{2+} release in PASMCs. The second aim is to investigate the CH-induced alterations of CD38-dependent Ca^{2+} pathways in PASMCs to elucidate their contributions in the pathophysiology of CHPH.*

This research successfully reveals the novel roles of CD38-dependent Ca^{2+} pathways in the physiological regulation of pulmonary vascular reactivity and the

pathophysiology of CH-induced PH. Proof of these concepts may lead to the discovery of a new therapeutic target for the treatment of CHPH.

CHAPTER 3

CD38 MEDIATES ANGIOTENSIN II-INDUCED INTRACELLUAR CALCIUM RELEASE IN RAT PULMONARY ARTERIAL SMOOTH MUSCLE CELL

Abstract

CD38 is a multifunctional enzyme that synthesizes the endogenous Ca^{2+} mobilizing messengers cADPR and NAADP. cADPR and NAADP activate ryanodine receptors (RyRs) of the endoplasmic/sarcoplasmic reticulum (ER/SR) and NAADP-sensitive endolysosomal Ca^{2+} stores, respectively; further, they are thought to play important roles in the regulation of $[Ca^{2+}]_i$ and vascular functions. However, information on the physiologic functions and the regulatory mechanisms of CD38 in PASMCs is scanty. This study characterized the expression of CD38, and its roles in angiotension II (Ang II)-induced vasoconstriction in PAs and Ang II-induced Ca^{2+} release (AICR) in PASMCs. Examination of the expression profile of CD38 in various rat arteries found a relatively high level of CD38 expression in PA-smooth muscle. Application of Ang II to PASMCs elicited Ca^{2+} response composed of both extracellular Ca^{2+} influx and intracellular Ca^{2+} release AICR activated in the absence of extracellular Ca^{2+} was significantly reduced by pharmacological or by siRNA inhibition of CD38, implying that CD38 mediates AICR in PASMCs. AICR was suppressed by the cADPR antagonist cADPR 8-Br-cADPR or the inhibition of the RyR-gated Ca^{2+} released with ryanodine. It was also suppressed by the NAADP-antagonist Ned-19 or the disruption of endolysosomal Ca^{2+} stores by the vacuolar H^+-ATPase inhibitor bafilomycin A1. Suppression of AICR by the inhibition of cADPR- and NAADP-dependent pathways was non-additive, indicating inter-dependence between RyR- and NAADP-gated Ca^{2+} release in PASMCs. Furthermore, AICR was inhibited by the PKC inhibitor staurosporine, the non-specific NADPH oxidase (NOX) inhibitor apocynin and DPI, the NOX2 specific inhibitor gp91ds-tat, and the ROS scavenger TEMPOL. These results, for the first time,

provide evidence that Ang II activates CD38-dependent Ca^{2+} release via the PKC-NOX2-ROS pathway in PASMCs.

Introduction

CD38 is a 45 kDa trans-membrane glycoprotein ubiquitously distributed in mammalian tissues, including inflammatory cells, brain tissue, pancreas, cardiac muscles, and airway and vascular smooth muscle cells [126,137,291]. CD38 is a multifunctional enzyme that serves as an ADP-ribosyl cyclase, synthesizes cyclic ADP-ribose (cADPR) from β-NAD^+, and acts as a catalase, producing nicotinic acid adenosine diphosphate (NAADP) from β-$NADP^+$ through a base-exchange reaction [148,149,152]. Additionally, both products, cADPR and NAADP, can be hydrolyzed by CD38 to form ADP-ribose and ADP-ribose phosphate, respectively [152,292,293]. cADPR is the endogenous ligand of RyRs [132,133]. It binds to the FK506 binding protein, an accessory protein that stabilizes RyRs on endoplasmic/sarcoplasmic reticulum (ER/SR), causing its dissociation from RyRs to initiate channel activation [134,135]. NAADP is the most potent Ca^{2+} mobilizing messenger to date, which triggers Ca^{2+} release from endolysosomes [150,151]. Recent studies identified the two-pore channels (TPC1 and TPC2) as the NAADP-activated Ca^{2+}-release channels [117,294,295]. It has been suggested that NAADP either binds directly to TPCs or to an accessory protein of the TPC complex to activate endo/lysosomal Ca^{2+} release [296].

To date, CD38 expression has been reported in various types of systemic arteries [186,187,188,196]. Endogenous vasoconstrictors such as norepinephrine (NE), endothelin-1 (ET-1), and angiotensin II (Ang II) can activate the cyclase and catalase activities of CD38, contributing to the elevation of $[Ca^{2+}]_i$ and vasoconstriction in

systemic arteries [120,168,193,297,298]. These agonists of mediated by G-protein coupled receptor (GPCR) signaling pathways activate phospholipase C (PLC) to synthesize inositol trisphosphate (IP_3) and diacyglycerol (DAG) from phosphatidylinositol bisphosphate. IP_3 activates the IP_3 receptor, which releases intracellular Ca^{2+} from SR in vascular smooth muscle cells (VSMCs) [299,300]. Evidence also demonstrated that Ang II can activate NAD(P)H oxidases (NOXs), in particular NOX2, to increase the production of reactive oxygen species (ROS) in VSMCs [301,302,303,304,305,306]. Ang II facilitates the assembly of NOX2 subunits by the phosphorylation of p47phox, leading to the coupling of p47phox and gp91phox, and ROS generation [307]. Moreover, previous studies showed that ROS production is associated CD38 activation [194,308,309,310], and that Ang II stimulates NOX to generate ROS, leading to enhanced ADP-ribosyl cyclase activity in afferent arterioles [305].

CD38 expression and its cyclase and hydrolase activity have been reported in rat pulmonary arteries (PA) and pulmonary arterial smooth muscle cells (PASMCs) [122,176,191]. ET-1 has also been shown to elicit Ca^{2+} responses in PASMCs, partially through NAADP-gated Ca^{2+} release and cross-activation of RyRs by Ca^{2+}-induced Ca^{2+} release [114,121]. Moreover, integrin-ligand GRGDSP increases the production of cADPR and activates Ca^{2+} release from both the RyR-gated Ca^{2+} stores and the endolysosomal Ca^{2+} store [122]. However, the mechanism underlying agonist-induced activation of CD38 in PASMCs is still unclear. In this study, we compared the expression of CD38 in pulmonary and systemic arteries, determined the contribution of CD38 in Ang II-induced Ca^{2+} release (AICR), and examined the signaling mechanism of Ang II-

induced activation of CD38 in PASMCs. We found that Ang II activates CD38 dependent Ca^{2+} release via the PKC-NOX2-ROS pathway in PASMCs.

Method

Preparation of rat PA tissue and PASMC All animal procedures in this study conformed with the Laboratory Animals Care and Use guidelines published by the United States National Institutes of Health and was approved by the Johns Hopkins University Animal Care and Use Committee. PA tissues were surgically dissected and PASMCs were enzymatically isolated from the tissues as previously described [311]. Briefly, lungs were harvested from male Wistar rats (150–200 g) anesthetized with an overdose of sodium pentobarbital (130 mg/kg intraperitoneally). Intrapulmonary arteries of second to fourth generations (800 to 300 μm) were then dissected in a 1.5 mM Ca^{2+} HEPES-buffered salt solution (HBSS) containing 130 mM NaCl, 5 mM KCl, 1.2 mM $MgCl_2$, 1.5 mM $CaCl_2$, 10 mM HEPES, and 10 mM glucose (pH 7.2 adjusted with 5 M NaOH). PAs were cleaned of connective tissue and cut open to remove their endothelial layers by rubbing the luminal surface thoroughly with a cotton swab. For the isolation of PASMCs, PA tissues were incubated in cold HBSS for 30 min, and then in HBSS with reduced Ca^{2+} (20 μM) at room temperature for 20 min. PAs were digested in a reduced-Ca^{2+} HBSS containing type I collagenase (1,750 U/ml), papain (9.5 U/ml), bovine serum albumin (2 mg/ml), and dithiothreitol (1 mM) at 37 °C for 20 min. After digestion, tissue was transferred to Ca^{2+}-free HBSS and the PASMCs were gently dispersed from the tissues by trituration in Ca^{2+}-free HBSS. The PASMCs were cultured transiently on 25 mm glass

cover slips (18–24 hrs) in HAM's F-12 media (#10-080-CV, Mediatech, Inc., VA) with 0.5% FBS and antibiotics for Ca^{2+} fluorescence experiments.

Preparation of protein Total protein was isolated from PA and other artery tissues, including the aorta, mesenteric (MA), renal (RA), femoral (FA), tail (TA), and cerebral artery (CA), and the PASMCs were cultured for Western blot analysis of CD38 expression. Endothelium-denuded PAs were frozen in liquid nitrogen and then pulverized with pestle and mortar in the liquid nitrogen. Ground tissues were transferred to a protein lysis buffer containing 50 mM Tris, 150 mM NaCl, 300 mM Sucrose, 0.5% NP-40, 1% deoxycholic acid, and 0.1% SDS with 5 mM EDTA and Halt™ protease inhibitor cocktail (Thermo Scientific, #78430). Tissue and cell lysate were centrifuged by 3,000 g at 4 °C for 10 min, and the protein concentrations were measured with the BCA Protein Assay Kit (Pierce, #23225).

Western blot Protein samples were separated with 10% polyacrylamide gel (20 μg from artery tissues and 10 μg from PASMCs per lane), and the separated proteins were transferred to an Immobilion®-P PVDF transfer membrane (#IPVH00010, EMD Millipore, Billerica, MA) using a tank system filled with transfer buffer containing 3.03 g/L Tris-base, 14.4 g/L glycine, and 10% methanol (80V, 3 hours, 4 °C). After blocking with 5% skim milk in PBS containing 0.0 1% Tween-20 (PBST) at room temperature for 1 hour, the membranes were incubated overnight with primary antibodies diluted in 3% BSA-PBST at 4 °C. The primary antibody for CD38 was diluted by 1:500 (#SC-7049, goat-anti rat, Santa Cruz Biotechnology, Inc.) and actin by 1: 5,000 (#SC-1615, goat-anti rat, Santa Cruz Biotechnology, Inc.). After a wash in PBST, the membranes were incubated with horseradish peroxidase-coupled secondary antibody (#SC-2020, donkey-

anti goat, Santa Cruz Biotechnology, Inc.) diluted by 1:5,000 in 3% BSA-PBST at room temperature for 1 hour, and then washed extensively. Upon incubation of the membrane with the enhanced chemiluminenscence substrate (#Pierce Biotechnologies), protein signals were detected on autoradiography film and quantified with Gel Logic 200 Image System (#Kodak, New Haven, CT). CD38 expression data were normalized with the actin level of each sample to correct sample variability.

Because of the similarity in size between actin and CD38 protein, the membrane was stripped and reprobed after the measurement of CD38. The membrane was gently agitated in 100 % acetonitrile for 10 min, submerged in stripping buffer (2% SDS, 62.5 mM Tris-HCL buffer pH 6.7) containing 100 mM 2-mercaptoethanol, and incubated at 50 ºC for 25 min. After a wash in PBST, the same protocol with typical a Western blot from a blocking step was undertaken.

Quantitative reverse-transcriptional PCR Endothelium-denuded PAs frozen in liquid nitrogen were mechanically homogenized with pestle and mortar. Total RNA from the PA tissues and cultured PASMCs was extracted using an RNeasy® minikit (#74104, Qiagen, Valencia, CA), followed by a first-strand cDNA synthesis using random hexamer primers and Superscript III-reverse transcriptase (#18080-051, Invitrogen, Grand Island, NY) according to the manufacturer's protocol. Quantitative real-time RT-PCR (qRT-PCR) data was used to quantify the expression of CD38 in PA and other arterial tissues with iQ SYBR Green PCR Supermix (#170-8880, Bio-Rad, Hercules, CA) following the manufacture's protocol. Gene-specific primers of qRT-PCR for 18S rRNA and CD38 of the following sequences were used: 18S rRNA forward 5′–CGGCTACCACATCCAAGG AA–3′ and reverse 5′–AGCTGGAATTACCGCGGC–3′ (accession number: 57149;

position: 452-639; expected size: 188 bp), CD38 forward 5′–TGGAGCAAGTCCAAAC ACCTGGC–3′, and reverse 5′–CTGGGGTCTCCACACCACCTGA–3′ (accession number: 6978628; position: 382-500; expected size: 119 bp). A qRT-PCR protocol, consisting of an initial step at 95°C for 5 min, followed by 40 cycles at 95°C for 15 s, 60°C for 30 s, and 72°C for 1 min, was performed using the iQ5 Multicolor real-time PCR detection system (Bio-Rad, Hercules, CA). Absolute copy numbers were calculated using standard curves generated from serial dilutions of the known copy number of the purified PCR products defined according to each product's size. All data were normalized by the copy number 18s rRNA in each sample to compensate for sample variability.

Calcium Imaging $[Ca^{2+}]_i$ was measured with fluorescent microscopy as previously described [311]. Fresh-isolated PASMCs on 25 mm cover-slip incubated overnight were loaded with fluo-3 AM (#F1242, Invitrogen, Grand Island, NY) and dissolved in DMSO containing 20% pluronic acid for 45 min at room temperature in the dark. Cells were washed with a 2 mM $CaCl_2$ tyrode solution containing 137 mM NaCl, 5.44 mM KCl, 1 mM $MgCl_2$, 10 mM D-glucose, and 10 mM HEPES, with pH 7.4 adjusted with NaOH, followed by 20 min of incubation for the deesterification of the cytosolic dye. Fluo-3 fluorescence, excited at 488 nm and emitted with 515 nm, was detected using a Diaphot microscope (Nikon TE2000U) equipped with epifluorescence attachments and a microfluometer (PTI, model D-104). Protocols were executed and data collected on-line with a Digidata analog-to-digital interface and the pClamp software package (Axon Instruments Inc.). Fluorescence intensity (F) was used to calculate the absolute $[Ca^{2+}]_i$ with the equation: $[Ca^{2+}]_i = [K_D \cdot (F - F_{bg})]/(F_{max} - F)$, where F_{bg} is the background

fluorescence and F max is the maximum fluorescence. The value for K_D of fluo-3 is 1.1 μM. F_{max} was determined in situ using the Ca^{2+} ionophore 4-Bromo-A23187 (#100107, Calbiochem, La Jolla, CA) and 10 mM Ca^{2+}, and F_{bg} was measured in an area devoid of cells after Mn^{2+} quenching.

Isometric tension measurements in PAs Isometric contraction of PAs induced by agonists were examined by an organ chamber experiment described previously [75]. Briefly, rat intralobar PAs (outer diameter: 300–800μm) were surgically harvested, endothelium-disrupted by gently rubbing the lumen with a fine wooden stick, and cut into ring segments of 4 mm in length. The PA rings were mounted in organ chambers warmed at 37°C and filled with Krebs solution (containing 118.3 mM NaCl, 4.7 mM KCl, 1.2 mM $MgSO_4$, 25 mM $NaHCO_3$, 11.1 mM glucose, 1.2 mM KH_2PO_4, and 2 mM $CaCl_2$,) and gassed with 16% O_2-5% CO_2 to maintain a pH of 7.4 during the entire experiment. Isometric tension was measured using force-displacement transducers (Grass Instruments, Quincy, MA), amplified by a PowerLab system controlled by the Chart software (ADInstruments Inc. Colorado Springs, CO). After equilibrium under a resting tension of approximately 0.8 g for 90 min, three 60 mM KCl-induced vasoconstrictions for 15 min each and washouts were performed to attain the stable optimal contraction of PA rings. Concentration-dependent responses to Ang II were examined by the cumulative addition (0.5 log unit increments) of Ang II into each chamber in the presence or absence of CD38 inhibitors. All inhibitors were preincubated for 10 min before the addition of AngII. At the end of experiments, the PA ring was exposed to phenylephrine (3×10^{-7} M) followed by acetylcholine (10^{-6} M) to verify the disruption of endothelium. Data from PA rings with >20% maximal contraction to the phenylephrine were discarded. The Ang II-

induced isometric tension was normalized to the maximal tension generated by 60 mM KCl. For the estimation of EC_{50} and maximum response (E_{max}), the concentration-response curves were analyzed using a 3-parameter logistic model or Hill equation as follows: $E= (E_{max})/\{1+([Agonist]/EC_{50})^{-b}\}]$, where E is the response and b is the slope factor.

siRNA knockdown of CD38 Isolated PASMCs in 0.5% FBS-containing HAM's F-12 media, incubated overnight, were cultured in 5% FBS-SmGM for 6 days with two cell passages. Short interfering RNA (siRNA) for CD38 was commercially purchased from Origene (#SR509476A, sequence: 5'-ACCAUACCAUGUAACAAGACUCUCT-3'), along with the scrambled control sequence. Prepared PASMCs were transfected with 100 nM siRNA or scramble control by electroporation using the Amaxa 96-well Shuttle^{TM} system (Lonza) and immediately seeded on 25 mm cover-slips in 5% FBS containing SmGM and incubated overnight. After 24 hrs, the medium was changed to serum-free SmGM for overnight starvation. Intracellular Ca^{2+} measurements and Western blots were performed within 48 hours of the siRNA transfection.

Chemicals and inhibitors All chemicals were commercially purchased: Ang II (#A9525), nicotinamide (#N0636, an ADP-ribosyl cyclase inhibitor), 8-Bromo-cADPR (#B5416, an antagonist of cADPR), staurosporine (#S-4400, PKC inhibitor), and diphenyleneiodonium (DPI, #D2926, NADPH oxidase inhibitor) from Sigma-Aldrich (St. Louis, MO); ryanodine (#181-00961, RyRs blocker) from Wako Pure Chemical Industries, LTD (Osaka, Japan); trans-Ned-19 (#270-503, a NAADP antagonist) and bafilomycin A1(#BML-CM110, a vacuolar-type H^+-ATPase inhibitor), from Enzo Life Sciences (Farmingdale, NY); apocynin (#178385, NADPH oxidase inhibitor) from EMD

millipore (Billerica, MA); and TEMPOL (#4653, ROS scavenger) from TOCRIS bioscience (Bristol, UK). The NOX2-specific peptide inhibitor gp91ds-tat (#63818) was purchased from ANASpec (Fremont, CA).

Statistical Analysis All data are shown as a mean ± S.E.M, calculated by Sigmaplot 11 (Systat Software Inc). The numbers of duplicates (n) are specified in the text. Statistical significance ($p<0.05$) was assessed with unpaired Student's t-tests, ANOVA with the Holm-Sidak method, or Newman-Keuls post hoc analyses if applicable.

Result

Profile of CD38 expression in vascular smooth muscle.

The expression of CD38 protein in endothelium-denuded rat arteries was detected by Western blot. The specificity of the CD38 antibody was verified using a specific blocking peptide (SC-7049P, Santa Cruz Biotechnology), which was pre-mixed with CD38 antibody (1 antibody: 5 antibody-blocking peptide) and incubated overnight at 4 °C before used. As shown in Figure. 3.1A, CD38 was detected as a single band of approximately 45 kDa in the resolved protein samples of PA, the renal artery (RA), and the cerebral artery (CA). The signals were completely blocked by the blocking peptide, whereas the non-specific signals of 50 kDa were unaffected. The molecular size of CD38 detected in CA samples was slightly smaller compared to those in PA and RA, presumably due to differences in the post-translational modification of glycosylation and phosphorylation.

We further compared CD38 protein expression in different types of arteries, including the aorta (Aor), PA, mesenteric artery (MA), femoral artery (FA), tail artery

(TA), RA and CA, as well as in isolated PASMCs (Fig. 3.1B). Immunoblots were performed using protein samples from different arteries at the same time. PDVF membranes were stripped and reprobed for actin as a loading control for normalization. Clear signals of CD38 were detected in PA, RA, CA, and PASMCs, compared to the weaker signals in Aor, MA, FA, and TA, with a CD38 expression profile of CA>RA=PA>MA>Aor=FA=TA (Fig. 3.1C). qRT-PCR was performed to further examine CD38 mRNA expression in the different types of arteries (Fig. 3.1D). CD38 transcript levels were similar to the protein levels with the exception of a relatively high mRNA level in the aorta. These results indicate that CD38 are differentially expressed in different types of arteries, with very clear expression in PA and PASMCs.

Ang II-induced activation of CD38 contributes to PA contraction.

To determine the contribution of CD38 activity in vasoreactivity, we examined the Ang II-induced isometric contraction of endothelium-denuded rat PA in the presence of 20 mM nicotinamide (NA) for the inhibition of CD38 (Fig. 3.2). Application of 0.1 nM to 100 nM Ang II activated concentration-dependent contraction expressed as % K-induced maximum response. Preincubation of PA rings with 20 mM nicotinamide (NA) for 20 min significantly reduced the maximal response (control : 89.60±5.06%, n=7; nicotinamide: 44.07±4.55%, n=7, $p<0.01$) and increased the EC_{50} (control: 1.48±0.25 nM, n=7; 3.76±0.53 nM, n=7, $p<0.01$) as compared to the control (Fig. 3.2A). Moreover, preincubation with 50 μM ryanodine for the inhibition of RyRs also caused a reduction in Ang II-induced maximum vasoconstriction (E_{max}=61.43±15.59%, n=5, p=0.016) compared to the control (E_{max}=111.72±9.78%, n=5), even though it had no significant

effect on EC_{50} (Fig. 3.2B). Suppression of Ang II-induced PA contraction by NA and ryanodine suggests that CD38 may play an important role in Ang II-induced pulmonary vasoconstriction.

Ang II-induced Ca^{2+} release in PASMCs is mediated in part by CD38.

Previous studies have demonstrated that CD38 contributes to agonist-induced Ca^{2+} mobilization in different types of cells and tissues [120,168,172,312]. Hence, we characterized Ang II-induced Ca^{2+} mobilization to determine the involvement of CD38 dependent mechanisms in PASMCs. The Ang II-induced Ca^{2+} response was determined in PASMCs in the presence extracellular Ca^{2+}, or after Ca^{2+} containing external solution was exchanged with 1 mM EGTA containing Ca^{2+}-free Tyrode solution 100 seconds prior to Ang II application to minimize changes in SR Ca^{2+} stores (Fig. 3.3). Ang II at concentrations between 10 nM to 1μM elicited concentration-dependent increases in $[Ca^{2+}]_i$, which rose rapidly to the peak and returned to the baseline within 100 seconds. The differences between the baseline and the peak $[Ca^{2+}]_i$ ($\Delta[Ca^{2+}]_i$) induced by 10 nM, 100 nM, and 1 μM Ang II were 88.5±32.6 (n= 6), 405.6±51.3 (n=7), and 741.4±122.5 nM (n=6), respectively, in the presence of 2 mM Ca^{2+}; and 69.6±26 (n=6), 165.5±68 (n=7) and 418.6±126.4 nM (n=6), respectively, in the absence of extracellular Ca^{2+}. Ca^{2+} responses activated by 100 nM Ang II were significantly reduced after the removal of extracellular Ca^{2+} ($p=0.016$). These results clearly suggest that Ang II-induced Ca^{2+} responses consisted of both Ca^{2+} release and Ca^{2+} influx in PASMCs.

To further elucidate whether AICR is dependent on the cyclase activity of CD38, PASMCs were incubated for 20 min with the ADP-cyclase inhibitor NA before the

application of 100 nM Ang II under Ca^{2+}-free condition (Fig. 3.4). NA at concentrations between 2–20 mM had no significant effect on the basal $[Ca^{2+}]_i$ in PASMCs. The kinetics of AICR was similar in the presence of NA. In contrast, peak Ca^{2+} response to 100 nM Ang II was reduced by NA in a concentration-dependent manner, with maximum $\Delta[Ca^{2+}]_i$ equal to 469.9±60.2 (n=10), 375±65.8 (n=8, p=N.S.), 268.9±49.3 (n=8, p=0.007), 221.7±31.6 (n=9, P<0.001), and 152.9±28.6 nM (n=10, p<0.001) at 0, 2 , 5 , 10, and 20 mM NA respectively.

Knockdown of CD38 expression decreases AngII-induced Ca^{2+} release in PASMCs.

To clarify whether AICR is indeed mediated by activation of CD38 in PASMCs, we examined AICR in siRNA-transfected PASMCs. The efficiency of siRNA treatment was determined by Western blot (Fig. 3.5A). CD38 protein levels were significantly reduced, by 69.05±5.35%, in siRNA transfected PASMCs compared to those in scrambled sequence transfected control cells (p=0.006, n=5). The reduced CD38 expression was associated with attenuated AICR in the siRNA transfected PASMCs (Fig. 3.5B). The AICR peaks $\Delta[Ca^{2+}]_i$ were 1028±114.5 nM in control cells (n=10) and 552.6±103.1 nM in CD38 siRNA (n=8)(p=0.003). Moreover, the significant reduction of AICR caused by 20 mM NA in the scrambled sequence transfected cells (637.8±119.2 nM, n=8, p=0.012) was not observed in the CD38 siRNA transfected PASMCs (574.6±71.9 nM, n=8). Accordingly, the proportion of the reduction in the peak $\Delta[Ca^{2+}]_i$ by 20 mM NA was 37.96±11.59% in the control group, and -3.97±13.02% in CD38 siRNA transfected PASMCs (p=0.031). These results provide direct evidence that AICR is mediated, in part, through CD38 activation in PASMCs.

AICR in PASMCs is mediated in part by the cADPR-RyRs and NAADP-TPCs pathway.

The cyclase activity of CD38 generates cADPR, which causes Ca^{2+} release via RyRs on the ER/SR in various types of cells, including vascular smooth muscle cells [100,141]. To examine the role of the cADPR-RyRs pathway in PASMCs, we determined the effects of the specific cADPR antagonist 8-Br-cADPR and ryanodine on the AICR in PASMCs (Fig. 3.6). Preincubation of PASMCs with various concentrations of 8-Bromo-cADPR for 20 min had no effect on the basal $[Ca^{2+}]_i$, but it caused significant reductions in the AICR peaks. The peaks $\Delta[Ca^{2+}]_I$ elicited by 100 nM Ang II were 333.5±32.2 (n=9), 234.2±31.3 (n=6, p=0.026), 198.3±24.4 (n=7, p=0.002), 185.3±26.5 (n=9, p<0.001), and 190.8±26.3 nM (n= 9, p<0.001) at 0, 0.1, 1, 10, and 100 μM 8-Br-cADPR, respectively (Fig. 3.6A). An apparent maximum inhibition of 40–50% of the control response was reached at 1 μM 8-Bromo-cADPR. Moreover, inhibition of RyRs by 50 μM ryanodine reduced the peak AICR from 299.5±57.3 to 125.4±21.1nM (n=9, p=0.034) (Fig. 3.6B). Hence, our data clearly suggest that Ang II-induced increases in $[Ca^{2+}]_i$ are mediated in part through the activation of ryanodine receptors by cADPR in PASMCs.

In addition to the cADPR-RyRs pathway, CD38 is responsible for Ca^{2+} mobilization through the activation of catalase, which generates NAADP targeting the two-pore channels (TPCs) that gate the endolysosomal Ca^{2+} stores [117]. To evaluate the contribution of the NAADP-lysosomal Ca^{2+} pathways, we have examined AICR in the presence of the specific NAADP antagonist Ned-19. Our previous study showed that 1 μM Ned-19 significantly inhibited intracellular Ca^{2+} release induced by membrane permeable NAADP-AM in PASMCs [114]. Preincubation of PASMCs with 1 μM Ned-

19 for 20 min significantly reduced the peak Ca^{2+} response induced by 100 nM Ang II from 186.9±44 to 67.6±14.8nM (n=9, p=0.021) (Fig. 3.7A). Moreover, 3μM bafilomycin A1(Baf A1), which blocks the vacuolar-type H^+-ATPase and disrupts the lysosomal proton gradient for Ca^{2+} uptake by the H^+-Ca^{2+} exchanger [313,314], significantly suppressed AICR (control: 299.5±57.3nM, n=9; Baf A1: 125.4±21.1nM, n=8, p=0.014) (Fig. 3.7B). These results suggest that NAADP-mediated Ca^{2+} release from endolysosomal stores also contributes significantly to the Ang II induced Ca^{2+} response in PASMCs.

CD38-dependent cADPR-RyRs and NAADP-lysosome pathways may operate independently or interdependently to facilitate Ang II induced Ca^{2+} mobilization. Our previous study provided evidence that Ca^{2+} release from NAADP-sensitive stores is amplified by cross-activation of Ca^{2+} release from RyRs-gated Ca^{2+} stores in PASMCs [114]. This possibility was examined by inhibiting both pathways with 10 μM 8-Br-cADPR and 1 μM Ned-19. The combined inhibitory effect of 8-Br-cADPR and Ned-19 (peak $\Delta [Ca^{2+}]_i$: control=330.4±40.8nM, n=12; 8-Br-cADPR+Ned-19=157.7±19.5nM, n=10, P=0.002) was similar to 8-Br-cADPR or Ned-19 alone, indicating that the effects of two inhibitors are non-additive (Fig. 3.7C). These results suggest that the two Ca^{2+} release pathways operate inter-dependently for AICR in PASMCs.

Ang II-induced CD38 activation is mediated by NADPH oxidase-dependent pathways in PASMC.

We further examined whether Ang II-induced CD38 activation is mediated by the PKC-NOX pathway (Fig. 3.8). Preincubation of PASMCs with the PKC inhibitor

staurosporine (STAS, 10 nM) for 20 min significantly reduced the peak Ca^{2+} response induced by 100 nM Ang II from 332.9±30.9 nM (n=8) to 204.7±34.3 nM (n=9, p=0.019). The addition of 20 mM NA to inhibit CD38 did not cause further reduction in the AICR (STAS+NA: 163.7±37.2 nM, n=10, p=0.432) (Fig. 3.8A). These results imply that activation of PKC is an upstream step in the signaling pathway for Ang II-induced CD38 activation.

To determine the contribution of NOX in Ang II-induced CD38 activation, AICR was measured in the absence or presence of the NOX inhibitors apocynin (APC) and diphenyleneiodonium (DPI). The peak Ca^{2+} response elicited by Ang II was significantly reduced by 30 μM APC (control: 304±56.9 nM, n=5; APC: 96.7±25.1 nM, n=6, p<0.001). Inhibition of CD38 by NA in the presence of APC did not lead to any additional decrease in AICR (APC+NA: 111.4±18.1nM, n=6, P=0.002) (Fig. 3.8B). Additionally, Ang II-induced peak Ca^{2+} was significantly reduced by 30 μM DPI (control: 333±30.9 nM, n=8; DPI: 205.7±34.3 nM, n=9, p=0.019). Likewise, NA did not lead to an additional decrease in AICR after inhibition of NOX by DPI (DPI+NA: 164±37.2 nM, n=10, p=0.003) (Fig. 3.8C). These results suggest that Ang II-induced CD38 activation is mediated by activation of NOX.

Furthermore, AICR was examined in the presence of the superoxide scavenger TEMPOL (TEMP). Preincubation of PASMCs with 100 μM TEMP caused a significant reduction in AICR (control: 227.6±33.9 nM, n= 8; TEMP: 120.5±18.4nM, n=9, p=0.007), but the addition of NA did not cause further reduction in the response (TEMP+NA: 92.7±22.4 nM, n=9, p=0.001) (Fig. 3.8D). These data indicate that Ang II-induced activation of CD38 is mediated by ROS produced by NOX.

Ang II-induced activation of CD38 is specifically mediated by NOX2.

To further examine the involvement of specific NOX subtypes in Ang II-mediated CD38 activation, we tested AICR in the presence of the small molecule NOX inhibitor VAS2870, the NOX1 specific antagonist ML171, and gp91ds-tat, a specific inhibitory peptide targeting NOX2. 30 μM VAS2870 had no significant effect on AICR (control: 275±38.9 nM, n=10; VAS2870: 248±49.5 nM, n=10, p=N.S.) (Fig. 3.9A); likewise, 2 μM ML171 did not suppress AICR (control: 326±51.3 nM, n=6; ML171: 315±61.4 nM, n=6, p=N.S.) in PASMCs (Fig. 3.9B).

In contrast, the pretreatment of PASMCs with 10μM gp91ds-tat caused significant reduction in the peak Ca^{2+} response (control: 364.6±38.7 nM, n=13; gp91ds-tat: 252.4±24.9 nM, n=13, p=0.045). Furthermore, there was no significant difference in the AICR between the gp91ds-tat and gp91ds-tat+NA treated cells (206.5±44.7 nM, n= 8, p=0.018). These results suggest that Ang II-induced CD38-dependent Ca^{2+} release is mediated primarily by the activation of NOX2 (Fig. 3.9C). In summary, these results suggest that Ang II activates CD38 through the PKC-dependent activation of ROS production from NOX2.

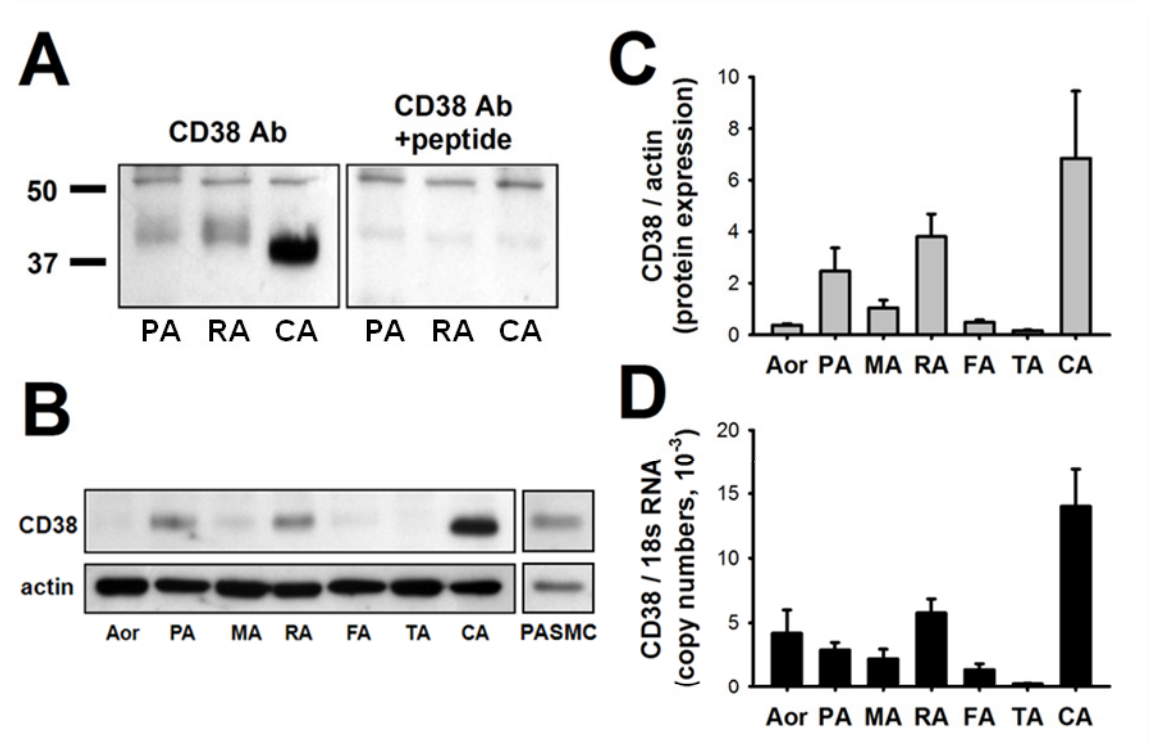

Figure 3.1. CD38 expression in rat pulmonary artery, systemic arteries and PASMCs. (A) Verification of the specificity of CD38 antibody in samples of pulmonary artery (PA), renal artery (RA), and cerebral artery (CA) with (right panel) and without (left panel) pretreatment of the antibody with a blocking peptide. (B) An immunoblot of CD38 from samples of aorta, PA, mesenteric (MA), renal (RA), femoral (FA), tail (TA) and CA arteries. (C) Averaged normalized CD38 protein level in various arteries using β-actin for normalization (n=5). (D) Quantitative real-time polymerase chain reaction of CD38 mRNA expression from different vascular smooth muscle tissues. The data are normalized with 18S RNA (n=5).

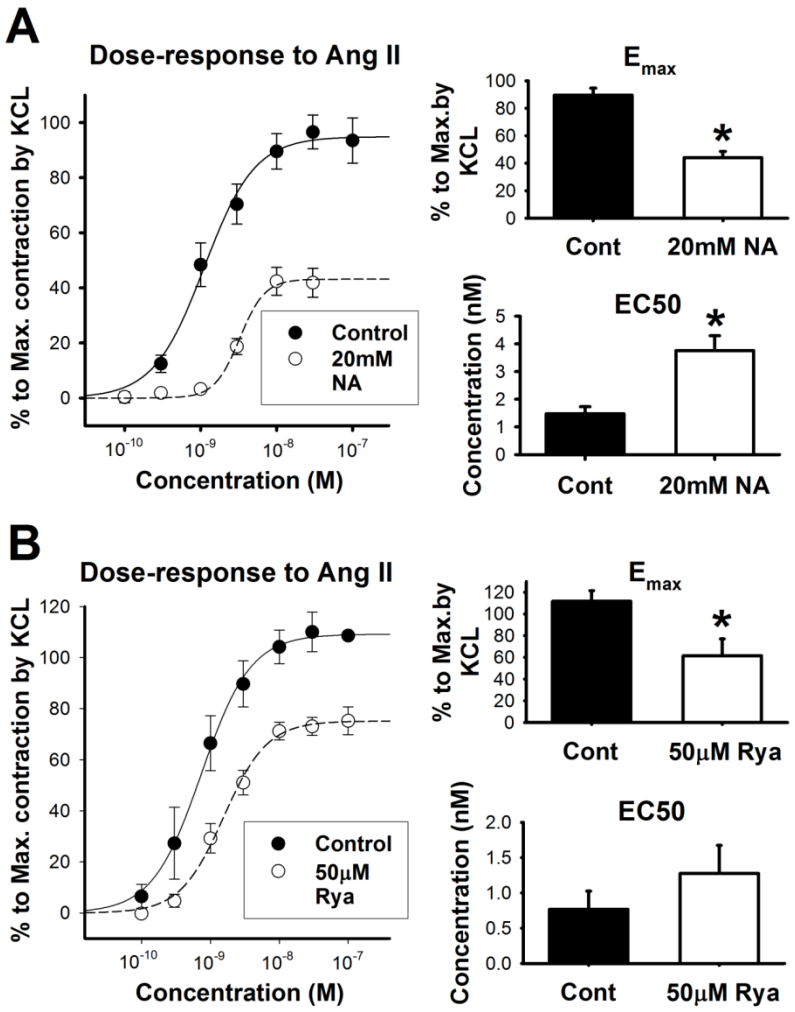

Figure 3.2. Inhibition of Ang II-induced isometric contraction of PA by nicotinamide and ryanodine. (A) Concentration-dependent curves of Ang II-induced PA contraction in the presence or absence of 20 mM nicotinamide (n=7, Left panel). Mean maximum contractile force (E_{max}, right upper panel) and EC_{50} (right-bottom panel) values of Ang II concentration-response curves. Asterisk (*) indicates significant difference compared to the untreated control ($p<0.001$, n=7). (B) Concentration-dependent curves of Ang II-induced PA contraction in the presence or absence of 50 μM ryanodine (n=5)(Left panel). E_{max} (right upper panel) and EC_{50} (right-bottom panel) values of Ang II concentration-response curves. * indicates significant inhibition by ryanodine compared to the untreated control ($p=0.016$, n=5). EC_{50} was not significantly increased in the ryanodine treated group ($p=0.311$).

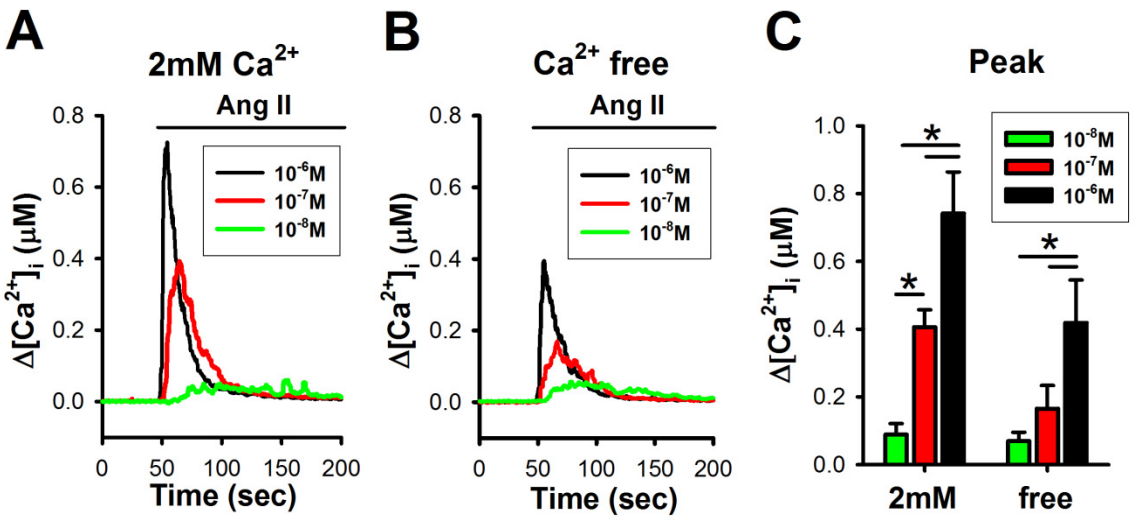

Figure 3.3. Concentration-dependent increase in $[Ca^{2+}]_i$ activated by Ang II in rat PASMCs. **(A and B)** Average Ca^{2+} transient ($\Delta[Ca^{2+}]_i$) activated by different concentrations of Ang II (10 nM, 100 nM and 1 μM) in the presence (2 mM Ca^{2+}) or absence (containing 1mM EGTA) of extracellular Ca^{2+}. (C) The average increase (Δ peak, right panel) in $[Ca^{2+}]_i$ induced by different concentrations of Ang II.

* indicates significant difference between the groups (n=6-7, $p<0.05$)

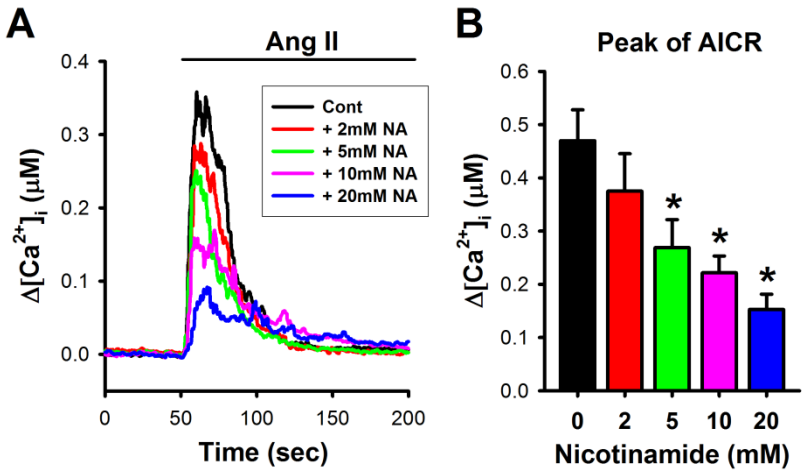

Figure 3.4. Inhibition of AICR by different concentrations of nicotinamide in PASMCs (A) Averaged traces of Ang II-induced Ca^{2+} transients elicited 100 seconds after removal of Ca^{2+} in the absence or presence of different concentrations (2 mM, 5 mM, 10 mM, and 20 mM) of the CD38 inhibitor nicotinamide. (B) Averaged peak change in $[Ca^{2+}]_i$ in the various groups. * indicates significant differences when compared to the control (5 mM, $p=0.007$; 10 mM, $p<0.001$; and 20 mM, $p<0.001$) (n=8–10).

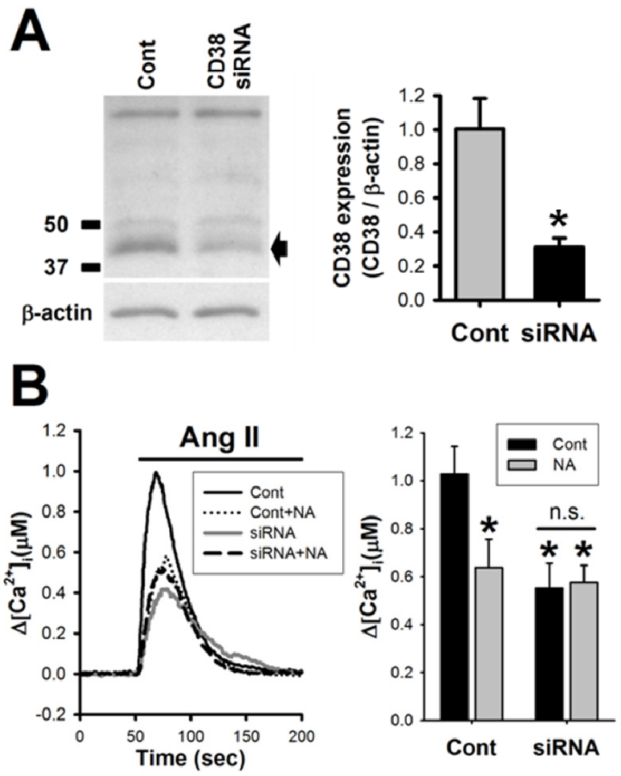

Figure 3.5. Effect of siRNA mediated suppression of CD38 expression on AICR in PASMCs. (A) Left panel shows an immunoblot of CD38 from samples of PASMCs transfected with a CD38-targeting siRNA and a control scrambled sequence. Right panel shows the mean CD38 expression data from the two groups after normalization with β-actin (n=5). * indicates significant decrease in expression compared to the scramble control (p=0.006). Note that there was no change in the pattern of the non-specific band between the scrambled control and the CD38 siRNA-transfected cells on the blot. (B) Left panel shows the mean traces of AICR in the transfected PASMCs in the absence or presence of 20 mM nicotinamide (NA). Right panel shows the mean peak $\Delta[Ca^{2+}]_i$ in the control scrambled sequence and CD38 siRNA transfected PASMCs in the absence or presence of 20 mM NA. n equals 8 for each group. * indicate significant difference from the control group in the absence of NA, and n.s. indicates no significant difference between the groups indicated.

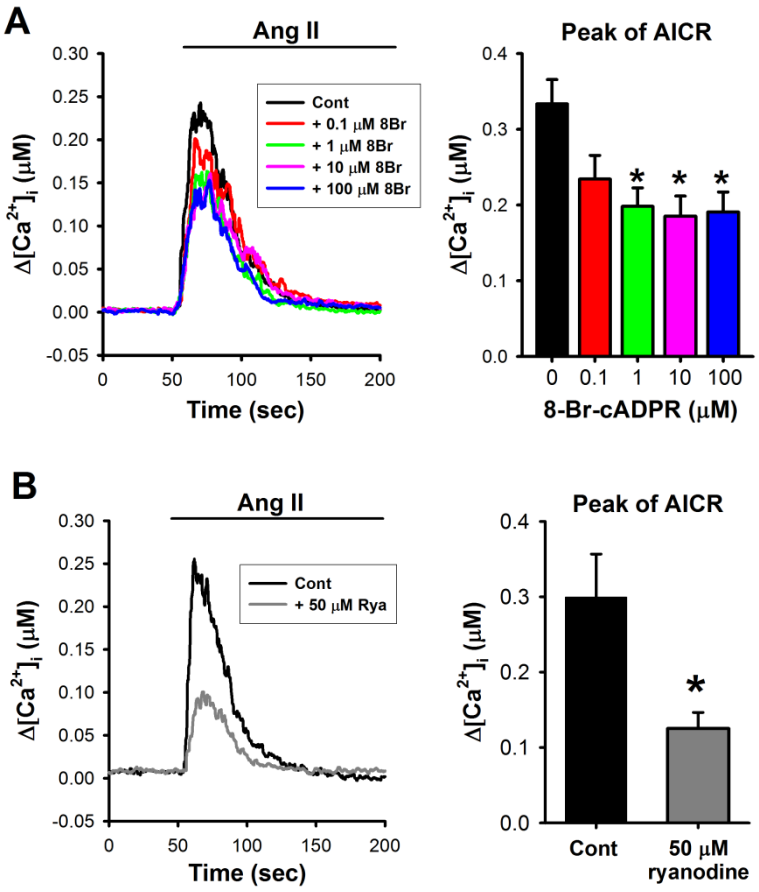

Figure 3.6. Effect of inhibition of cADPR-dependent Ca^{2+} release on AICR in PASMCs. (A) Left panel shows mean traces of Ang II-induced changes in $[Ca^{2+}]_i$ in the absence or presence of different concentrations of the cADPR antagonist 8-Br-cADPR. Right panel shows the mean data from each group. * indicates significant difference from control, 1μM (p=0.002), 10μM (p<0.001) and 100μM (p<0.001)(n=6-9). (B) Left panel shows Ang II-induced changes in $[Ca^{2+}]_i$ in the absence or presence of 50μM ryanodine. Preincubation with ryanodine significantly decreased AICR (n=9, p=0.034).

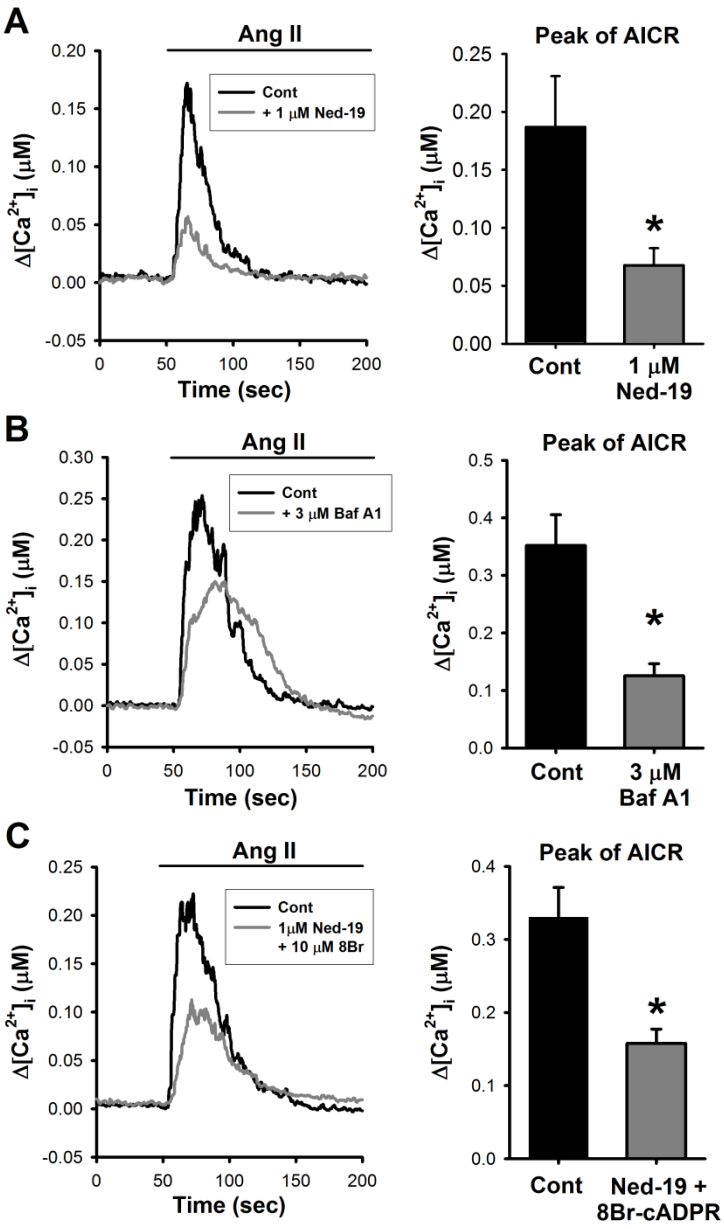

Figure 3.7 Effect of inhibition of NAADP-dependent pathway on AICR in PASMCs. (A) Left panel shows the mean traces of Ang II-induced changes in $[Ca^{2+}]_i$ in the absence or presence of the NAADP antagonist Ned-19 (1μM). Right panel shows the peak change in $[Ca^{2+}]_i$ in each group (n=9, p=0.021). (B) AICR in PASMCs with or without preincubation with the vacuolar H+-ATPase blocker Bafilomycin A1 (3μM)(n=8~9, p=0.014). (C) AICR in PASMCs with or without treated with both 8-Br-cADPR (10μM) and Ned-19 (1 μM) (n=10–12, p=0.002). * indicates significant difference from the control.

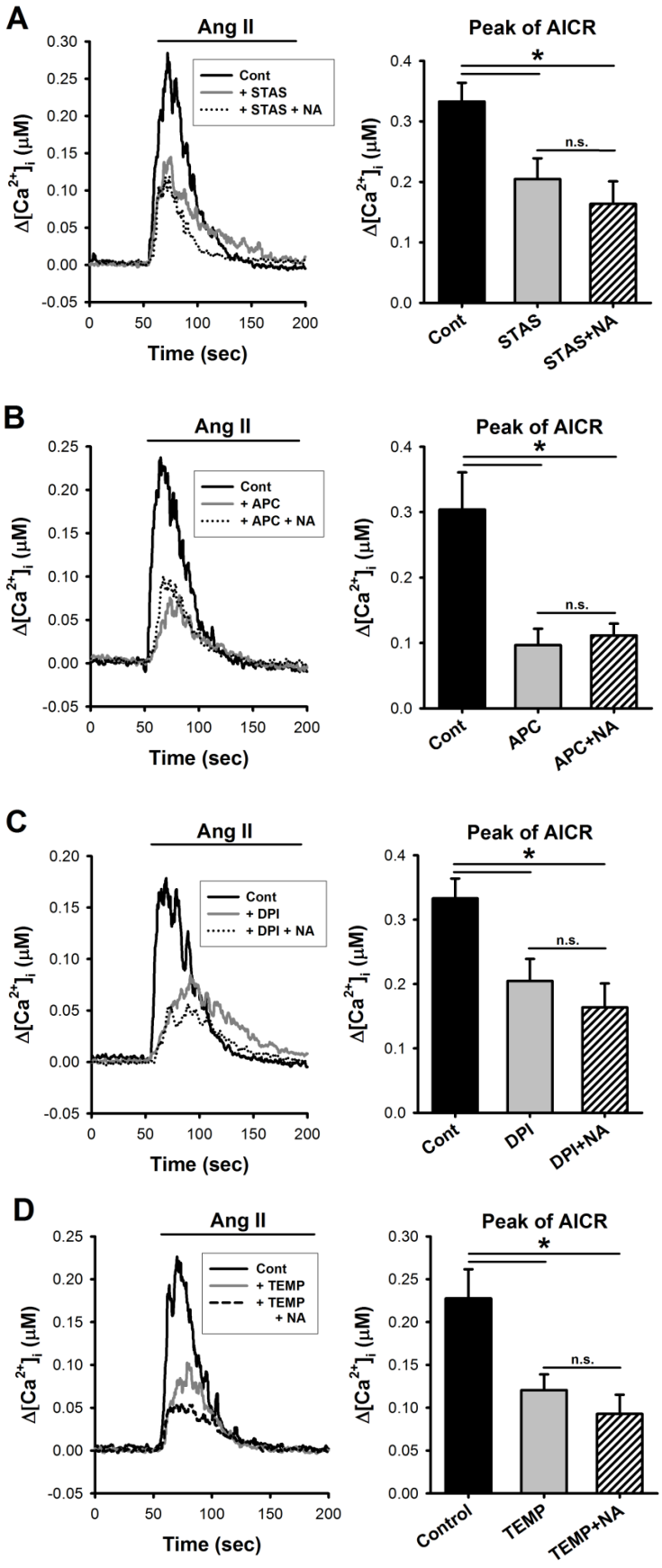
A
Ang II
Cont
+ STAS
+ STAS + NA
Δ[Ca2+]i (μM)
Time (sec)
Peak of AICR
*
n.s.
Cont
STAS
STAS+NA
B
Ang II
Cont
+ APC
+ APC + NA
Δ[Ca2+]i (μM)
Time (sec)
Peak of AICR
*
n.s.
Cont
APC
APC+NA
C
Ang II
Cont
+ DPI
+ DPI + NA
Δ[Ca2+]i (μM)
Time (sec)
Peak of AICR
*
n.s.
Cont
DPI
DPI+NA
D
Ang II
Cont
+ TEMP
+ TEMP
+ NA
Δ[Ca2+]i (μM)
Time (sec)
Peak of AICR
*
n.s.
Control
TEMP
TEMP+NA

Figure 3.8 PKC-NOX dependent activation of CD38 in PASMCs. (A) The effect of PKC inhibition with staurosporine (STAS, 10 nM) on AICR in PASMCs. Left panel shows the mean traces of AICR in the absence or presence of STAS and STAS+NA (20 mM). Right panel shows the mean peak $\Delta[Ca^{2+}]_i$ in the control (n=8), STAS (n=9, p=0.019), and STAS+NA (n=10, p=0.002) treated group. Note that there was no additional reduction of $\Delta[Ca^{2+}]_i$ in the STAS+NA group. (B and C) The effect of the NOX inhibitor apocynin (APC, 30μM) and diphenyleneiodonium (DPI, 30μM) on AICR in PASMCs. * indicates significant inhibition of AICR by APC (n=6, $p<0.001$) and APC+NA (n=6, p=0.002) compared to control (n=5). There was no significant difference between APC and APC+NA treated cells. Likewise, there was significant inhibition of AICR by DPI (n=9, p=0.019) and DPI+NA (n=10, p=0.003) compared to the control (n=8), while no significant difference between APC and APC+NA treated cells was observed. (D) The effect of the ROS scavenger tempol (TEMP, 100 μM) on AICR Preincubation of TEMP (n=9, p=0.007) and TEMP+NA^+ (n=9, p=0.001), showing a significant reduction in AICR, whereas there was no additional inhibition of AICR in cells treated with the two inhibitor.

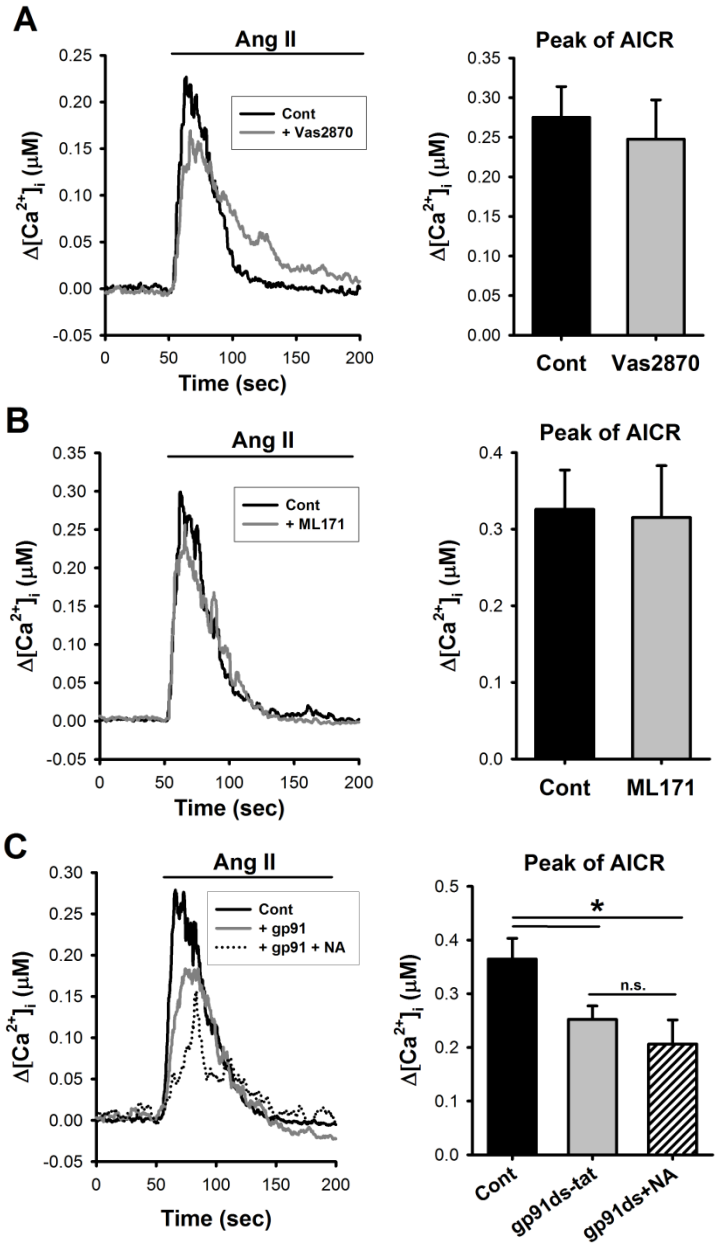

Figure 3.9. The effects of NOX1 and NOX2 specific antagonist on AICR in PASMCs
(A and B) The effect of the NOX1 specific inhibitor VAS2870 (30μM) and ML171 (30μM) on AICR in PASMCs. Treatment of the specific NOX inhibitors VAS2870 (n=10) and ML171 (n=6) failed to decrease AICR. (C) The effects of the NOX2 specific peptide inhibitor gp91ds-tat (10μM) on AICR in PASMCs. There was a significant reduction in AICR with gp91ds-tat (n=13, p=0.045) and gp91ds-tat+NA (n=8, p=0.018) treated cells compared to the untreated control. There was no significant different between gp91ds-tat and gp91ds-tat+NA cells.

Discussion

CD38, through its multifunctional enzymatic activities, generates cADPR and NAADP, which contribute to a wide variety of physiologic responses, such as egg fertilization [315], vascular smooth muscle contraction [316], insulin secretion [302,317], and the asthmatic phenotype in smooth muscle airways [175]. In the present study, we found that the expression level of CD38 protein and mRNA in PA smooth muscle is relatively higher compared to other vascular smooth muscles. Ang II evokes vasoconstriction in PA smooth muscle and induces intracellular Ca^{2+} release in part through both the cADPR- and NAADP-dependent pathways by activating CD38 in PASMCs. Furthermore, Ang II induces CD38 activation through the PKC-dependent activation of NOX2 in PASMCs. These results provide clear evidence that CD38 is a potent regulator of Ca^{2+} homeostasis in pulmonary vasculature and establish the signaling pathway for AICR in PASMCs.

CD38 expression has been reported in various types of arteries including systemic arteries and PA [122,186,187,188,191,196]. Comparing CD38 expression in different arteries, we found that CD38 protein levels vary greatly in different vascular smooth muscle tissues, with the highest level in the cerebral artery, followed by the PA and renal arteries; whereas the expression in the aorta, mesenteric artery, femoral artery, and tail artery are minimal. These observations indicate that CD38 contributes quite differently to the physiological functions of various vasculatures. The functions of CD38 have not been examined in cerebral arteries; however, they are well characterized in renal arteries and arterioles [120,192,197,298,305,316]. It has been shown that CD38-dependent pathways mediate significant changes in cytosolic $[Ca^{2+}]_i$ and contractile functions in renal afferent

arteries and arterioles, and can account for more than 50% of the contractile response during Ang II, ET-1 and NE stimulation [197]. Comparable expressions of CD38 protein in PA and renal arteries suggest that CD38 may play a similarly significant role in pulmonary vasculatures.

The important contribution of CD38-dependent pathways in Ca^{2+} signaling in pulmonary vasculature is clearly evident in this study of AICR in PASMCs. Removal of extracellular Ca^{2+} revealed that about 50% of the Ca^{2+} response is mediated by intracellular Ca^{2+} release, implying that Ang II-induced Ca^{2+} mobilization is composed of extracellular Ca^{2+} influx and intracellular Ca^{2+} release. When focusing on the mechanism of Ca^{2+} release in PASMCs, both pharmacological inhibition of CD38 with NA and genetic suppression with CD38 siRNA proved to cause significant inhibition of AICR, indicating the participation of CD38 in the Ca^{2+} release process. The specificity of the inhibitory effect of NA was verified under our experimental conditions, as NA did not cause further reduction of AICR in CD38 siRNA-transfected cells. Moreover, nicotinamide caused significant reduction in the sensitivity, and 60% reduction in the maximal contraction, induced by Ang II in isolated PAs. This further suggests a significant contribution of CD38 in pulmonary vascular reactivity.

AICR in PASMCs is mediated in part by the cADPR-dependent Ca^{2+} release from RyR-gated stores and by the NAADP-dependent Ca^{2+} release from the acidic endolysosomes. Antagonism of cADPR with the 8-bromo-cADPR [318] and inhibition of RyRs with ryanodine were each effective in suppressing AICR. Inhibition of NAADP with its specific antagonist Ned-19 [319], or depleting endolysosomal Ca^{2+} stores by disrupting the H^+ gradient for H^+-Ca^{2+} exchange with the vacuolar H^+-ATPase inhibitor

Baf A1 [320], also reduced AICR. These results suggest that Ang II stimulates both the cyclase and catalase activities of CD38 for the production of cADPR and NAADP, respectively.

It is interesting to note that the cADPR- and NAADP-dependent mechanisms operate interdependently during AICR because the suppression of AICR by co-inhibition of cADPR and NAADP remain comparable to the inhibition of either cADPR or NAADP alone. These results are consistent with previous findings including ours on the cross-activation of RyRs by NAADP-mediated Ca^{2+} release in PASMCs [114,121,200], implying that NAADP-channels are coupled with Ca^{2+} release via RyRs, and that cADPR may sensitize RyRs for the cross-activation by Ca^{2+}-induced Ca^{2+} release under physiological stimulation. The remaining AICR in PASMCs, after co-inhibition of cADPR and NAADP, was likely due to IP_3R-gated Ca^{2+} release mediated by the well-recognized PLC-IP_3 pathway of angiotensin receptors [321,322].

An increasing amount of evidence suggests that Ang II enhances ROS production through the activation of NOX, contributing to the Ca^{2+} response in vascular smooth muscle cells [323]. Several studies have demonstrated that CD38 activity is regulated by redox-state and oxidative stress [191,194,309,324,325]. However, the mechanism of Ang II-induced CD38 activation in PASMCs has not been established. This study demonstrates that Ang II activates CD38 in PASMCs via ROS generation by NOX. This is based on the finding that AICR, which is mediated by the activation of CD38, was inhibited significantly by the NOX inhibitors APC and DPI, and the ROS scavenger TEMPOL. Inhibition of CD38 with NA in the presence of the NOX inhibitors or the ROS scavenger did not further suppress the Ang II-induced Ca^{2+} response in PASMCs,

suggesting that ROS plays a pivotal role in the activation of CD38 in PASMCs. These observations are consistent with findings on renal afferent arterioles and cardiac myocytes that Ang II stimulates NOX to generate ROS, leading to enhanced ADP-ribosyl cyclase activity [305,326].

There are five NOX homologues (NOX1–5) with different subunit compositions and localizations [323,327]. It has been reported that Ang II-induced ROS production in vascular smooth muscle cells from large arteries is mediated by NOX1 [328] and, in resistance arteries, is mainly depend on NOX2 [307]. NOX1 and NOX2 can be activated through Rac1 [323,327,329]. It has been shown that ET-1 stimulates Rac1-NOX1-dependent ROS production to activate CD38 in coronary arteries [329]. NOX2 can also be activated by PKC dependent phosphorylation of p47phox to facilitate the assembly of the oxidase complex [323]. We found that preincubation of PASMCs with specific NOX1 inhibitors ML171 [330] and VAS2870 [331] had no significant inhibitory effect on AICR. In contrast, the NOX2 specific peptide inhibitor gp91ds-tat caused a significant decrease in AICR but no further reduction with inhibition of CD38 by NA, indicating that the Ang II-induced activation of CD38 is specifically mediated by NOX2. Moreover, inhibition of PKC with STAS also suppressed AICR. These results, therefore, are consistent with Ang II-induced CD38 activation through the PKC-NOX2-ROS pathway to elicit Ca^{2+} release in PASMCs.

In this study, NA was used as a CD38 inhibitor. Although NA may have other non-specific effects, NA has been widely used and accepted for the purpose of CD38 inhibition in previous as well as recent studies [167,298,332]. Since the activity of CD38 is dependent on the substrate NAD^+, high concentration of the NAD^+ analog operates as a

competitive antagonist to inhibit the CD38 enzyme activity. In fact, recent studies on novel CD38 inhibitors have continuously designed analogs, which are structurally derived from NAD^+ [333]. Despite the high concentration used in this study, the cell morphology and resting $[Ca^{2+}]_i$ were not altered in the presence of NA during Ca^{2+} imaging experiment, indicating that NA does not cause significant disturbance in Ca^{2+} homeostasis. A recent study demonstrated that apigenin, a flavonoid, is a specific inhibitor for NADase activity of CD38 *in vivo* [334]. However, apigenin could not applicable for AICR measurement due to its toxicity during the preincubation. Nonetheless, NA could not cause additional reduction in AICR when CD38 was knockdown by siRNA suggesting that NA is useful tool in our research on CD38 dependent Ca^{2+} release in PASMC.

In conclusion, this study systematically characterized the mechanism of Ca^{2+} release induced by Ang II in PASMCs and demonstrated that it is in part mediated by CD38 activation through NOX2-dependent ROS production, leading to the synergistic Ca^{2+} release from cADPR- and NAADP-gated Ca^{2+} stores. These findings, hence, provide the evidence to support a critical role for CD38 in Ca^{2+} signaling of pulmonary vasculature.

Acknowledgement

This research was supported by R01 HL071835 and R01 HL075134National Institutes of Health.

CHAPTER 4

CHRONIC HYPOXIA REGULATES THE EXPRESSION AND ACTIVITY OF CD38 IN RAT PULMONARY ARTERIAL SMOOTH MUSCLE CELL

Abstract

The pathophysiological changes in chronic hypoxia-induced pulmonary hypertension (CHPH) are multi-factorial and complex. Accumulating evidence suggests a role for aberrant alterations in the regulation of intracellular Ca^{2+} of pulmonary arterial smooth muscle cells (PASMCs). Previous studies have reported elevation of $[Ca^{2+}]_i$ in PASMCs due to enhanced Ca^{2+} influx in CHPH, but the changes of intracellular Ca^{2+} release under chronic hypoxia (CH) have not been examined. This study characterized the CH-induced alterations in the expression and functions of CD38, a multi-functional enzyme that produces the Ca^{2+} mobilizing messengers cyclic ADP-ribose and nicotinic acid adenine dinucleotide phosphate in PASMCs. The expression of CD38 protein and mRNA were both significantly upregulated in the PA smooth muscle of CH rats. This upregulation of CD38 in PA of CH rats was time-dependent, observed after 3–7 days of hypoxic exposure and declining after 3 weeks of CH. NADase activity of CD38 in PA smooth muscle was significantly increased, whereas the same activity in whole lung was decreased after 1-week hypoxia, suggesting specific CD38 upregulation in hypoxic PA. Angiotensin II-induced Ca^{2+} release (AICR), which is mediated in part by CD38, was significantly increased in PASMCs isolated from CH rats. The difference between AICR in PASMCs of normoxic and 1-week CH rats was completely abolished by the CD38 inhibitor nicotinamide. The CH-induced upregulation of CD38 expression and activity were due to the direct effect of hypoxia on PASMCs. *In vitro* exposure of PASMCs from normoxic rats to hypoxia for 3 days caused significant increase in CD38 expression and enhancement in AICR, which was equalized by nicotinamide. Sequence analysis of the putative promoter region of CD38 gene found multiple putative binding motifs of nuclear

factor of activated T-cells (NFAT). CH-induced upregulation of CD38 expression in isolated PASMCs was inhibited by the specific NFAT-inhibitor VIVIT and the calcineurin inhibitor cyclosporine A, indicating that CH-induced CD38 upregulation in PASMCs is mediated by the calcineurin/NFAT-pathway. Moreover, the expressions of the NAADP-sensitive channels (TPC1 and TPC2) were significantly increased in the PA smooth muscle of CH rat. All these results clearly indicate that CH has a profound effect on CD38-dependent mechanisms that may play crucial roles in the alterations of Ca^{2+} homeostasis in PASMCs.

Introduction

Chronic alveolar hypoxia (CH), as occur in high altitude inhabitants or patients with chronic pulmonary diseases such as COPD, triggers the development of pulmonary hypertension (PH). CH-induced pulmonary hypertension (CHPH) is characterized by increased vascular tone, altered vasoreactivity, and profound vascular remodeling, leading to an increase in pulmonary vascular resistance, right heart hypertrophy and eventually right heart failure [335,336,337]. The mechanism for the pathogenesis of CHPH is complex and multifactorial [338], but many of the pathophysiological changes in the pulmonary vasculature in CHPH is clearly associated with the alteration in Ca^{2+} homeostasis of pulmonary arterial smooth muscle cells (PASMCs) [238,239]. It is well recognized that CH leads to the elevation of cytoplasmic $[Ca^{2+}]_i$ in PASMCs via many different mechanisms; for example, downregulation of voltage-gated K^+ (K_v) channels [66,70,247,339], enhanced Ca^{2+} entry mediated through upregulation of store-operated Ca^{2+} entry (SOCE) [52,238,265,279], receptor-operated Ca^{2+} entry [38,238,340],

mechanosensitive cation channels [37,39], acid-sensing ion channels (ASIC) [278,279,280], voltage-dependent Ca^{2+} channels (VDCC) [35,276], and Ca^{2+}-activated Cl^- channels [75]. However, there is very limited information on the effects of CH on intracellular Ca^{2+} release pathways in PASMCs.

CD38 is a multifunctional enzyme, that syntheses the Ca^{2+} mobilization second messenger cADPR and NAADP, which are endogenous ligands of ryanodine receptors (RyRs) of sarcoplasmic reticulum and NAADP-sensitive channels of endolysosomes, respectively [144,341]. Hence, it plays important roles in regulating intracellular Ca^{2+} release. Moreover, Ca^{2+} release from RyRs may further enhance Ca^{2+} influx by initiating SOCE [342,343], and activating Ca^{2+}-activated Cl^- channels (CaCC) to cause membrane depolarization and activation of VDCC [74,76]. However, only few studies provided evidence that CD38 plays a role in $[Ca^{2+}]_i$ regulation in response to hypoxia in PASMCs. Previous studies had shown that acute hypoxia promotes accumulation of cADPR causing Ca^{2+} release from RyR-gated Ca^{2+} stores to initiate pulmonary vasoconstriction [191,324]. Indeed, it has been proposed that CD38 acts as a redox sensor for HPV. A reduction of β-NAD^+:β-NADH ratio during hypoxia stimulates cyclase activity and inhibits hydrolase activity of CD38, leading to the accumulation of cADPR to cause intracellular Ca^{2+} release. However, this hypothesis is challenged by a recent study which showed that HPV in isolated PAs requires neither cADPR- nor NAADP-dependent Ca^{2+} release in the absence of preconstriction, but rather is mediated by SOCE independent of CD38 mediated Ca^{2+} release [290]. Besides these studies, there is no published record on the regulation of CD38 expression and activity by CH in PASMCs.

In this study, we tested the hypothesis that CD38-dependent mechanisms play a crucial role in the alterations of Ca^{2+} homeostasis in PAs and PASMCs of CH rats. We examined CD38 expression and the CD38-dependent angiotensin II (Ang II) induced Ca^{2+} release (AICR) in PAs of CH rats and hypoxic PASMCs, as well as the transcriptional regulation of CD38 by CH. Furthermore, we examined the expression of the NAADP-sensitive channels (two-pore channels, TPC1 and TRPC2) in PAs of CH rats, as to understand the regulation of Ca^{2+} release mediated by CD38 under CH.

Methods

Animal care All animal procedures were compliant with the Guide for the Care and Use of Laboratory Animals published by the United States National Institutes of Health and was approved by the Johns Hopkins University Animal Care and Use Committee. Male Wistar rats (150–200g) were commercially purchased from Harlan laboratories.

Hypoxia exposure Adult male rats were placed in hypoxic chamber (10% O_2) for maximum 3–4 weeks (wk) as described previously [344]. Hypoxic air, a mixture of N_2 and room air, was continuously flushed into chamber. O_2 concentration in the chamber was continuously monitored. Food and water were replenished two times a week. PA tissues were harvested at different time-point based on the experimental protocol. Isolated PASMCs from hypoxic rats were placed in a modular incubation chamber (Billups-Rothenberg Inc.) filled with 4% O_2 hypoxic air. PASMCs from normoxic rat were cultured under 2% O_2 for 3 days to induce the hypoxic response.

Preparation of rat PA tissues and PASMCs Intralobar PA tissues and PASMCs were isolated as described in Chapter II. Briefly, rats were anesthetized using sodium

pentobarbital (130 mg/kg intraperitoneally) and the second to the fourth generations (800 to 300 μm) of intralobar PA were harvested in HEPES-buffer. After endothelium-denudation, PASMCs were enzymatically digested and cultured in HAM's F-12 media overnight. PASMCs were platted on 25 mm glass cover slips and transiently cultured for 12–18 hours before the Ca^{2+} fluorescence experiments. PASMCs were cultured in Smooth muscle Cell Basal Medium (#CC-3181, Lonza, MD) with 5% FBS and antibiotics for 3 days after overnight incubation with HAM's F-12 media for protein and mRNA determination.

Western blot Total protein was isolated from PA tissues and cultured PASMCs for Western blot analysis of CD38 expression as previously described in Chapter II. Briefly, tissue and cell lysates were resolved by 10% polyacrylamide gel and transferred to PVDF transfer membrane using a tank system filled with transfer buffer. After blocking, the membrane was incubated with primary antibodies diluted in 3% BSA-PBST at 4 °C overnight. The primary antibody for CD38 was diluted by 1:500 (#SC-7049, goat, Santa Cruz Biotechnology, Inc.), TPC1 by 1:500 (#ab80961, rabbit, Abcam), TPC 2 by 1:2,500 (#ACC-072, rabbit, Alomone Labs), actin by 1:5,000 (#SC-1615, goat, Santa Cruz Biotechnology, Inc.), and β-actin by 1:50,000 (#A1978, mouse, Sigma-Aldrich). After wash, membranes were incubated with horseradish peroxidase-coupled secondary antibody diluted by 1:5,000 for CD38 and actin (#SC-2020, donkey anti-goat, Santa Cruz Biotechnology, Inc.), 1:5,000 for TPC1/2 (#SC- 2313, donkey anti-rabbit, Santa Cruz Biotechnology, Inc.) and 1:50,000 for β-actin (#NA931V, sheep anti- mouse, GE healthcare UK limited) in 3% BSA-PBST. Protein signals were detected by enhanced chemiluminescence (Pierce) on autoradiography film and quantified by Gel Logic 200

Image System (Kodak, New Haven, CT). After CD38 determination, the membrane was stripped and reprobed for actin/β-actin in the same blot as previously described in Chapter 3.

Quantitative reverse-transcription PCR Total RNA was extracted from endothelium-denuded PA tissues and cultured PASMCs using RNeasy® minikit (#74104, Qiagen, Valencia, CA) and followed by first-strand cDNA synthesis using random hexamer primers and Superscript III-reverse transcriptase (#18080-051, Invitrogen, Grand Island, NY) according to the manufacturer's protocol. Quantitative real-time RT-PCR (qRT-PCR) using iQ SYBR Green PCR Supermix (#170-8880, Bio-Rad, Hercules, CA) was used to quantify the expression of CD38 in PAs and PASMCs. The sequence for the gene-specific primers was described in table 1. The copy number of target mRNA expression was normalized by the copy number of TATA-box binding protein (TBP) as an internal control.

Ca^{2+} imaging for intracellular Ca^{2+} release $[Ca^{2+}]_i$ was measured with fluorescent

Table 4.1. Primer sequence for qRT-PCR

Gene	Primer	Sequence	Tm (°C)	% GC	Position (5'→3')	Amplicon Size (nt)
CD38	sense	TGGAGCAAGTCCAAACACCTGGC	65	56	382-404	119
	anti-sense	CTGGGGTCTCCACACCACCTGA	65	63	479-500	
TPC 1	sense	TCCGCTGTGGGGATATTG	60	56	34-51	108
	anti-sense	TCAGGGGCATCTTCTAGGG	60	58	124-141	
TPC 2	sense	GACTACTTCCAACAACCCTGATG	59	48	833-855	77
	anti-sense	CTCGGAACTGATTATAGATGATGG	59	42	886-909	
TBP	sense	CCCACCAGCAGTTCAGTAGC	61	60	1029-1048	75
	anti-sense	CAATTCTGGGTTTGATCATTCTG	56	39	1081-1103	

microscopy as previously described in Chapter II. Briefly, fluo-3 AM (#F1242, Invitrogen, Grand Island, NY) was loaded into isolated PASMCs on 25 mm cover-slip and incubated for 45 min at room temperature in the dark. After washed and incubation for deesterification of cytosolic dye, Fluo-3 was excited at 488 nm and the emitted light at 515 nm was detected by inverted microscope (Diaphot, Nikon TE2000U) equipped with epifluorescence attachments and a microfluometer (PTI, model D-104). PASMCs were pretreated with the CD38 inhibitor nicotinamide for 20 min. To examine intracellular Ca^{2+} release, Ca^{2+} containing (2 mM) Tyrode solution was changed with Ca^{2+}-free Tyrode (containing 1 mM EGTA) 100 seconds prior to the application of Ang II. Fluorescence intensity (F) was used to calculate the absolute $[Ca^{2+}]_i$ using the equation: $[Ca^{2+}]_i = [K_D \cdot (F - F_{bg})]/(F_{max} - F)$. F_{bg} is the background fluorescence, F_{max} is the maximum fluorescence, and K_D of fluo-3 is 1.1. F_{max} was determined in situ using the Ca^{2+} ionophore 4-Bromo-A23187 (#100107, Calbiochem, La Jolla, CA) and 10 mM Ca^{2+}, and F_{bg} was measured in a cell-free area after Mn^{2+} quenching

Identification of putative transcription factor binding motifs in CD38 gene Rat CD38 promoter region sequence was pulled from the Rat Genome Database, and the ALGGEN PROMO, which uses TRANSFAC database for transcription factor binding sites, was utilized to determine putative transcription factor binding motifs for NFAT, HIF-1, NF-κB, and CREB-like motif. The sequences were manually validated for the presence of putative HIF-1 (ACGTG or CACGT), NFAT (GGAAA or TTTCC), NF- κB (GGGATTCC or GGGGC) and CREB-like (TGGCGTCA) binding core motif.

Determination of NADase activity Measurement of NADase activity was performed by a fluorometric method (by Dr. Eduardo Chini's laboratory) as previously described

[345,346]. The enzyme activity was determined by measuring change in fluorescence with excitation (300 nm) and emission (410 nm) wavelengths in the presence of the NADase substrate 1-etheno-NAD. Tissue samples from PA and whole lung tissue with a final protein concentration of 0.5 mg per ml were incubated in a medium containing 0.2 mM 1-etheno-NAD, 0.25 M sucrose, and 40 mM Tris–HCl (pH 7.2) at 37°C. After baseline fluorescence was recorded, 80 μM of 1-etheno-NAD was added to start the reaction and fluorescence was recorded for 200 sec. The activity was calculated as the fluorescence units per unit time normalized by the amount of protein in the samples (unit/sec/mg protein).

Chemicals and inhibitors All chemicals were commercially available to be purchased; Ang II (#A9525, Sigma-Aldrich), nicotinamide (#N0636, Sigma-Aldrich), cell-permeable VIVIT (#480401, Calbiochem) and cyclosporine A (#C-6000, LC Laboratories).

Statistical Analysis All data are expressed as mean ± S.E.M. The numbers of replicates (n) are specified in the text. Statistical significance ($p<0.05$) was assessed by unpaired Student's t-tests or ANOVA with Holm-Sidak method if applicable.

Results

CD38 expression in PA smooth muscle tissue was increased in PA tissue from CH rat for 3–4wk.

As the first step of investigating the effects of CH on CD38 dependent mechanisms, we determined the expression of CD38 protein and mRNA in PAs of normoxic and CH rats (Fig. 4.1A). Immunoblot analysis showed that the expression of CD38 protein in endothelium-denuded PAs of 3–4 week CH rats (1.21±0.06) was slightly

but significantly increased compared to that of normoxic rats (1.00±0.07) (n=12, p=0.042). The CD38 mRNA level, quantified by qRT-PCR, was also significantly higher in the PA of CH rats. (CH: 0.199±0.032; normoxia: 0.094±0.019, n=7, p=0.016).

To examine the possible changes in the functional activity of CD38 caused by CH, AICR was determined in PASMCs isolated from normoxic control and 3–4 week CH rats (Fig. 4.1B). Intracellular Ca^{2+} release was elicited by 100 nM Ang II 100 seconds after removal of extracellular Ca^{2+}. Similar to the expression of CD38 protein, the peak $\Delta[Ca^{2+}]_i$ ($[Ca^{2+}]_{i,\ peak}$ - $[Ca^{2+}]_{i,\ baseline}$) of AICR was slightly but significantly elevated in PASMCs of CH rat (353.6±26.8 nM , n=11) compared to those of normoxic control (274.3± 21.6 nM, n=12) (p=0.05). These results implied that CH increases the expression and functional activity of CD38 in PASMCs.

CD38 expression and activity in PA were greatly enhanced during the early development of CHPH.

A previous study showed spontaneous rhythmic contractions, spike-like membrane depolarization, and elevated resting $[Ca^{2+}]_i$ in the PAs of rats after 1 weeks of CH [281]. These activities were blocked by ryanodine or cyclopiazonic acid and subsided after prolonged CH exposure (4 week). These results indicate that intracellular Ca^{2+} release contributes to spontaneous contraction of PA during the early development of CHPH.

To examine the possible changes in CD38 dependent mechanism during the early stage of CHPH development, we examined the time-course of change in CD38 expression in PAs of CH rats. CD38 protein expression in PAs was determined after 0, 1,

2, 3, and 7 days of CH exposure, with normalized values of 1.03±0.15, 0.89±0.12, 1.63±0.26, 2.00±0.13, 2.52±0.22, respectively (n=5 for each group) (Fig. 4.2A). CD38 protein levels significantly increased by day 3 and day 7 ($p=0.001$ and $p<0.001$, respectively), compared to the day 0 control. Similar time-course changes were found in the mRNA level of CD38 in the PAs after CH exposure (day 0: 0.27±0.05; day 1: 0.19±0.03; day 2: 0.34±0.09; day 3: 0.57±0.05; and day 7: 0.88±0.26, n=5 for each group) (Fig. 4.2B). The mRNA level of CD38 was significantly upregulated in PAs after 3 and 7 days of CH exposure ($p=0.003$ and $p=0.008$, respectively). These results indicate that the CH upregulates the expression of CD38 protein and mRNA of PA smooth muscle in a time-dependent manner. The 2–3 fold increase in CD38 expression after 3 to 7 days of hypoxic exposure, as compared to the marginal increase in 3–4 weeks CH suggests that CD38 may be more involved during the early development of CHPH.

NADase activity was increased in PA smooth muscle from hypoxic rat.

To examine whether the upregulation of CD38 expression by CH was associated with increased enzymatic activity, NADase activity (i.e. CD38) was measured (collaboration with Dr. Eduardo N. Chini, in Mayo Clinic, Rochester, MN) (Fig.4.2C). NADase activity was significantly increased in PAs of 1-week CH rats, with 6.61±2.03 units/sec/mg protein in normoxic control and 18.38±3.15 units/sec/mg protein in CH PAs ($n=9$, $p=0.006$). In contrast, NADase activity was significantly lower in whole lung tissue in hypoxic rat (38.03±2.33 units/sec/mg protein) compared to normoxic control (51.33±5.02 units/sec/mg protein) ($n=6$, $p=0.037$). These data suggest that the effects of CH on CD38 activity, and perhaps expression, are different in the whole lung and PA

tissues. We also examined the weight of whole lung tissue, and right heart hypertrophy (RV/(LV+S)) from normoxic and CH rats (Fig. 4.3). The weight of lungs of 1 week hypoxic rat (1.29±0.10 g, n=9) was significantly higher than that of normoxic control (0.93±0.05 g, n=9) ($p<0.001$, respectively). Likewise, the weight of PA smooth muscle tissue of 1 week hypoxic rat (0.0461±0.00206 g, n=16) was significantly higher than the normoxic control (0.0351±0.00235 g, n=16, p=0.001). RV/(LV+S) was also significantly higher in 1-week hypoxic rats (control: 27.63±0.73 %, n=12; CH: 44.29±0.80 %, n=12, $p<0.001$). These results implicate that the 1 week hypoxia exposure causes the development of CHPH including right heart hypertrophy, pulmonary vascular remodeling, and alteration in CD38 activity.

AICR was increased in PASMCs of 1 week hypoxic rats.

To examine the CD38 dependent Ca^{2+} release processes, AICR was determined in PASMCs of normoxic control and 1 week hypoxic rats (Fig. 4.4). Ca^{2+} release induced by 100 nM Ang II was examined and recorded in the presence or absence of 20 mM nicotinamide (NA) (Fig. 4.4A). AICR was significant greater in hypoxic PASMCs (455.3±63.3 nM, n=12) than in normoxic PASMCs (289.9±32.3 nM, n=9, p=0.04). The Ca^{2+} response was significantly suppressed by inhibition of CD38 with NA (normoxic: 124.3±20.4 nM, n=8, $p<0.001$; CH: 115.4±15.7 nM, n=9, p=0.037), and there was no difference between the two groups in the presence of NA (Fig. 4.4B). The percent inhibition of AICR by NA was significantly greater in the hypoxic cells (74.65±4.16%) compared to the normoxic cells (55.61±6.16%, p=0.014) (Fig. 4.4C). These results

suggest that the CD38-dependent Ca^{2+} release activated by Ang II was potentiated in PASMCs of 1 week CH rats.

Hypoxia directly enhanced CD38 expression and activity in PASMCs of normoxic rats.

Upregulation of CD38 expression in the CH rat model could be related to multiple factors. To determine whether hypoxia induces CD38 expression through a direct effect on PASMCs, PASMCs isolated from normoxic rat were exposed to 21 or 2% O_2 for 3 days, and the expression of CD38 in the two groups were compared (Fig. 4.5A). Western blot analysis showed that CD38 protein level was significantly increased in the hypoxia PASMCs (2.19±0.35, n=5) compared to the normoxic control (1.25±0.05, n=5, p=0.025). The CD38 mRNA level of hypoxic PASMCs ($5.43\pm0.13\times10^5$) was also significantly higher than that of normoxic cells ($2.07\pm0.42\times10^5$, n=5, p=0.036). These data clearly indicate that hypoxia exerts a direct effect on PASMCs to upregulate the expression of CD38.

AICR was performed to examine the functional changes in CD38 activity caused by the direct effect of hypoxia (2% O_2, 3 days) in PASMCs (Fig. 4.5B). Peak $\Delta[Ca^{2+}]_i$ induced by Ang II (100 nM) was 325.2±16.6 nM in normoxic (n=14) and 593.3±77.0 nM in hypoxic PASMCs (n=15) in the absence of NA; and 152.9±21.0 nM in normoxic (n=7) and 111.5±31.9 nM in hypoxic PASMCs (n=6) after CD38 was blocked by 20 mM NA. AICR was significant greater in the hypoxic PASMCs compared to the normoxic control (p=0.002). The Ca^{2+} response was significantly suppressed by the inhibition of CD38 ($p<0.001$ for both), but there was no significant difference between the normoxic and hypoxic PAMSCs in the presence 20 mM NA. The percent inhibition of AICR by 20 mM

NA was 81.21±5.37% in hypoxic PASMCs and 52.98±6.47% in normoxic cell. The percent inhibition was significantly greater in the hypoxic PASMCs (p=0.007). These data show that the upregulation of CD38 expression in PASMCs caused by direct hypoxia exposure was associated with enhanced CD38-dependent Ca^{2+} response.

NFAT is putative regulatory transcription factor for CD38 expression in rat PASMCs.

To further investigate the molecular mechanism of CD38 upregulation by hypoxia, the putative binding sites for transcription factors in the promoter region of rat CD38 gene were explored in a 3.0 kbp 5'-UTR promoter region of CD38 (Fig. 4.6). We found that there are ten NFAT, three HIF, two NF-κB, and one CREB-like putative binding-motifs in the region, indicating that these transcriptional factors could be involved in the upregulation of CD38 expression by hypoxia.

CH-induced CD38 upregulation was dependent on the calcineurin/NFAT pathway.

Since there are multiple putative NFAT binding sites in the promoter region of the CD38 gene, we tested the involvement of the calcineurin/NFAT pathway in the hypoxia-induced upregulation of CD38 in PASMCs. Expression of CD38 protein was examined in PASMCs isolated from normoxic rat and cultured under hypoxia (2% O_2) for three days in the absence or presence of the peptide inhibitor of NFAT activation VIVIT (3 μM) or the calcineurin inhibitor cyclosporine A (Cyc A, 5 μM) (Fig. 4.7). Semi-quantitative Western blot analysis showed that the relative CD38 protein level was 0.984±0.0632 in normoxic control, 0.844±0.0603 in VIVIT treated, and 0.808±0.0477 in Cyc A treated normoxic cells (n=5). It was not significantly altered by VIVIT and Cyc A treatment for 3

days. CD38 was significantly increased in the hypoxic cells (1.562±0.0633, p=0.005) compared to normoxic control. The hypoxia-induced increase in CD38 protein was blocked by VIVIT (1.131±0.167, p<0.001) and Cyc A (1.070±0.199, p<0.001). There was no significant upregulation of CD38 by hypoxia in the presence of both inhibitors. These results suggest that the hypoxia-induced upregulation of CD38 in PASMCs is mediated by calcineurin/NFAT-dependent pathway.

CH alters the expression of NAADP-sensitive Ca^{2+} release channels in PA smooth muscle.

To further elucidate the changes in the CD38-dependent mechanism in PASMCs under CH exposure, we examined the expression of the NAADP-sensitive Ca^{2+} channels TPC1 and TPC2 in PAs of normoxic and CH rats (Fig. 4.8). Semi-quantitative Western blot analysis found that the expression of TPC1 protein in PA tissue of 3–4 week hypoxic rat (0.65±0.21, n=6) was significantly increased compared to that of normoxic rats (0.14±0.05, n=6, p=0.031) (Fig. 4.8A). Similar increase in TPC2 expression was observed in hypoxic PAs (normoxic: 0.94±0.15, n=6; CH: 1.75±0.26, n=6, p=0.021). We also examined the expression of TPC1 and TPC2 protein in PAs of rats exposed to CH for different durations (Fig. 4.8B). The relative TPC1 protein level was 0.88±0.12 in day 0, 0.99±0.19 in day 1, 1.18±0.25 in day 2, 1.27±0.18 in day 3 and 1.47±0.29 in day 7 (n=5 rats for each time-point). The expression level of TPC2 protein was 1.49±0.52 in day 0, 1.58±0.41 in day 1, 4.49±0.99 in day 2, 6.12±1.45 in day 3 and 5.24±0.98 in day 7 (n=5 rats for each time-point). The TPC2 protein level was significantly increased in PAs of rats after 2, 3, and 7 days of CH (p=0.028, p=0.010, and p=0.033, respectively)

compared to that of normoxic control. TPC1 protein showed a tendency of increase while there is no statistical significance in the hypoxic PA tissue. In contrast, mRNA level of TPC1/2 in PA tissue was not significantly changed in CH rats compared to the normoxic control. These results suggest that CH exposure induces TPC1/2 protein expression in PA smooth muscle in a time-dependent manner possibly through a post-transcriptional mechanism.

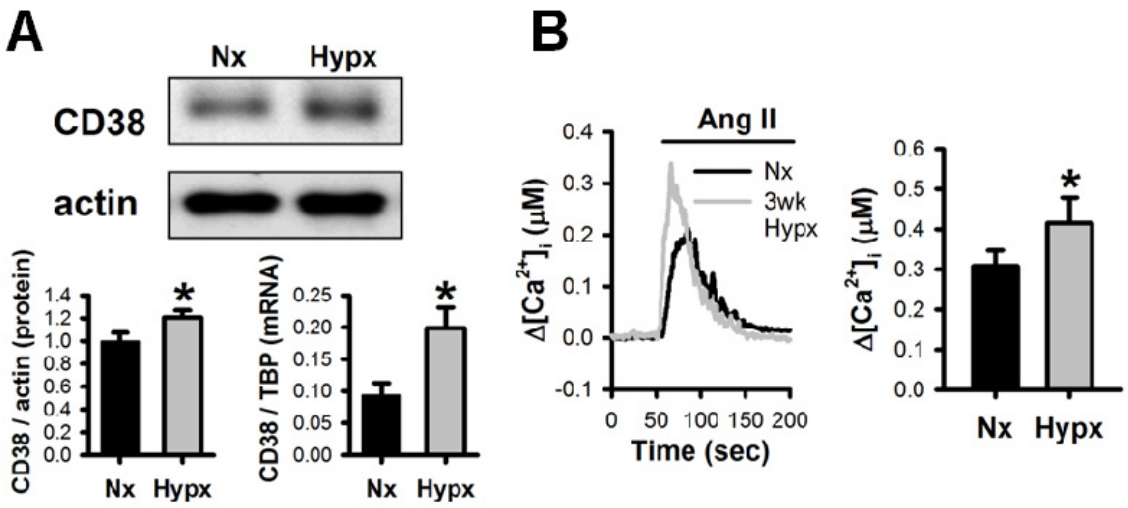

Figure 4.1. Upregulation of CD38 in PA smooth muscle tissue and enhancement of AICR in PASMCs of 3–4 week CH rat (A) Upper panel shows representative immunoblot of CD38 and β-actin in PA samples of normoxic (Nx) and CH (Hypx) rats. Lower panels show mean data of semi-quantitative Western blot and quantitative real-time polymerase chain reaction (qRT-PCR) analysis of CD38 protein and mRNA in PA smooth muscle of 3–4 week hypoxic and normoxic rats. Asterisk (*) indicates significant increase compared to Nx rats (n=7 for each groups, P=0.042 for CD38 protein and p=0.0014 for CD38 mRNA). (B) Mean traces of An II-induced increase in $[Ca^{2+}]_i$ (left pannel) and mean peak $\Delta[Ca^{2+}]_i$ elicited in PASMCs of normoxic (n=11) and CH rats (n=12) (right panel). * indicates significant increase in Ca^{2+} response compared to normoxic control (p=0.05).

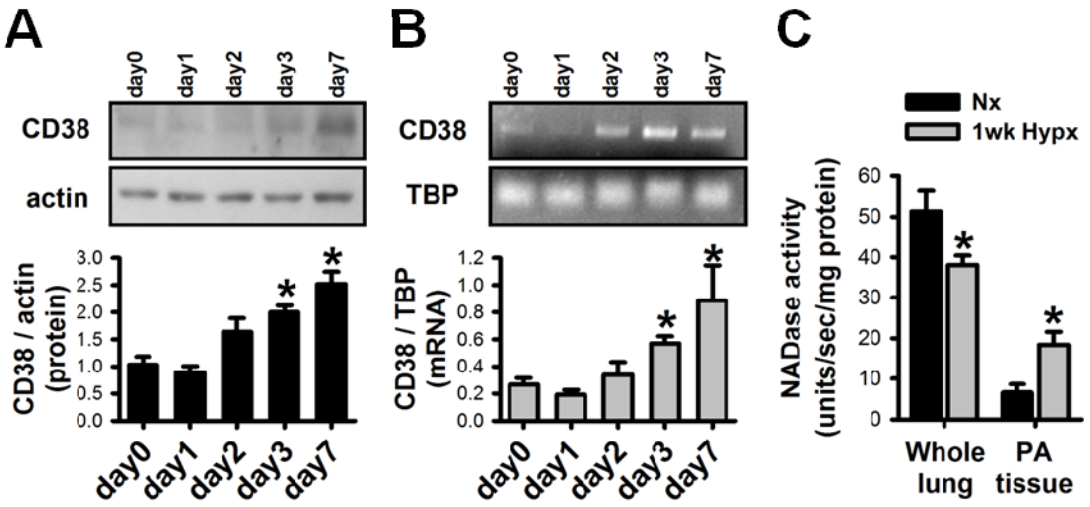

Figure 4.2. CD38 expression and activity in PA smooth muscle of rats after different periods of CH (10% O_2) exposure (A) Western blot analysis of CD38 protein expression in PA of rat at different time-points of CH exposure. * indicates that CD38 protein increased significantly in day 3 (n=5, $p<0.001$) and day 7 (n=5, $p<0.001$) compared to day 0. (B) Conventional RT-PCR (upper panel) and qRT-PCR (lower panel) analysis of CD38 mRNA expression in PA tissue. * indicates that CD38 mRNA increased significantly in day 3 (n=5, 0.004), and day 7 (n=5, $p<0.001$) compared to day 0. (C) NADase (i.e. CD38) activity measured in whole lung lobe and PA smooth muscle of normoxic and 1wk hypoxic rats.* indicates that NADase activity in PAs of 1week hypoxic rat was significantly increased (n=9, p=0.006), while the activity in whole lung lobe tissue of 1wk hypoxic rat was significantly decreased (n=6, p=0.037), compared to those of normoxic control.

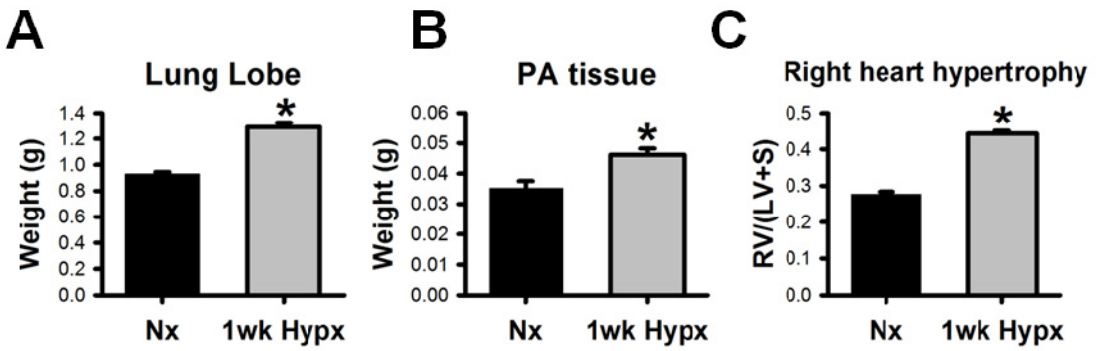

Figure 4.3. CH-induced lung, PA and cardiac remodeling (A and B) The weight of whole lung lobe and PA of 1 week hypoxic rat. * indicates significant difference in lung lobe (n=9, $p<0.001$) and PA tissue (n=16, $p=0.001$) compared to Nx control (n=9 and n=16, respectively). (C) Measurement of RV/(LV+S) for right heart hypertrophy. * indicates that RV/(LV+S) was significantly higher in hypoxic rats (n=12) compared to the value of Nx control (n=12, $p<0.001$).

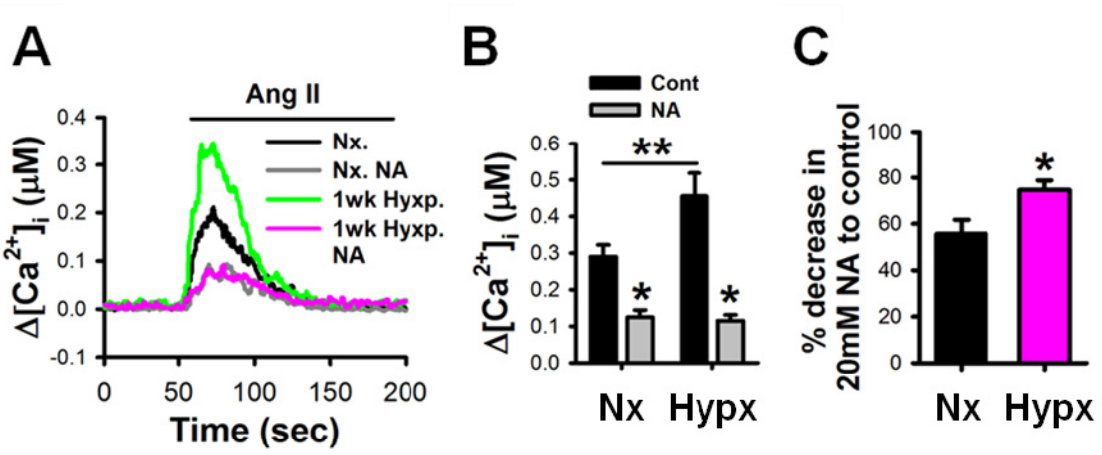

Figure 4.4. CH-induced increase in AICR mediated by CD38 (A) Mean trace of $[Ca^{2+}]_i$ by 100nM Ang II in PASMCs from 1wk Hypx and Nx rat in the presence of 20 mM nicotinamide (NA) to inhibit CD38. (B) Mean peak $\Delta[Ca^{2+}]_i$ of AICR. Double asterisk (**) demonstrates the significant enhancement of peak $\Delta[Ca^{2+}]_i$ of AICR in PASMCs from Hypx rat (n=12) compared to Nx control (n=9, p=0.04). * indicates that NA significantly suppressed peak $\Delta[Ca^{2+}]_i$ of AICR in both Hypx (n=9) and Nx PASMCs (n=8) compared to its experimental control ($p<0.001$ and $p=0.037$, respectively). Note that inhibition of CD38 by NA lead to no difference in AICR between Hypx and Nx PASMCs. (C) The proportion of inhibition of peak $[Ca^{2+}]$ by NA (%decrease in 20 mM NA to control) in hypoxic PASMCs was significantly higher than the proportion in normoxic cells (p=0.014).

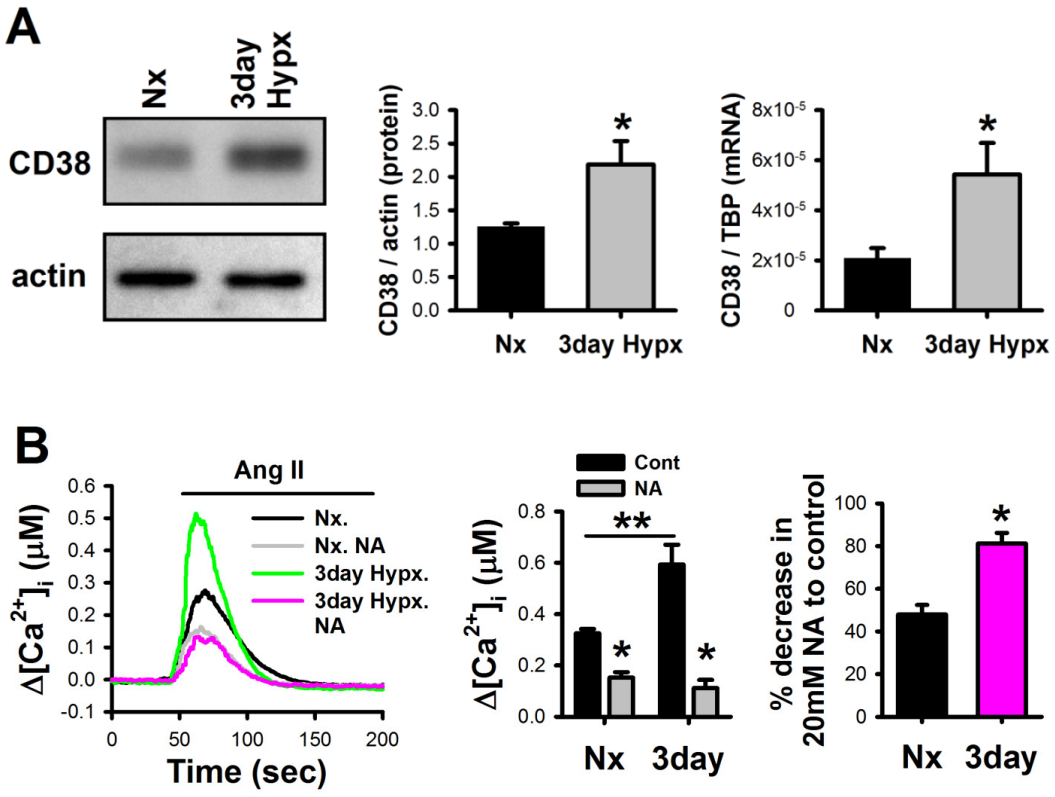

Figure 4.5. Hypoxic-induced enhancement of CD38 expression and AICR in PASMCs *in vitro* (A) The expression of CD38 protein and mRNA in rat PASMCs isolated from normoxic rat cultured under normoxic (21% O_2) and hypoxic conditions (2% O_2) for 3 days. * indicates that CD38 protein and mRNA in Hypx PASMCs (n=6 and n=5, respectively) were significantly increased compared to the expression in Nx control PASMCs (n=6, p=0.025 and n=5, p=0.036, respectively). (B) Mean traces of $\Delta[Ca^{2+}]_i$ activated by 100 nM Ang II in Hypx and Nx PASMCs in the absence or presence of 20 mM NA (left panel). Mean peak $\Delta[Ca^{2+}]_i$ of AICR (middle panel). ** indicates significant enhancement of peak $\Delta[Ca^{2+}]_i$ of AICR in Hypx PASMCs (n=15) compared to Nx control (n=14, p=0.02).* indicates that NA significantly suppressed the peak $\Delta[Ca^{2+}]_i$ of AICR in both Hypx (n=7) and Nx PASMCs (n=6) ($p<0.001$ for both). Inhibition of CD38 by NA lead to no difference in the peak $\Delta[Ca^{2+}]_i$ of AICR between Hypx and Nx PASMCs. The proportion of inhibition of peak $[Ca^{2+}]$ by NA (% decrease in 20 mM NA to control) in hypoxic PASMCs was significantly higher than the proportion in normoxic cells (p=0.007).

GCTCAGCAAATAAAGACACAGAGAAGGGCAGTCTGAAAGCCGAGTAAACAGGCCTCAGAAGGAGAC
ACCCATGCAGAAACCCTGATCTTGAACGTCCAGCTTTCAGTAGTGCAAGACAATACATTTCTTTTGTTT
AAGACATCCAGTGTATGGTGTGGTATGCTGCTATGGCACCTCCAGCAGACTGAACTTTGACCTTTTTTT
CCGGTATTTTCCTAAGTAGTGGGTGTGGTTGCACAAACACTGGTTCACTAACTGGCCTCTTTTTGAACT
TTTGACCATTTAATGACACCCTGAGGCCTTGTCTAACCTGCACCCTGATTAGACTCCATCAGTGCTCGG
TGCTGTTCCCCACCACAGGATCTTTCCCTTTTTACAGCATGAAGGAAGCAATCAGGAGAGAATGTCCTC
TAAAGCCTCACCCCACCCCCACCCCTATTCTCCACCTCTCTTTTGTGAGGAACGAGAGCTCTCGAGCTC
CTGCCCACATCCTGACCATGCCTCAGATTCCTCACACCATCTCCTACATTTGTCAAGTGTTTCTGTGCTA
GTGAGTCAGCCTCCAAAAGTTCTGTGGGAAGTCTGATCTCAGAACAGGAAGCTGTTTCCTGACTCCCA
GGCTGCTATTACTTTCTCATTATTGAGAAAAAATGTCCAACGTGACAACTAAAGAGAATTTCACTTTGG
TTCAGTTTTAGAGGATTTGATCCATGGTCTCTTGGCGTCATGCTTTTGGGTAGAACATTATATGGCATA
GGAGATTAGTTCACATCATGACCAACTACAAGGCAGAGAACGGGACAGGAAGTTACCAGGGATAACA
CAGCATCAAAGACTTTTAACCAGTGACCCAAGTCCTCCATCTTGGTCCCTCCTCCTAAATGTATAAACC
TTCCAAAATAGTTCCCCAACCTGAGGTCCAAGAGTTCAAAATCATGATCCTTTAGAGAAGTTTACATAT
CTAAGTCATAATACTCAGCGCCTTCTAATTGCATCCTTATTTTTCTGTTCCTTCTGACATTAAAAAACCA
ACCAAACAAAACCGCTTCCCTTTTCAACACAACTGCACTCTAACTTACTTTTAGAACCTTCAAACATTC
TCTTGAACCTAATCTGCTAGGCCGTGTCCTTCATTTAAGAGTGTTTGCTGCTCTTGCAGAAAACTGGAG
TTAGGATGTAGCATCCACACTGGGCAACTCACAACCATTTACAATGTCAACTCTGGAGACTTGATGCC
CTATTTTGGCTGGTATGGGCACCGCACATAGGAGCATGCACACACATACACAGATACTATGTTAGGTT
TTTAATCTTTTTGAGCTCCCGTTAGTTAAGAACCATTTTTTCTTTTTCAGGTGTCATCCTTCCAAGTTCCT
CTTGCTGGGATTCCCACGTTTTTCTGACTCCTACTTCAAGAATGTTCCCCAAGGTTTTGAAACTTCTCCA
TTCTGTCTGTTACAGTCTTTCTGAGACATGACAGCCCTCTTTACAAACCATGTGCTGAACCCTCATCTA
CCAGGTCATTTAAGGTCACTGATCTTAAATGGTTTAAAACAGAAATGTGTGCTGGTGAAATGGCCCAA
CCTGTTCAGTCCTCTCTGCTCTCAAGCCTGATGACCTCAGTTCAATGCCTTGGACACACATGGGAGAGA
GAGAGAAAAGACCTCTCAAAGTTGTCCTTTGACCTACACACACACACACACACACACACACACACACA
CACACACACTCACAGAGGCACACAAAATGAATAAGCAAAATGACAGCAAACATTTTTAAAAAAATGA
AATGCACAGTCTAAAAATGTCCCGCTGACATAGGAAGCTGCAGAGACCTCCTCTCCTGCTGCTTTCAG
AAGGATTCTCTCTCTGTTCATCCTCTAGTCCAGCTGCAATGGCTGCTTTCCCACTCCTTAAAACAACAC
AAGGGGCTTTCCTGTCCCAGTCTCTTCATCTAGTATTCCCGCTGCCTGGAAAATGTCCCATGAAGATCC
AGCGTTGTGATCCTTATGTGACAAGACTCTGTTTAAGCAATATATGTCTTCATAGGAAGGAGAGGCAG
GAAGAGCGTCTGCATTTTGGGGTTCCTATGTGGGATGACGTATCAGTGCACATGAGACGGGTTGCAGG
CATCCTATCAACTATAAAACCCTATTTGACAACACCCTAGAGCAAGCAGCAATAACTTATATTTATTGA
GTAATCAGTTATTATGTTTTAGGGATTATACAAACACCTAGGCGATATTAACTCACCGAACCAAAGCA
AGCTGTGATGTAATTAATGTGAGTCTCTGCTCACGTCTATCTGGTTCAGAGAGGTGAGTTAACAGCATT
TTAGCAGCTGGGGCTGGGTTTGAACTGATAACTCCCGAGAAGAGGAACAGAGTGATGCTGAGACTTTA
AAGATATCTGGGTAGGATTTTTATCAAAGTTCAGAATTAGAGGTGGGACATTCATTGCCAGGCATTTG
GGTGAACAGAGAGAGGGGGAGGGAGGAAAGAGGGAGAAGGAGAGTGGGAAAGAGGCAGAGAGATG
GAGAGAGAGAGAGATGGAGAGAGAGAAGAGAGAGAGAGAGGGAGAGAGAGAAGAGAGAGAGGGA
GAGAGAGAGGGAGGAATTTTTACCCTCCGGGGCACATATGTAGCGAAAGTGTCAAGTGCACAGGTGA
CAGGGGGCGTTGGCCAGGAGTATCCTGAAGCTCTTGTTTGTGCACCCACAGAGGCTAAAGTGCTGTCT
TCTCTTGGAGAGAGAGGTTCGGGTCAGTCTGCTCTGGAGTCTGGAAGTAAGCAGCTGGAGCGCCTGTT
GACAACCCAAAAGCCTTGTTAGTCTAGTCACCCCCGGTGGAACTCTGAAGCAGGAGTAGGGGGTGGG
AAAGGAAGCAGATAAAAGGCAAGTGAAAGAAAGGAGGAGGGGCAGGCTCTGACCCAGCCAGCCCTG
TGCTCTCTTCCTGCCTAGCCTGGGCCAGTCTCCAGGAGCC

NFAT (10), Hif-1 (3), NF-κB (2), and CREB-like (1) motifs.

Figure 4.6. DNA sequence of the putative 3.0 kbp 5'-UTR promoter region of rat CD38 gene Transcription factor-binding sites are underlined. Note that there are multiple putative binding motifs for NFAT (10), HIF-1 (3), NF-κB (2) and CREB-like (1) in the region.

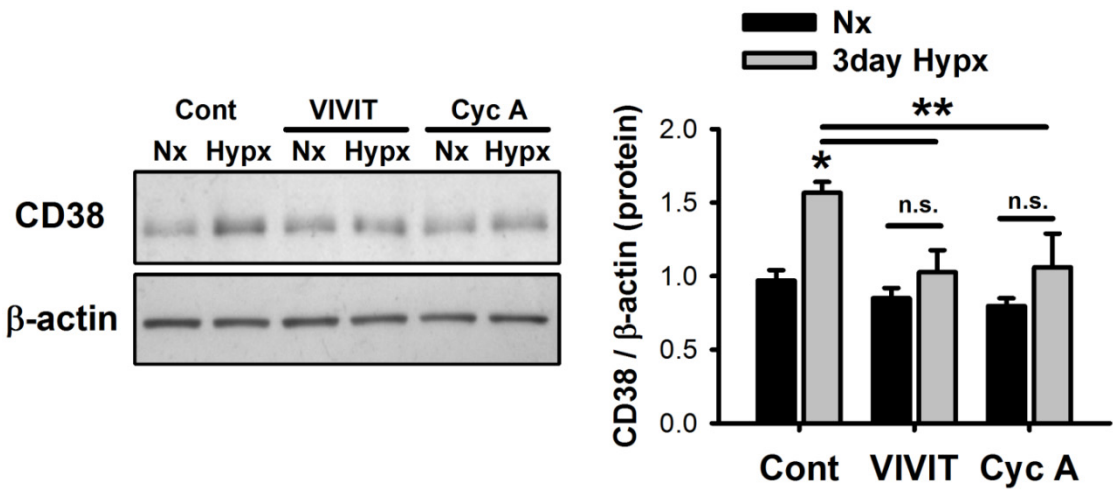

Figure 4.7. Suppression of CH-induced CD38 upregulation by inhibition of calcineurin/NFAT-pathway Western blot analysis for CD38 expression in PASMCs cultured under normoxic or hypoxic conditions for 3 days in the absence or presence of 3 μM VIVIT (NFAT inhibitor) and 5 μM cyclosporin A (Cyc A) (n=5). * indicates that CD38 expression in PASMCs was significantly upregulated by hypoxic exposure for 3 days in control (p=0.005), while the upregulation of CD38 was blocked in the presence of VIVIT or Cyc A. ** indicates that there was a significant difference between control and the VIVIT (p=0.015) or Cyc A (p=0.013) treated hypoxic cells. Note that hypoxia-induced CD38 upregulation was blocked in the presence of VIVIT and Cyc A compared to the experimental control group (n.s.).

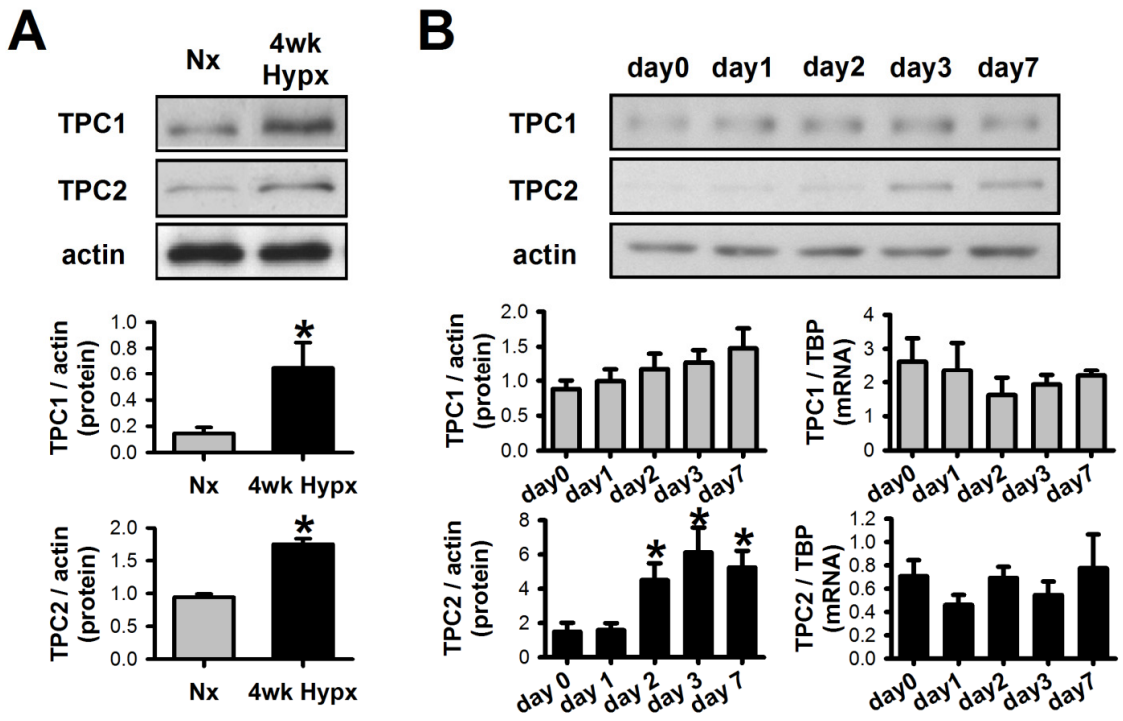

Figure 4.8. Increased expression of TPC1/2 in PA smooth muscle tissue of CH rats (10% O_2) (A) Western blot analysis of TPC1/2 protein in PA smooth muscle tissue from 4 week CH rats for. * indicates significant increase in both TPC1 and 2 in Hypx compared to Nx PA (n=6, p=0.031 and p=0.021, respectively). (B) Hypoxia-induced alteration of TPC1/2 protein and mRNA in PA tissues of rats after different period of hypoxic exposure. * indicates that TPC2 protein increased significantly in day 2, 3 and 7 compared to day 0 (n=5, p=0.028, p=0.010, and p=0.033, respectively), whereas there was no significant increase in TPC1 protein in CH PAs. Note that mRNA expression of TPC1/2 was not altered by hypoxic exposure up to 1 week compared to the expression in day 0 control.

Discussion

The major finding of this research project is that CH enhances the expression and activity of CD38 in rat PASMCs. While CD38 expression and activity in smooth muscle is known to be regulated by various cytokines and hormones such as TNF-α, endothelin-1, and Ang II [138,316,347], there is no systematic research on the regulation of CD38 in PASMCs with an emphasis on prolonged hypoxic exposure. This study first characterized the effect of CH on CD38 expression in the PAs of rats and found that CD38 expression was increased in a time-dependent manner in the first week of hypoxia exposure. The increase in CD38 expression was associated with enhanced CD38 enzymatic activity in PA smooth muscle and CD38-dependent AICR in PASMCs of CH rats. The effect of hypoxia on CD38 was reproduced in cultured PASMCs isolated from normoxic rats *in vitro*, indicating that these effects are due to the direct actions of hypoxia on PASMCs. Furthermore, CH-induced CD38 upregulation in hypoxic PASMCs was blocked by the inhibition of calcineurin or NFAT, suggesting that it underlies the calcineurin/NFAT pathway. Additionally, the expression of TPC2, which is the NAADP-sensitive Ca^{2+} release channel in the endolysosomes, were significantly increased in the PA smooth muscle of CH rat. These results provide the first evidence that CD38 may participate in the development of CHPH.

This study clearly demonstrated that CH induces CD38 expression in the PAs of rats. This effect of CH is time-dependent, with CD38 protein and mRNA increasing gradually in the first week of CH exposure, followed by a decline in the protein level after 3–4 week of CH, while the increased mRNA level remained unchanged. Since most of the changes in the development of PH, including increased PA pressure and vascular

remodeling, occur within the first week of hypoxia exposure [348,349,350], the upregulation of CD38 protein specifically in this period suggest that this could be related primarily to the progression, rather than the maintenance, of CHPH.

The significant increase found in the functional CD38 in the PA of week 1 hypoxic rats is supported by the enhanced enzymatic activity of CD38. It is well established that CD38 is the major multi-catalytic NAD^+-glycohydrolase (NADase), influencing the activity of cyclase, catalase, and hydrolase in the lungs [351] and other tissues [125]. We found that NADase activity was significantly increased in the PAs, while it decreased in the whole lung tissue, of hypoxic rats. Although we have not determined the individual enzymatic functions of the NADase activity due to its multifunctionality, the results clearly suggest that hypoxia alters the activity of CD38 specifically in PA, independent of the other lung tissues. These results, hence, suggest that CD38 upregulation in PA could be a unique characteristic in the development of CHPH.

In additional to NADase activity, we examined AICR to gauge the functional activity of CD38 in PASMCs. As shown in Chapter 3, Ang II induces CD38-dependent Ca^{2+} release in PASMCs. The magnitude of AICR in the PASMCs of week 4 CH rats was slightly but significantly increased, consistent with the moderate increase in CD38 expression, suggesting that CD38 may contribute to enhanced Ca^{2+} release in CH PASMCs. Consistent with CD38 expression data, AICR in the PASMCs of week 1 hypoxic rats was greatly enhanced compared to that of the normoxic control. The augmentation of AICR is clearly related to the upregulation of CD38, because the difference between PASMCs of week 1 hypoxic and normoxic rats was completely

eliminated in the presence of the CD38 inhibitor NA, and the percent inhibition of AICR in PASMCs of the hypoxic rats was significantly greater than in those of the normoxic cells. It has been reported that members of the Ang II signaling pathway, including the level of Ang II and the Ang receptors, are elevated in animals and patients with pulmonary hypertension and that this is associated with the pathophysiology of CHPH [352,353,354,355]. The enhanced CD38-dependent Ca^{2+} release can provide an additional mechanism for the increased vasoreactivity to Ang II in CHPH. Our previous studies found that other vasoactive agonists, such as ET-1 and integrin-ligands GRGDSP, also activate Ca^{2+} release through CD38 dependent mechanisms [114,122]. Our present results, hence, suggest that the increased CD38 expression may contribute to the enhanced agonist induced vasoreactivity in hypoxic PASMCs.

Hypoxia may exert its effect on CD38 expression by the direct modulation of gene expression in PASMCs or indirectly through other endocrinal or paracrinal agents/ factors released in the circulation and in the lung tissues [336]. Our observations that incubation of PASMCs from normoxic rats in 2% O_2 for 3 days evoked a significant increase in CD38 protein and mRNA and that AICR was enhanced in hypoxic PASMCs clearly suggest that hypoxia alone can directly lead to CD38 upregulation, even through when the participation of other mechanisms under *in vivo* conditions are not excluded.

To date, there is no report on the regulation of CD38 expression by CH in PASMCs or any other tissue. However, previous studies have shown that several transcriptional factors, such as HIF and NFAT, play very important roles in gene regulation during CH [216,356,357,358]. We analyzed the 3.0 kbp 5'-UTR promoter region of CD38 in rats and found multiple putative binding sites for transcription factors

including HIF-1, NF-κB, CREB, and NFAT. Among the candidates, the putative binding motifs for NFAT are most abundant in that region, and a similar observation was made in the promoter regions of human and mouse CD38 genes (data not shown). This raises the interesting possibility that CD38 upregulation by hypoxia may be dependent on the NFAT-signaling pathway. NFAT is a transcription factor ubiquitously distributed in various cell types and regulated by dephosphorylation by calcineurin [359]. Indeed, NFATc3 plays a pivotal role in vascular development [360,361], cell proliferation, cell differentiation [362,363], and the characteristic of smooth muscle cell contractility [364,365]. Studies have also demonstrated that CH induces pulmonary arterial remodeling mediated, in part, by the activation of NFATc3 [366].

To test this possibility, we designed two different approaches to inhibit the NFAT pathway: inhibiting calcineurin with Cyc A and blocking the dephosphorylation site of NFAT with the specific peptide antagonist VIVIT. Both inhibitors mitigated the increased expression of CD38 by hypoxia in PASMCs. These results suggest that the hypoxic-induced upregulation of CD38 in PASMCs requires a functional activation of the NFAT signaling pathways. However, the possible roles of other hypoxia-related transcription factors such as HIF-1 and NF-κB in the regulation of CD38 expression in PASMCs require further investigation.

In addition to the enhancement of CD38 expression and activity, other members of the CD38-dependent Ca^{2+} release pathway, such as the RyRs and TPC channels, could also be affected by CH. We have previously shown that NAADP evokes intracellular Ca^{2+} release via TPC1/2 of the endolysosomes and cross-activates RyRs to amplify Ca^{2+} release in PAMSCs [114]. In this study, we observed that TPC2 protein expression in PA

smooth muscle tissue was enhanced by CH exposure in a time-dependent manner during the early development of CHPH. Interestingly, CD38 expression was highest at 1 week and declined at 3–4 weeks of CH exposure, while elevated TPC1/2 protein levels were sustained. In particular, TPC1 protein, which was not significantly increased at 1 week, was significantly increased after 4 weeks of CH. These data suggest that CH differentially regulates the components of the CD38-dependent mechanism at different stages in the development of CHPH.

Previous studies provided the evidence that the mechanism of CHPH development is complex and depends on many factors. Studies have established that an increased $[Ca^{2+}]_i$ in PASMCs of CH animals stimulates pathophysiological changes including cell contraction, migration, and proliferation, eventually resulting in pulmonary vascular remodeling under CH. The current consensus on the alteration of Ca^{2+} levels in CH PASMCs is that it is due to the inhibition of the voltage-dependent K^+ channel in exposure to CH, leading to membrane depolarization and an increase in $[Ca^{2+}]_i$ [274,339]. It is recognized that CH also affects other Ca^{2+} influx mechanisms, including store-operated and receptor-operated Ca^{2+} entry [238], mechanosensitive Ca^{2+} channels [37,39], and Ca^{2+} activated Cl^- channels in PASMCs [75], leading to the elevation of $[Ca^{2+}]_i$. Moreover, recent studies have clearly demonstrated the differential roles of transient receptor potential (TRP) channels, including TRPC1, TRPC6 and TRPV4, in the development of CHPH and the alteration of vasoreactivity in PA from CH animals [37,38,367]. The diversity of $[Ca^{2+}]_i$ the regulation mechanism in PASMC under CH is not fully understood, particularly for intracellular Ca^{2+} release. Our findings clearly

indicate that CH induces alterations of intracellular Ca^{2+} release mechanisms via an increase in the expression and activity of CD38 in PASMCs.

In conclusion, this study demonstrated that CH upregulates CD38 expression and activity in PASMCs and enhances the functional activity in response to Ang II. The upregulation of CD38 expression is mediated by Ca^{2+} dependent NFAT-pathways in PASMCs. These findings, therefore, provide novel information for improving our understanding of the mechanism for the development of CHPH.

Acknowledgement

This research was supported by National Institutes of Health grants R01 HL071835R01 and HL075134. Measurement of NADase activity was collaborated with Dr. Eduardo N. Chini at the Mayo Clinic (Rochester, Minnesota).

CHAPTER 5

SUMMARY AND FUTURE DIRECTIONS

Summary

Ca^{2+} homeostasis is crucial for almost every physiological function and is maintained by different types of regulatory mechanisms in response to various environmental stimuli including hypoxic exposure. It is clearly recognized that $[Ca^{2+}]_i$ is elevated in pulmonary arterial smooth muscle cells (PASMCs) from chronic hypoxia-induced pulmonary hypertension (CHPH) animals due to CH-induced increase in Ca^{2+} influx via functional and expressional enhancement of Ca^{2+} mobilization gated by membrane channels. Yet, the changes in the other part of Ca^{2+} regulation, intracellular Ca^{2+} release, have not been clearly established in PASMCs. An increasing number of studies have provided evidence that the multifunctional enzyme CD38 plays crucial roles in Ca^{2+} release, leading to multiple physiological responses in various cell types. However, the regulatory mechanism of CD38 has not been systematically established in PASMCs. Further, no study has investigated whether chronic hypoxia (CH) modulates the expression and activity of CD38 in PASMCs.

Based on these two questions, the work presented in this dissertation was proposed to describe the mechanisms of intracellular Ca^{2+} release mediated by CD38 in PASMCs and the alteration of the CD38 induced by CH exposure. The hypothesis and major findings for each aim are summarized as follows.

1. The first hypothesis in this dissertation states that CD38 plays a role in intracellular Ca^{2+} in PASMCs and contributes to agonist-induced vasoconstriction in pulmonary arterial (PA) smooth muscle. CD38 is highly expressed in PA smooth muscle and PASMCs compared to other vascular smooth muscles. CD38 partially mediates angiotensin II (Ang II)-induced vasoconstriction in PA smooth muscle. Ang II-induced

intracellular Ca^{2+} release (AICR) in PASMCs is significantly reduced by pharmacological or by siRNA inhibition of CD38, indicating that AICR in PASMC is mediated by CD38. AICR is subsided with the inhibition of cADPR- and NAADP-dependent Ca^{2+} release. In particular, suppression of these two Ca^{2+} release mechanisms is non-additive, indicating the inter-dependence between RyR- and NAADP-gated Ca^{2+} release in PASMCs. The Ang II-induced CD38-dependent intracellular Ca^{2+} release in PASMCs is mediated via PKC-NADPH oxidase 2-reactive oxygen species. For the first time, these results establish the signaling mechanism of CD38 activation in response to Ang II leading to Ca^{2+} release in PAMSCs.

2. The second hypothesis of this dissertation states that the expression and activity of CD38 is altered by CH in PASMCs. CH induces the upregulation of CD38 expression in PASMCs in both *in vivo* and *in vitro* experiments. In particular, the activity of CD38 in PA smooth muscle from hypoxic rat was significantly increased compared to that from normoxic control rat, whereas the same activity in whole lung was decreased, suggesting a specific CD38 upregulation in hypoxic PA. AICR is significantly increased in hypoxic PASMCs both *in vivo and in vitro*. The difference between AICR in CH and normoxic PASMCs is completely abolished by the inhibition of CD38, indicating that CH stimulates the enhancement of CD38 activity in PASMCs. The CH-induced upregulation of CD38 expression in isolated PASMCs is inhibited by calcineurin/NFAT pathway, indicating that CH-induced CD38 upregulation in PASMCs is mediated by the calcineurin/NFAT-pathway. Beside, the NAADP-dependent Ca^{2+} channel TPC 1 and TPC 2 is increased in CH PA. Hence, for the first time, these results clearly support our

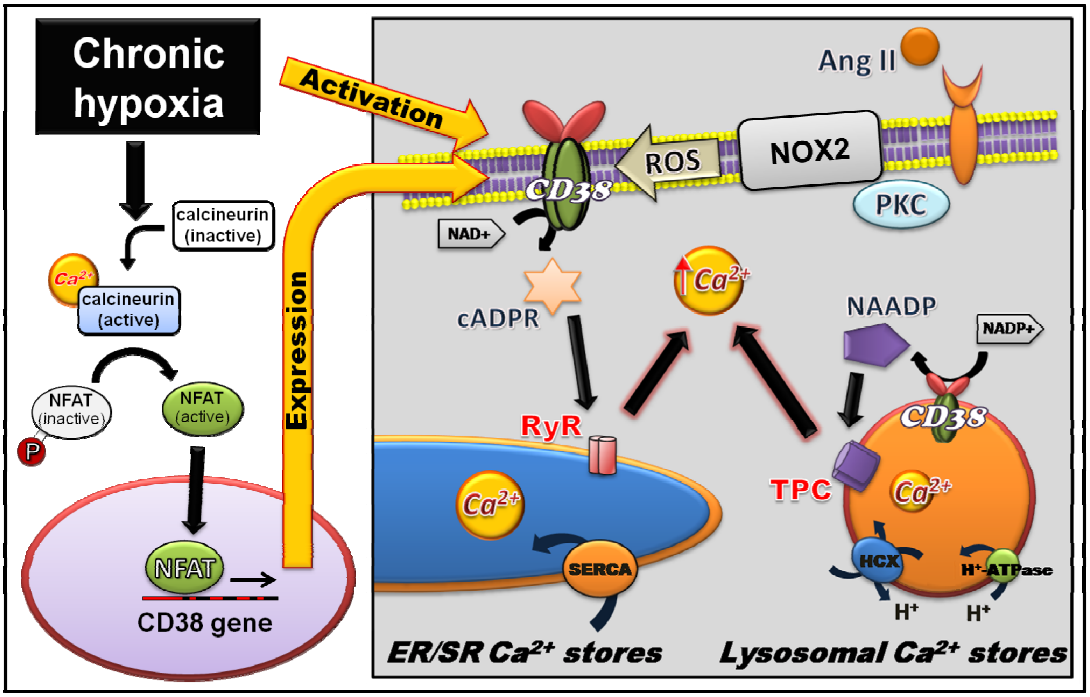

Figure 5.1. Summary of the thesis research CD38 in PASMCs plays an important role in the regulation of Ca^{2+} release from two different stores, RyR- and NAADP-gated Ca^{2+} stores activated by cADPR and NAADP, respectively. The signaling mechanism of Ang II-induced CD38 activation is mediated by PKC-NOX2-ROS pathways. CH triggers enhancement of CD38 activity and expression. In particular, CH-induced CD38 regulation is mediated by calcineurin/NFAT pathway in PASMCs.

hypothesis that CH increases the expression and activity of CD38 and the CD38-dependent Ca^{2+} release in PASMCs.

In conclusion, the results of this thesis reveal that CH triggers an increase in expression and activity of CD38, leading to alteration of Ca^{2+} homeostasis through increased Ca^{2+} in PASMCs. These results may suggest that CD38 is associated with development of CHPH and is a novel therapeutic target for pulmonary vasculature disease.

Future directions

While the experimental results revealed the novel aspects of expression and function of CD38 in PASMCs, particularly related to the alteration of Ca^{2+} signaling in the CHPH model, it also opens up many interesting directions for future research.

First, it is important to explore the detailed mechanism of how CH induces CD38 upregulation beyond the calcineurin/NFAT-dependent pathway. For example, the role of hypoxia-inducible factor-1 (HIF-1) in the regulation of CD38 expression in PASMCs during CH has not been adequately described. It will be interesting to examine whether there is any interactions between HIF-1 and NFAT-pathways in the regulation of CD38 in CH PASMCs. Further researches are required for establishing the translational mechanism of CH-induced upregulation of CD38 in PASMCs.

Secondly, future studies should provide evidence as to whether increased CD38 expression and activity contribute to the alteration of PA properties such as myogenic tone and vasoreactivity in CHPH. It is well known that CH contributes to augmented vasoreactivity in mouse PA [75,211]. However, it is still unknown whether CD38 contributes to changes in pulmonary vascular physiology through regulation of intracellular Ca^{2+} release during CHPH. These questions could be approached using the measurement of isometric contraction in PA smooth muscle tissues from CH rat in the presence of inhibitors for CD38-dependent mechanism (e.g., nicotinamide, 8-brom-cADPR, and Ned-19), similar to the methods in chapter 2. In addition to the findings in chapter 4, such evidence could elucidate how the changes in mechanism of Ca^{2+} release potentiate and contribute to the development of vascular remodeling during CHPH.

Finally, it is important to further explore the roles and mechanisms of other CD38 agonists that are clearly associated with CHPH. ET-1 is a potential candidate and plays an important role in Ca^{2+} regulation during CH by altering the activity of Ca^{2+} regulatory molecules including augmentation of NCX and the voltage-gated Ca^{2+} channel, inhibition of voltage-gated K^{+} channels, and increased myofilament sensitivity in PASMCs [227,277,368]. Likewise, there has been no systematic research on the signaling mechanism of ET-1-induced activation of CD38 in PASMCs. Understanding the systematic mechanism of agonist-induced CD38 activation could elicit the novel aspects and strategies for development of CHPH.

REFERENCES

1. Kahl CR, Means AR (2003) Regulation of cell cycle progression by calcium/calmodulin-dependent pathways. Endocr Rev 24: 719-736.

2. Artalejo AR, Ellory JC, Parekh AB (1998) Ca2+-dependent capacitance increases in rat basophilic leukemia cells following activation of store-operated Ca2+ entry and dialysis with high-Ca2+-containing intracellular solution. Pflugers Arch 436: 934-939.

3. Malcuit C, Kurokawa M, Fissore RA (2006) Calcium oscillations and mammalian egg activation. J Cell Physiol 206: 565-573.

4. Endo M (2009) Calcium-induced calcium release in skeletal muscle. Physiol Rev 89: 1153-1176.

5. Fomina AF, Nowycky MC (1999) A current activated on depletion of intracellular Ca2+ stores can regulate exocytosis in adrenal chromaffin cells. J Neurosci 19: 3711-3722.

6. Wu XS, McNeil BD, Xu J, Fan J, Xue L, et al. (2009) Ca(2+) and calmodulin initiate all forms of endocytosis during depolarization at a nerve terminal. Nat Neurosci 12: 1003-1010.

7. Clapham DE (2007) Calcium signaling. Cell 131: 1047-1058.

8. Berridge MJ, Lipp P, Bootman MD (2000) The versatility and universality of calcium signalling. Nat Rev Mol Cell Biol 1: 11-21.

9. Allen DG, Eisner DA, Orchard CH (1984) Factors influencing free intracellular calcium concentration in quiescent ferret ventricular muscle. J Physiol 350: 615-630.

10. Eltit JM, Yang T, Li H, Molinski TF, Pessah IN, et al. (2010) RyR1-mediated Ca2+ leak and Ca2+ entry determine resting intracellular Ca2+ in skeletal myotubes. J Biol Chem 285: 13781-13787.

11. Kahn AM, Seidel CL, Allen JC, O'Neil RG, Shelat H, et al. (1993) Insulin reduces contraction and intracellular calcium concentration in vascular smooth muscle. Hypertension 22: 735-742.

12. Parfitt AM (1987) Bone and plasma calcium homeostasis. Bone 8 Suppl 1: S1-8.

13. Borle AB (1981) Control, Modulation, and regulation of cell calcium. Rev Physiol Biochem Pharmacol 90: 13-153.

14. Berridge MJ, Bootman MD, Roderick HL (2003) Calcium signalling: dynamics, homeostasis and remodelling. Nat Rev Mol Cell Biol 4: 517-529.

15. Parekh AB, Putney JW, Jr. (2005) Store-operated calcium channels. Physiol Rev 85: 757-810.

16. Petersen OH (1988) Calcium channels. Nature 336: 528.

17. Petersen OH, Gerasimenko OV, Gerasimenko JV, Mogami H, Tepikin AV (1998) The calcium store in the nuclear envelope. Cell Calcium 23: 87-90.

18. Walsh MP (1994) Calmodulin and the regulation of smooth muscle contraction. Mol Cell Biochem 135: 21-41.

19. Gao N, Huang J, He W, Zhu M, Kamm KE, et al. (2013) Signaling through myosin light chain kinase in smooth muscles. J Biol Chem 288: 7596-7605.

20. Gao Y, Ye LH, Kishi H, Okagaki T, Samizo K, et al. (2001) Myosin light chain kinase as a multifunctional regulatory protein of smooth muscle contraction. IUBMB Life 51: 337-344.

21. Yang XR, Lin MJ, Sham JS (2010) Physiological functions of transient receptor potential channels in pulmonary arterial smooth muscle cells. Adv Exp Med Biol 661: 109-122.

22. Guibert C, Ducret T, Savineau JP (2008) Voltage-independent calcium influx in smooth muscle. Prog Biophys Mol Biol 98: 10-23.

23. Ertel EA, Campbell KP, Harpold MM, Hofmann F, Mori Y, et al. (2000) Nomenclature of voltage-gated calcium channels. Neuron 25: 533-535.

24. Wanstall JC, O'Donnell SR (1989) Age influences responses of rat isolated aorta and pulmonary artery to the calcium channel agonist, Bay K 8664, and to potassium and calcium. J Cardiovasc Pharmacol 13: 709-714.

25. Leach RM, Twort CH, Cameron IR, Ward JP (1992) A comparison of the pharmacological and mechanical properties in vitro of large and small pulmonary arteries of the rat. Clin Sci (Lond) 82: 55-62.

26. Mikkelsen E, Pedersen OL (1983) Regional differences in the response of isolated human vessels to vasoactive substances. Gen Pharmacol 14: 89-90.

27. Abd El-Rahman RR, Harraz OF, Brett SE, Anfinogenova Y, Mufti RE, et al. (2013) Identification of L- and T-type Ca2+ channels in rat cerebral arteries: role in myogenic tone development. Am J Physiol Heart Circ Physiol 304: H58-71.

28. Schleifer KJ (1999) Stereoselective characterization of the 1,4-dihydropyridine binding site at L-type calcium channels in the resting state and the opened/inactivated state. J Med Chem 42: 2204-2211.

29. Hansen PB, Poulsen CB, Walter S, Marcussen N, Cribbs LL, et al. (2011) Functional importance of L- and P/Q-type voltage-gated calcium channels in human renal vasculature. Hypertension 58: 464-470.

30. Rodman DM, Reese K, Harral J, Fouty B, Wu S, et al. (2005) Low-voltage-activated (T-type) calcium channels control proliferation of human pulmonary artery myocytes. Circ Res 96: 864-872.

31. Firth AL, Remillard CV, Platoshyn O, Fantozzi I, Ko EA, et al. (2011) Functional ion channels in human pulmonary artery smooth muscle cells: Voltage-dependent cation channels. Pulm Circ 1: 48-71.

32. Sommer N, Dietrich A, Schermuly RT, Ghofrani HA, Gudermann T, et al. (2008) Regulation of hypoxic pulmonary vasoconstriction: basic mechanisms. Eur Respir J 32: 1639-1651.

33. McMurtry IF (1985) BAY K 8644 potentiates and A23187 inhibits hypoxic vasoconstriction in rat lungs. Am J Physiol 249: H741-746.

34. Rodman DM, Harral J, Wu S, West J, Hoedt-Miller M, et al. (2005) The low-voltage-activated calcium channel CAV3.1 controls proliferation of human pulmonary artery myocytes. Chest 128: 581S-582S.

35. Wan J, Yamamura A, Zimnicka AM, Voiriot G, Smith KA, et al. (2013) Chronic hypoxia selectively enhances L- and T-type voltage-dependent Ca2+ channel activity in pulmonary artery by upregulating Cav1.2 and Cav3.2. Am J Physiol Lung Cell Mol Physiol 305: L154-164.

36. Nilius B, Owsianik G (2011) The transient receptor potential family of ion channels. Genome Biol 12: 218.

37. Xia Y, Fu Z, Hu J, Huang C, Paudel O, et al. (2013) TRPV4 channel contributes to serotonin-induced pulmonary vasoconstriction and the enhanced vascular reactivity in chronic hypoxic pulmonary hypertension. Am J Physiol Cell Physiol 305: C704-715.

38. Xia Y, Yang XR, Fu Z, Paudel O, Abramowitz J, et al. (2013) Classical Transient Receptor Potential 1 and 6 Contribute to Hypoxic Pulmonary Hypertension Through Differential Regulation of Pulmonary Vascular Functions. Hypertension.

39. Yang XR, Lin AH, Hughes JM, Flavahan NA, Cao YN, et al. (2012) Upregulation of osmo-mechanosensitive TRPV4 channel facilitates chronic hypoxia-induced myogenic tone and pulmonary hypertension. Am J Physiol Lung Cell Mol Physiol 302: L555-568.

40. Wickman KD, Clapham DE (1995) G-protein regulation of ion channels. Curr Opin Neurobiol 5: 278-285.

41. Meng F, To WK, Gu Y (2008) Inhibition effect of arachidonic acid on hypoxia-induced [Ca(2+)](i) elevation in PC12 cells and human pulmonary artery smooth muscle cells. Respir Physiol Neurobiol 162: 18-23.

42. McFadzean I, Gibson A (2002) The developing relationship between receptor-operated and store-operated calcium channels in smooth muscle. Br J Pharmacol 135: 1-13.

43. Berridge MJ (2009) Inositol trisphosphate and calcium signalling mechanisms. Biochim Biophys Acta 1793: 933-940.

44. Hofer AM, Brown EM (2003) Extracellular calcium sensing and signalling. Nat Rev Mol Cell Biol 4: 530-538.

45. Yamamura A, Guo Q, Yamamura H, Zimnicka AM, Pohl NM, et al. (2012) Enhanced Ca(2+)-sensing receptor function in idiopathic pulmonary arterial hypertension. Circ Res 111: 469-481.

46. Putney JW, Jr. (1986) A model for receptor-regulated calcium entry. Cell Calcium 7: 1-12.

47. Hoth M, Penner R (1992) Depletion of intracellular calcium stores activates a calcium current in mast cells. Nature 355: 353-356.

48. Li SW, Westwick J, Poll CT (2002) Receptor-operated Ca2+ influx channels in leukocytes: a therapeutic target? Trends Pharmacol Sci 23: 63-70.

49. Cahalan MD (2009) STIMulating store-operated Ca(2+) entry. Nat Cell Biol 11: 669-677.

50. Baba Y, Hayashi K, Fujii Y, Mizushima A, Watarai H, et al. (2006) Coupling of STIM1 to store-operated Ca2+ entry through its constitutive and inducible movement in the endoplasmic reticulum. Proc Natl Acad Sci U S A 103: 16704-16709.

51. Brandman O, Liou J, Park WS, Meyer T (2007) STIM2 is a feedback regulator that stabilizes basal cytosolic and endoplasmic reticulum Ca2+ levels. Cell 131: 1327-1339.

52. Ng LC, Gurney AM (2001) Store-operated channels mediate Ca(2+) influx and contraction in rat pulmonary artery. Circ Res 89: 923-929.

53. Wang J, Shimoda LA, Sylvester JT (2004) Capacitative calcium entry and TRPC channel proteins are expressed in rat distal pulmonary arterial smooth muscle. Am J Physiol Lung Cell Mol Physiol 286: L848-858.

54. Ng LC, McCormack MD, Airey JA, Singer CA, Keller PS, et al. (2009) TRPC1 and STIM1 mediate capacitative Ca2+ entry in mouse pulmonary arterial smooth muscle cells. J Physiol 587: 2429-2442.

55. Salido GM, Jardin I, Rosado JA (2011) The TRPC ion channels: association with Orai1 and STIM1 proteins and participation in capacitative and non-capacitative calcium entry. Adv Exp Med Biol 704: 413-433.

56. Ng LC, Ramduny D, Airey JA, Singer CA, Keller PS, et al. (2010) Orai1 interacts with STIM1 and mediates capacitative Ca2+ entry in mouse pulmonary arterial smooth muscle cells. Am J Physiol Cell Physiol 299: C1079-1090.

57. Penna A, Demuro A, Yeromin AV, Zhang SL, Safrina O, et al. (2008) The CRAC channel consists of a tetramer formed by Stim-induced dimerization of Orai dimers. Nature 456: 116-120.

58. Lee KP, Yuan JP, Hong JH, So I, Worley PF, et al. (2010) An endoplasmic reticulum/plasma membrane junction: STIM1/Orai1/TRPCs. FEBS Lett 584: 2022-2027.

59. Syed NI, Tengah A, Paul A, Kennedy C (2010) Characterisation of P2X receptors expressed in rat pulmonary arteries. Eur J Pharmacol 649: 342-348.

60. Nassar T, Yarovoi S, Fanne RA, Waked O, Allen TC, et al. (2011) Urokinase plasminogen activator regulates pulmonary arterial contractility and vascular permeability in mice. Am J Respir Cell Mol Biol 45: 1015-1021.

61. Cheng KT, Chan FL, Huang Y, Chan WY, Yao X (2003) Expression of olfactory-type cyclic nucleotide-gated channel (CNGA2) in vascular tissues. Histochem Cell Biol 120: 475-481.

62. Yao X, Leung PS, Kwan HY, Wong TP, Fong MW (1999) Rod-type cyclic nucleotide-gated cation channel is expressed in vascular endothelium and vascular smooth muscle cells. Cardiovasc Res 41: 282-290.

63. Pauvert O, Lugnier C, Keravis T, Marthan R, Rousseau E, et al. (2003) Effect of sildenafil on cyclic nucleotide phosphodiesterase activity, vascular tone and calcium signaling in rat pulmonary artery. Br J Pharmacol 139: 513-522.

64. Standen NB, Quayle JM (1998) K+ channel modulation in arterial smooth muscle. Acta Physiol Scand 164: 549-557.

65. Clapp LH, Gurney AM (1992) ATP-sensitive K+ channels regulate resting potential of pulmonary arterial smooth muscle cells. Am J Physiol 262: H916-920.

66. Yuan XJ, Wang J, Juhaszova M, Golovina VA, Rubin LJ (1998) Molecular basis and function of voltage-gated K+ channels in pulmonary arterial smooth muscle cells. Am J Physiol 274: L621-635.

67. Albarwani S, Robertson BE, Nye PC, Kozlowski RZ (1994) Biophysical properties of Ca(2+)- and Mg-ATP-activated K+ channels in pulmonary arterial smooth muscle cells isolated from the rat. Pflugers Arch 428: 446-454.

68. Gutman GA, Chandy KG, Adelman JP, Aiyar J, Bayliss DA, et al. (2003) International Union of Pharmacology. XLI. Compendium of voltage-gated ion channels: potassium channels. Pharmacol Rev 55: 583-586.

69. Remillard CV, Yuan JX (2005) High altitude pulmonary hypertension: role of K+ and Ca2+ channels. High Alt Med Biol 6: 133-146.

70. Yuan XJ (1995) Voltage-gated K+ currents regulate resting membrane potential and [Ca2+]i in pulmonary arterial myocytes. Circ Res 77: 370-378.

71. Brayden JE, Nelson MT (1992) Regulation of arterial tone by activation of calcium-dependent potassium channels. Science 256: 532-535.

72. Berkefeld H, Fakler B, Schulte U (2010) Ca2+-activated K+ channels: from protein complexes to function. Physiol Rev 90: 1437-1459.

73. Zhang WM, Yip KP, Lin MJ, Shimoda LA, Li WH, et al. (2003) ET-1 activates Ca2+ sparks in PASMC: local Ca2+ signaling between inositol trisphosphate and ryanodine receptors. Am J Physiol Lung Cell Mol Physiol 285: L680-690.

74. Hartzell C, Putzier I, Arreola J (2005) Calcium-activated chloride channels. Annu Rev Physiol 67: 719-758.

75. Sun H, Xia Y, Paudel O, Yang XR, Sham JS (2012) Chronic hypoxia-induced upregulation of Ca2+-activated Cl- channel in pulmonary arterial myocytes: a mechanism contributing to enhanced vasoreactivity. J Physiol.

76. Yuan XJ (1997) Role of calcium-activated chloride current in regulating pulmonary vasomotor tone. Am J Physiol 272: L959-968.

77. Yang YD, Cho H, Koo JY, Tak MH, Cho Y, et al. (2008) TMEM16A confers receptor-activated calcium-dependent chloride conductance. Nature 455: 1210-1215.

78. Manoury B, Tamuleviciute A, Tammaro P (2010) TMEM16A/anoctamin 1 protein mediates calcium-activated chloride currents in pulmonary arterial smooth muscle cells. J Physiol 588: 2305-2314.

79. Forrest AS, Joyce TC, Huebner ML, Ayon RJ, Wiwchar M, et al. (2012) Increased TMEM16A-encoded calcium-activated chloride channel activity is associated with pulmonary hypertension. Am J Physiol Cell Physiol 303: C1229-1243.

80. Albrieux M, Lee HC, Villaz M (1998) Calcium signaling by cyclic ADP-ribose, NAADP, and inositol trisphosphate are involved in distinct functions in ascidian oocytes. J Biol Chem 273: 14566-14574.

81. Zhu MX, Ma J, Parrington J, Galione A, Evans AM (2010) TPCs: Endolysosomal channels for Ca2+ mobilization from acidic organelles triggered by NAADP. FEBS Lett 584: 1966-1974.

82. Lanner JT, Georgiou DK, Joshi AD, Hamilton SL (2010) Ryanodine receptors: structure, expression, molecular details, and function in calcium release. Cold Spring Harb Perspect Biol 2: a003996.

83. Berridge MJ (1993) Inositol trisphosphate and calcium signalling. Nature 361: 315-325.

84. Patel S, Joseph SK, Thomas AP (1999) Molecular properties of inositol 1,4,5-trisphosphate receptors. Cell Calcium 25: 247-264.

85. Yoshikawa F, Iwasaki H, Michikawa T, Furuichi T, Mikoshiba K (1999) Cooperative formation of the ligand-binding site of the inositol 1,4, 5-trisphosphate receptor by two separable domains. J Biol Chem 274: 328-334.

86. Narayanan D, Adebiyi A, Jaggar JH (2012) Inositol trisphosphate receptors in smooth muscle cells. Am J Physiol Heart Circ Physiol 302: H2190-2210.

87. Mikoshiba K (2007) The IP3 receptor/Ca2+ channel and its cellular function. Biochem Soc Symp: 9-22.

88. Ozawa T (2008) Effects of FK506 on ca release channels (review). Perspect Medicin Chem 2: 51-55.

89. Miyakawa T, Mizushima A, Hirose K, Yamazawa T, Bezprozvanny I, et al. (2001) Ca(2+)-sensor region of IP(3) receptor controls intracellular Ca(2+) signaling. EMBO J 20: 1674-1680.

90. Bultynck G, Sienaert I, Parys JB, Callewaert G, De Smedt H, et al. (2003) Pharmacology of inositol trisphosphate receptors. Pflugers Arch 445: 629-642.

91. Janiak R, Wilson SM, Montague S, Hume JR (2001) Heterogeneity of calcium stores and elementary release events in canine pulmonary arterial smooth muscle cells. Am J Physiol Cell Physiol 280: C22-33.

92. Weidelt T, Isenberg G (2000) Augmentation of SR Ca(2+) release by rapamycin and FK506 causes K(+)-channel activation and membrane hyperpolarization in bladder smooth muscle. Br J Pharmacol 129: 1293-1300.

93. Yang XR, Lin MJ, Yip KP, Jeyakumar LH, Fleischer S, et al. (2005) Multiple ryanodine receptor subtypes and heterogeneous ryanodine receptor-gated Ca2+ stores in pulmonary arterial smooth muscle cells. Am J Physiol Lung Cell Mol Physiol 289: L338-348.

94. Takeshima H, Nishimura S, Matsumoto T, Ishida H, Kangawa K, et al. (1989) Primary structure and expression from complementary DNA of skeletal muscle ryanodine receptor. Nature 339: 439-445.

95. Endo M, Tanaka M, Ogawa Y (1970) Calcium induced release of calcium from the sarcoplasmic reticulum of skinned skeletal muscle fibres. Nature 228: 34-36.

96. Bouchard R, Pattarini R, Geiger JD (2003) Presence and functional significance of presynaptic ryanodine receptors. Prog Neurobiol 69: 391-418.

97. Hakamata Y, Nakai J, Takeshima H, Imoto K (1992) Primary structure and distribution of a novel ryanodine receptor/calcium release channel from rabbit brain. FEBS Lett 312: 229-235.

98. Timerman AP, Ogunbumni E, Freund E, Wiederrecht G, Marks AR, et al. (1993) The calcium release channel of sarcoplasmic reticulum is modulated by FK-506-binding protein. Dissociation and reconstitution of FKBP-12 to the calcium release channel of skeletal muscle sarcoplasmic reticulum. J Biol Chem 268: 22992-22999.

99. Lee HC, Aarhus R (1991) ADP-ribosyl cyclase: an enzyme that cyclizes NAD+ into a calcium-mobilizing metabolite. Cell Regul 2: 203-209.

100. Lee HC (1993) Potentiation of calcium- and caffeine-induced calcium release by cyclic ADP-ribose. J Biol Chem 268: 293-299.

101. Wang YX, Zheng YM, Mei QB, Wang QS, Collier ML, et al. (2004) FKBP12.6 and cADPR regulation of Ca2+ release in smooth muscle cells. Am J Physiol Cell Physiol 286: C538-546.

102. Nelson MT, Cheng H, Rubart M, Santana LF, Bonev AD, et al. (1995) Relaxation of arterial smooth muscle by calcium sparks. Science 270: 633-637.

103. Jaggar JH, Porter VA, Lederer WJ, Nelson MT (2000) Calcium sparks in smooth muscle. Am J Physiol Cell Physiol 278: C235-256.

104. Rios E, Brum G (1987) Involvement of dihydropyridine receptors in excitation-contraction coupling in skeletal muscle. Nature 325: 717-720.

105. Endo M (2005) Mechanisms of calcium release from the sarcoplasmic reticulum in skeletal muscle. Adv Exp Med Biol 565: 233-247; discussion 247, 397-403.

106. Endo M (2007) Calcium-induced release of calcium from the sarcoplasmic reticulum. Adv Exp Med Biol 592: 275-285.

107. Lohn M, Jessner W, Furstenau M, Wellner M, Sorrentino V, et al. (2001) Regulation of calcium sparks and spontaneous transient outward currents by RyR3 in arterial vascular smooth muscle cells. Circ Res 89: 1051-1057.

108. Lohn M, Furstenau M, Sagach V, Elger M, Schulze W, et al. (2000) Ignition of calcium sparks in arterial and cardiac muscle through caveolae. Circ Res 87: 1034-1039.

109. Smani T, Iwabuchi S, Lopez-Barneo J, Urena J (2001) Differential segmental activation of Ca2+ -dependent CI-and K+ channels in pulmonary arterial myocytes. Cell Calcium 29: 369-377.

110. Remillard CV, Zhang WM, Shimoda LA, Sham JS (2002) Physiological properties and functions of Ca(2+) sparks in rat intrapulmonary arterial smooth muscle cells. Am J Physiol Lung Cell Mol Physiol 283: L433-444.

111. Zhang F, Xia M, Li PL (2010) Lysosome-dependent Ca(2+) release response to Fas activation in coronary arterial myocytes through NAADP: evidence from CD38 gene knockouts. Am J Physiol Cell Physiol 298: C1209-1216.

112. Chini EN, Beers KW, Dousa TP (1995) Nicotinate adenine dinucleotide phosphate (NAADP) triggers a specific calcium release system in sea urchin eggs. J Biol Chem 270: 3216-3223.

113. Patel S, Ramakrishnan L, Rahman T, Hamdoun A, Marchant JS, et al. (2011) The endo-lysosomal system as an NAADP-sensitive acidic Ca(2+) store: role for the two-pore channels. Cell Calcium 50: 157-167.

114. Jiang YL, Lin AH, Xia Y, Lee S, Paudel O, et al. (2013) Nicotinic acid adenine dinucleotide phosphate (NAADP) activates global and heterogeneous local Ca2+ signals from NAADP- and ryanodine receptor-gated Ca2+ stores in pulmonary arterial myocytes. J Biol Chem 288: 10381-10394.

115. Lee HC (2012) Cyclic ADP-ribose and nicotinic acid adenine dinucleotide phosphate (NAADP) as messengers for calcium mobilization. J Biol Chem 287: 31633-31640.

116. Guse AH, Lee HC (2008) NAADP: a universal Ca2+ trigger. Sci Signal 1: re10.

117. Calcraft PJ, Ruas M, Pan Z, Cheng X, Arredouani A, et al. (2009) NAADP mobilizes calcium from acidic organelles through two-pore channels. Nature 459: 596-600.

118. Ruas M, Rietdorf K, Arredouani A, Davis LC, Lloyd-Evans E, et al. (2010) Purified TPC isoforms form NAADP receptors with distinct roles for Ca(2+) signaling and endolysosomal trafficking. Curr Biol 20: 703-709.

119. Zhang F, Zhang G, Zhang AY, Koeberl MJ, Wallander E, et al. (2006) Production of NAADP and its role in Ca2+ mobilization associated with lysosomes in coronary arterial myocytes. Am J Physiol Heart Circ Physiol 291: H274-282.

120. Thai TL, Churchill GC, Arendshorst WJ (2009) NAADP receptors mediate calcium signaling stimulated by endothelin-1 and norepinephrine in renal afferent arterioles. Am J Physiol Renal Physiol 297: F510-516.

121. Kinnear NP, Boittin FX, Thomas JM, Galione A, Evans AM (2004) Lysosome-sarcoplasmic reticulum junctions. A trigger zone for calcium signaling by

nicotinic acid adenine dinucleotide phosphate and endothelin-1. J Biol Chem 279: 54319-54326.

122. Umesh A, Thompson MA, Chini EN, Yip KP, Sham JS (2006) Integrin ligands mobilize Ca2+ from ryanodine receptor-gated stores and lysosome-related acidic organelles in pulmonary arterial smooth muscle cells. J Biol Chem 281: 34312-34323.

123. Reinherz EL, Kung PC, Goldstein G, Levey RH, Schlossman SF (1980) Discrete stages of human intrathymic differentiation: analysis of normal thymocytes and leukemic lymphoblasts of T-cell lineage. Proc Natl Acad Sci U S A 77: 1588-1592.

124. Ramaschi G, Torti M, Festetics ET, Sinigaglia F, Malavasi F, et al. (1996) Expression of cyclic ADP-ribose-synthetizing CD38 molecule on human platelet membrane. Blood 87: 2308-2313.

125. Chini EN (2009) CD38 as a regulator of cellular NAD: a novel potential pharmacological target for metabolic conditions. Curr Pharm Des 15: 57-63.

126. Lee HC (2006) Structure and enzymatic functions of human CD38. Mol Med 12: 317-323.

127. Clapper DL, Walseth TF, Dargie PJ, Lee HC (1987) Pyridine nucleotide metabolites stimulate calcium release from sea urchin egg microsomes desensitized to inositol trisphosphate. J Biol Chem 262: 9561-9568.

128. Lee HC, Aarhus R (1993) Wide distribution of an enzyme that catalyzes the hydrolysis of cyclic ADP-ribose. Biochim Biophys Acta 1164: 68-74.

129. Bai N, Lee HC, Laher I (2005) Emerging role of cyclic ADP-ribose (cADPR) in smooth muscle. Pharmacol Ther 105: 189-207.

130. Lee HC, Walseth TF, Bratt GT, Hayes RN, Clapper DL (1989) Structural determination of a cyclic metabolite of NAD+ with intracellular Ca2+-mobilizing activity. J Biol Chem 264: 1608-1615.

131. Lee HC, Aarhus R, Graeff R, Gurnack ME, Walseth TF (1994) Cyclic ADP ribose activation of the ryanodine receptor is mediated by calmodulin. Nature 370: 307-309.

132. Galione A, White A (1994) Ca2+ release induced by cyclic ADP-ribose. Trends Cell Biol 4: 431-436.

133. Galione A, Churchill GC (2000) Cyclic ADP ribose as a calcium-mobilizing messenger. Sci STKE 2000: PE1.

134. Tang WX, Chen YF, Zou AP, Campbell WB, Li PL (2002) Role of FKBP12.6 in cADPR-induced activation of reconstituted ryanodine receptors from arterial smooth muscle. Am J Physiol Heart Circ Physiol 282: H1304-1310.

135. Noguchi N, Takasawa S, Nata K, Tohgo A, Kato I, et al. (1997) Cyclic ADP-ribose binds to FK506-binding protein 12.6 to release Ca2+ from islet microsomes. J Biol Chem 272: 3133-3136.

136. Yamasaki-Mann M, Demuro A, Parker I (2009) cADPR stimulates SERCA activity in Xenopus oocytes. Cell Calcium 45: 293-299.

137. States DJ, Walseth TF, Lee HC (1992) Similarities in amino acid sequences of Aplysia ADP-ribosyl cyclase and human lymphocyte antigen CD38. Trends Biochem Sci 17: 495.

138. Jude JA, Solway J, Panettieri RA, Jr., Walseth TF, Kannan MS (2010) DIFFERENTIAL INDUCTION OF CD38 EXPRESSION BY TNF-{alpha} IN ASTHMATIC AIRWAY SMOOTH MUSCLE CELLS. Am J Physiol Lung Cell Mol Physiol.

139. Orciani M, Trubiani O, Guarnieri S, Ferrero E, Di Primio R (2008) CD38 is constitutively expressed in the nucleus of human hematopoietic cells. J Cell Biochem 105: 905-912.

140. Kang BN, Jude JA, Panettieri RA, Jr., Walseth TF, Kannan MS (2008) Glucocorticoid regulation of CD38 expression in human airway smooth muscle cells: role of dual specificity phosphatase 1. Am J Physiol Lung Cell Mol Physiol 295: L186-193.

141. Deshpande DA, White TA, Dogan S, Walseth TF, Panettieri RA, et al. (2005) CD38/cyclic ADP-ribose signaling: role in the regulation of calcium homeostasis in airway smooth muscle. Am J Physiol Lung Cell Mol Physiol 288: L773-788.

142. Khoo KM, Chang CF (2002) Identification and characterization of nuclear CD38 in the rat spleen. Int J Biochem Cell Biol 34: 43-54.

143. Graeff R, Munshi C, Aarhus R, Johns M, Lee HC (2001) A single residue at the active site of CD38 determines its NAD cyclizing and hydrolyzing activities. J Biol Chem 276: 12169-12173.

144. Lee HC (2000) Enzymatic functions and structures of CD38 and homologs. Chem Immunol 75: 39-59.

145. Jackson DG, Bell JI (1990) Isolation of a cDNA encoding the human CD38 (T10) molecule, a cell surface glycoprotein with an unusual discontinuous pattern of expression during lymphocyte differentiation. J Immunol 144: 2811-2815.

146. Howard M, Grimaldi JC, Bazan JF, Lund FE, Santos-Argumedo L, et al. (1993) Formation and hydrolysis of cyclic ADP-ribose catalyzed by lymphocyte antigen CD38. Science 262: 1056-1059.

147. Takasawa S, Tohgo A, Noguchi N, Koguma T, Nata K, et al. (1993) Synthesis and hydrolysis of cyclic ADP-ribose by human leukocyte antigen CD38 and inhibition of the hydrolysis by ATP. J Biol Chem 268: 26052-26054.

148. Kim H, Jacobson EL, Jacobson MK (1993) Synthesis and degradation of cyclic ADP-ribose by NAD glycohydrolases. Science 261: 1330-1333.

149. Aarhus R, Graeff RM, Dickey DM, Walseth TF, Lee HC (1995) ADP-ribosyl cyclase and CD38 catalyze the synthesis of a calcium-mobilizing metabolite from NADP. J Biol Chem 270: 30327-30333.

150. Lee HC, Aarhus R (1995) A derivative of NADP mobilizes calcium stores insensitive to inositol trisphosphate and cyclic ADP-ribose. J Biol Chem 270: 2152-2157.

151. Churchill GC, Okada Y, Thomas JM, Genazzani AA, Patel S, et al. (2002) NAADP mobilizes Ca(2+) from reserve granules, lysosome-related organelles, in sea urchin eggs. Cell 111: 703-708.

152. Graeff R, Liu Q, Kriksunov IA, Hao Q, Lee HC (2006) Acidic residues at the active sites of CD38 and ADP-ribosyl cyclase determine nicotinic acid adenine

dinucleotide phosphate (NAADP) synthesis and hydrolysis activities. J Biol Chem 281: 28951-28957.

153. Revollo JR, Grimm AA, Imai S (2007) The regulation of nicotinamide adenine dinucleotide biosynthesis by Nampt/PBEF/visfatin in mammals. Curr Opin Gastroenterol 23: 164-170.

154. Revollo JR, Korner A, Mills KF, Satoh A, Wang T, et al. (2007) Nampt/PBEF/Visfatin regulates insulin secretion in beta cells as a systemic NAD biosynthetic enzyme. Cell Metab 6: 363-375.

155. Barbosa MT, Soares SM, Novak CM, Sinclair D, Levine JA, et al. (2007) The enzyme CD38 (a NAD glycohydrolase, EC 3.2.2.5) is necessary for the development of diet-induced obesity. FASEB J 21: 3629-3639.

156. Guse AH (2000) Cyclic ADP-ribose. J Mol Med 78: 26-35.

157. Zhao YJ, Lam CM, Lee HC (2012) The membrane-bound enzyme CD38 exists in two opposing orientations. Sci Signal 5: ra67.

158. Sumoza-Toledo A, Penner R (2011) TRPM2: a multifunctional ion channel for calcium signalling. J Physiol 589: 1515-1525.

159. Zholos A, Johnson C, Burdyga T, Melanaphy D (2011) TRPM channels in the vasculature. Adv Exp Med Biol 704: 707-729.

160. Fleig A, Penner R (2004) The TRPM ion channel subfamily: molecular, biophysical and functional features. Trends Pharmacol Sci 25: 633-639.

161. Lange I, Yamamoto S, Partida-Sanchez S, Mori Y, Fleig A, et al. (2009) TRPM2 functions as a lysosomal Ca2+-release channel in beta cells. Sci Signal 2: ra23.

162. Sano Y, Inamura K, Miyake A, Mochizuki S, Yokoi H, et al. (2001) Immunocyte Ca2+ influx system mediated by LTRPC2. Science 293: 1327-1330.

163. Beck A, Kolisek M, Bagley LA, Fleig A, Penner R (2006) Nicotinic acid adenine dinucleotide phosphate and cyclic ADP-ribose regulate TRPM2 channels in T lymphocytes. FASEB J 20: 962-964.

164. Inamura K, Sano Y, Mochizuki S, Yokoi H, Miyake A, et al. (2003) Response to ADP-ribose by activation of TRPM2 in the CRI-G1 insulinoma cell line. J Membr Biol 191: 201-207.

165. Deterre P, Berthelier V, Bauvois B, Dalloul A, Schuber F, et al. (2000) CD38 in T- and B-cell functions. Chem Immunol 75: 146-168.

166. Campana D, Suzuki T, Todisco E, Kitanaka A (2000) CD38 in hematopoiesis. Chem Immunol 75: 169-188.

167. Wei WJ, Sun HY, Ting KY, Zhang LH, Lee HC, et al. (2012) Inhibition of cardiomyocytes differentiation of mouse embryonic stem cells by CD38/cADPR/Ca2+ signaling pathway. J Biol Chem 287: 35599-35611.

168. Gul R, Kim SY, Park KH, Kim BJ, Kim SJ, et al. (2008) A novel signaling pathway of ADP-ribosyl cyclase activation by angiotensin II in adult rat cardiomyocytes. Am J Physiol Heart Circ Physiol 295: H77-88.

169. Higashida H, Hashii M, Yokoyama S, Hoshi N, Asai K, et al. (2001) Cyclic ADP-ribose as a potential second messenger for neuronal Ca2+ signaling. J Neurochem 76: 321-331.

170. Kadoyama K, Takahashi Y, Higashida H, Tanabe T, Yoshimoto T (2001) Cyclooxygenase-2 stimulates production of amyloid beta-peptide in

neuroblastoma x glioma hybrid NG108-15 cells. Biochem Biophys Res Commun 281: 483-490.

171. Sun L, Adebanjo OA, Moonga BS, Corisdeo S, Anandatheerthavarada HK, et al. (1999) CD38/ADP-ribosyl cyclase: A new role in the regulation of osteoclastic bone resorption. J Cell Biol 146: 1161-1172.

172. Kim SY, Cho BH, Kim UH (2010) CD38-mediated Ca2+ signaling contributes to angiotensin II-induced activation of hepatic stellate cells: attenuation of hepatic fibrosis by CD38 ablation. J Biol Chem 285: 576-582.

173. Kato I, Yamamoto Y, Fujimura M, Noguchi N, Takasawa S, et al. (1999) CD38 disruption impairs glucose-induced increases in cyclic ADP-ribose, [Ca2+]i, and insulin secretion. J Biol Chem 274: 1869-1872.

174. Cosker F, Cheviron N, Yamasaki M, Menteyne A, Lund FE, et al. (2010) The ecto-enzyme CD38 is a nicotinic acid adenine dinucleotide phosphate (NAADP) synthase that couples receptor activation to Ca2+ mobilization from lysosomes in pancreatic acinar cells. J Biol Chem 285: 38251-38259.

175. Deshpande DA, Walseth TF, Panettieri RA, Kannan MS (2003) CD38/cyclic ADP-ribose-mediated Ca2+ signaling contributes to airway smooth muscle hyper-responsiveness. FASEB J 17: 452-454.

176. Evans AM, Dipp M (2002) Hypoxic pulmonary vasoconstriction: cyclic adenosine diphosphate-ribose, smooth muscle Ca(2+) stores and the endothelium. Respir Physiol Neurobiol 132: 3-15.

177. Dipp M, Nye PC, Evans AM (2001) Hypoxic release of calcium from the sarcoplasmic reticulum of pulmonary artery smooth muscle. Am J Physiol Lung Cell Mol Physiol 281: L318-325.

178. Fukushi Y, Kato I, Takasawa S, Sasaki T, Ong BH, et al. (2001) Identification of cyclic ADP-ribose-dependent mechanisms in pancreatic muscarinic Ca(2+) signaling using CD38 knockout mice. J Biol Chem 276: 649-655.

179. Partida-Sanchez S, Cockayne DA, Monard S, Jacobson EL, Oppenheimer N, et al. (2001) Cyclic ADP-ribose production by CD38 regulates intracellular calcium release, extracellular calcium influx and chemotaxis in neutrophils and is required for bacterial clearance in vivo. Nat Med 7: 1209-1216.

180. Andrade MC, Ferreira SB, Goncalves LC, De-Paula AM, de Faria ES, et al. (2013) Cell surface markers for T and B lymphocytes activation and adhesion as putative prognostic biomarkers for head and neck squamous cell carcinoma. Hum Immunol.

181. Nakayama S, Yokote T, Hirata Y, Iwaki K, Akioka T, et al. (2012) Immunohistological analysis in diagnosis of plasma cell myeloma based on cytoplasmic kappa/lambda ratio of CD38-positive plasma cells. Hematology 17: 317-320.

182. de Weers M, Tai YT, van der Veer MS, Bakker JM, Vink T, et al. (2011) Daratumumab, a novel therapeutic human CD38 monoclonal antibody, induces killing of multiple myeloma and other hematological tumors. J Immunol 186: 1840-1848.

183. Polzonetti V, Carpi FM, Micozzi D, Pucciarelli S, Vincenzetti S, et al. (2012) Population variability in CD38 activity: correlation with age and significant effect of TNF-alpha -308G>A and CD38 184C>G SNPs. Mol Genet Metab 105: 502-507.

184. Sobko EA, Kraposhina A, Demko IV, Salmina AB (2013) [CD38/ADP-ribosyl cyclase, a marker of endothelial dysfunction in bronchial asthma]. Klin Med (Mosk) 91: 34-38.

185. Cockayne DA, Muchamuel T, Grimaldi JC, Muller-Steffner H, Randall TD, et al. (1998) Mice deficient for the ecto-nicotinamide adenine dinucleotide glycohydrolase CD38 exhibit altered humoral immune responses. Blood 92: 1324-1333.

186. Mitsui-Saito M, Kato I, Takasawa S, Okamoto H, Yanagisawa T (2003) CD38 gene disruption inhibits the contraction induced by alpha-adrenoceptor stimulation in mouse aorta. J Vet Med Sci 65: 1325-1330.

187. de Toledo FG, Cheng J, Liang M, Chini EN, Dousa TP (2000) ADP-Ribosyl cyclase in rat vascular smooth muscle cells: properties and regulation. Circ Res 86: 1153-1159.

188. Jia SJ, Jin S, Zhang F, Yi F, Dewey WL, et al. (2008) Formation and function of ceramide-enriched membrane platforms with CD38 during M1-receptor stimulation in bovine coronary arterial myocytes. Am J Physiol Heart Circ Physiol 295: H1743-1752.

189. Yu JZ, Zhang DX, Zou AP, Campbell WB, Li PL (2000) Nitric oxide inhibits Ca(2+) mobilization through cADP-ribose signaling in coronary arterial smooth muscle cells. Am J Physiol Heart Circ Physiol 279: H873-881.

190. de Toledo FG, Cheng J, Dousa TP (1997) Retinoic acid and triiodothyronine stimulate ADP-ribosyl cyclase activity in rat vascular smooth muscle cells. Biochem Biophys Res Commun 238: 847-850.

191. Wilson HL, Dipp M, Thomas JM, Lad C, Galione A, et al. (2001) Adp-ribosyl cyclase and cyclic ADP-ribose hydrolase act as a redox sensor. a primary role for cyclic ADP-ribose in hypoxic pulmonary vasoconstriction. J Biol Chem 276: 11180-11188.

192. Fellner SK, Arendshorst W (2007) Endothelin-A and -B receptors, superoxide, and Ca2+ signaling in afferent arterioles. Am J Physiol Renal Physiol 292: F175-184.

193. Fellner SK, Arendshorst WJ (2005) Angiotensin II Ca2+ signaling in rat afferent arterioles: stimulation of cyclic ADP ribose and IP3 pathways. Am J Physiol Renal Physiol 288: F785-791.

194. Zhang AY, Yi F, Teggatz EG, Zou AP, Li PL (2004) Enhanced production and action of cyclic ADP-ribose during oxidative stress in small bovine coronary arterial smooth muscle. Microvasc Res 67: 159-167.

195. Ge ZD, Zhang DX, Chen YF, Yi FX, Zou AP, et al. (2003) Cyclic ADP-ribose contributes to contraction and Ca2+ release by M1 muscarinic receptor activation in coronary arterial smooth muscle. J Vasc Res 40: 28-36.

196. Giulumian AD, Meszaros LG, Fuchs LC (2000) Endothelin-1-induced contraction of mesenteric small arteries is mediated by ryanodine receptor Ca2+ channels and cyclic ADP-ribose. J Cardiovasc Pharmacol 36: 758-763.

197. Arendshorst WJ, Thai TL (2009) Regulation of the renal microcirculation by ryanodine receptors and calcium-induced calcium release. Curr Opin Nephrol Hypertens 18: 40-49.

198. Yusufi AN, Cheng J, Thompson MA, Chini EN, Grande JP (2001) Nicotinic acid-adenine dinucleotide phosphate (NAADP) elicits specific microsomal Ca2+ release from mammalian cells. Biochem J 353: 531-536.

199. Yusufi AN, Cheng J, Thompson MA, Burnett JC, Grande JP (2002) Differential mechanisms of Ca(2+) release from vascular smooth muscle cell microsomes. Exp Biol Med (Maywood) 227: 36-44.

200. Boittin FX, Galione A, Evans AM (2002) Nicotinic acid adenine dinucleotide phosphate mediates Ca2+ signals and contraction in arterial smooth muscle via a two-pool mechanism. Circ Res 91: 1168-1175.

201. Vadula MS, Kleinman JG, Madden JA (1993) Effect of hypoxia and norepinephrine on cytoplasmic free Ca2+ in pulmonary and cerebral arterial myocytes. Am J Physiol 265: L591-597.

202. Sylvester JT, Shimoda LA, Aaronson PI, Ward JP (2012) Hypoxic pulmonary vasoconstriction. Physiol Rev 92: 367-520.

203. Liu Q, Sham JS, Shimoda LA, Sylvester JT (2001) Hypoxic constriction of porcine distal pulmonary arteries: endothelium and endothelin dependence. Am J Physiol Lung Cell Mol Physiol 280: L856-865.

204. Stringham R, Shah NR (2010) Pulmonary arterial hypertension: an update on diagnosis and treatment. Am Fam Physician 82: 370-377.

205. Simonneau G, Robbins IM, Beghetti M, Channick RN, Delcroix M, et al. (2009) Updated clinical classification of pulmonary hypertension. J Am Coll Cardiol 54: S43-54.

206. Rabinovitch M (2007) Pathobiology of pulmonary hypertension. Annu Rev Pathol 2: 369-399.

207. McLaughlin VV, Archer SL, Badesch DB, Barst RJ, Farber HW, et al. (2009) ACCF/AHA 2009 expert consensus document on pulmonary hypertension: a report of the American College of Cardiology Foundation Task Force on Expert Consensus Documents and the American Heart Association: developed in collaboration with the American College of Chest Physicians, American Thoracic Society, Inc., and the Pulmonary Hypertension Association. Circulation 119: 2250-2294.

208. Newman JH, Fanburg BL, Archer SL, Badesch DB, Barst RJ, et al. (2004) Pulmonary arterial hypertension: future directions: report of a National Heart, Lung and Blood Institute/Office of Rare Diseases workshop. Circulation 109: 2947-2952.

209. Orchard CH, Sanchez de Leon R, Sykes MK (1983) The relationship between hypoxic pulmonary vasoconstriction and arterial oxygen tension in the intact dog. J Physiol 338: 61-74.

210. Marshall BE, Marshall C, Benumof J, Saidman LJ (1981) Hypoxic pulmonary vasoconstriction in dogs: effects of lung segment size and oxygen tension. J Appl Physiol 51: 1543-1551.

211. Shimoda LA, Sham JS, Sylvester JT (2000) Altered pulmonary vasoreactivity in the chronically hypoxic lung. Physiol Res 49: 549-560.

212. Miao Q, Shi XP, Ye MX, Zhang J, Miao S, et al. (2012) Polydatin Attenuates Hypoxic Pulmonary Hypertension and Reverses Remodeling through Protein Kinase C Mechanisms. Int J Mol Sci 13: 7776-7787.

213. Berger MM, Dehnert C, Bailey DM, Luks AM, Menold E, et al. (2009) Transpulmonary plasma ET-1 and nitrite differences in high altitude pulmonary hypertension. High Alt Med Biol 10: 17-24.

214. Yu AY, Shimoda LA, Iyer NV, Huso DL, Sun X, et al. (1999) Impaired physiological responses to chronic hypoxia in mice partially deficient for hypoxia-inducible factor 1alpha. J Clin Invest 103: 691-696.

215. Bonnet S, Rochefort G, Sutendra G, Archer SL, Haromy A, et al. (2007) The nuclear factor of activated T cells in pulmonary arterial hypertension can be therapeutically targeted. Proc Natl Acad Sci U S A 104: 11418-11423.

216. Bierer R, Nitta CH, Friedman J, Codianni S, de Frutos S, et al. (2011) NFATc3 is required for chronic hypoxia-induced pulmonary hypertension in adult and neonatal mice. Am J Physiol Lung Cell Mol Physiol 301: L872-880.

217. de Frutos S, Caldwell E, Nitta CH, Kanagy NL, Wang J, et al. (2010) NFATc3 contributes to intermittent hypoxia-induced arterial remodeling in mice. Am J Physiol Heart Circ Physiol 299: H356-363.

218. Steudel W, Scherrer-Crosbie M, Bloch KD, Weimann J, Huang PL, et al. (1998) Sustained pulmonary hypertension and right ventricular hypertrophy after chronic hypoxia in mice with congenital deficiency of nitric oxide synthase 3. J Clin Invest 101: 2468-2477.

219. DiCarlo VS, Chen SJ, Meng QC, Durand J, Yano M, et al. (1995) ETA-receptor antagonist prevents and reverses chronic hypoxia-induced pulmonary hypertension in rat. Am J Physiol 269: L690-697.

220. Keegan A, Morecroft I, Smillie D, Hicks MN, MacLean MR (2001) Contribution of the 5-HT(1B) receptor to hypoxia-induced pulmonary hypertension: converging evidence using 5-HT(1B)-receptor knockout mice and the 5-HT(1B/1D)-receptor antagonist GR127935. Circ Res 89: 1231-1239.

221. Launay JM, Herve P, Peoc'h K, Tournois C, Callebert J, et al. (2002) Function of the serotonin 5-hydroxytryptamine 2B receptor in pulmonary hypertension. Nat Med 8: 1129-1135.

222. MacLean MR, Morecroft I (2001) Increased contractile response to 5-hydroxytryptamine1-receptor stimulation in pulmonary arteries from chronic hypoxic rats: role of pharmacological synergy. Br J Pharmacol 134: 614-620.

223. Sakurada S, Okamoto H, Takuwa N, Sugimoto N, Takuwa Y (2001) Rho activation in excitatory agonist-stimulated vascular smooth muscle. Am J Physiol Cell Physiol 281: C571-578.

224. Homma N, Nagaoka T, Morio Y, Ota H, Gebb SA, et al. (2007) Endothelin-1 and serotonin are involved in activation of RhoA/Rho kinase signaling in the

chronically hypoxic hypertensive rat pulmonary circulation. J Cardiovasc Pharmacol 50: 697-702.

225. Ward JP, McMurtry IF (2009) Mechanisms of hypoxic pulmonary vasoconstriction and their roles in pulmonary hypertension: new findings for an old problem. Curr Opin Pharmacol 9: 287-296.

226. Bailly K, Ridley AJ, Hall SM, Haworth SG (2004) RhoA activation by hypoxia in pulmonary arterial smooth muscle cells is age and site specific. Circ Res 94: 1383-1391.

227. Weigand L, Sylvester JT, Shimoda LA (2006) Mechanisms of endothelin-1-induced contraction in pulmonary arteries from chronically hypoxic rats. Am J Physiol Lung Cell Mol Physiol 290: L284-290.

228. Liu JQ, Zelko IN, Erbynn EM, Sham JS, Folz RJ (2006) Hypoxic pulmonary hypertension: role of superoxide and NADPH oxidase (gp91phox). Am J Physiol Lung Cell Mol Physiol 290: L2-10.

229. Fike CD, Slaughter JC, Kaplowitz MR, Zhang Y, Aschner JL (2008) Reactive oxygen species from NADPH oxidase contribute to altered pulmonary vascular responses in piglets with chronic hypoxia-induced pulmonary hypertension. Am J Physiol Lung Cell Mol Physiol 295: L881-888.

230. Hoshikawa Y, Ono S, Suzuki S, Tanita T, Chida M, et al. (2001) Generation of oxidative stress contributes to the development of pulmonary hypertension induced by hypoxia. J Appl Physiol (1985) 90: 1299-1306.

231. Jankov RP, Kantores C, Pan J, Belik J (2008) Contribution of xanthine oxidase-derived superoxide to chronic hypoxic pulmonary hypertension in neonatal rats. Am J Physiol Lung Cell Mol Physiol 294: L233-245.

232. Zaidi SH, You XM, Ciura S, Husain M, Rabinovitch M (2002) Overexpression of the serine elastase inhibitor elafin protects transgenic mice from hypoxic pulmonary hypertension. Circulation 105: 516-521.

233. Ooi CY, Wang Z, Tabima DM, Eickhoff JC, Chesler NC (2010) The role of collagen in extralobar pulmonary artery stiffening in response to hypoxia-induced pulmonary hypertension. Am J Physiol Heart Circ Physiol 299: H1823-1831.

234. Platoshyn O, Yu Y, Golovina VA, McDaniel SS, Krick S, et al. (2001) Chronic hypoxia decreases K(V) channel expression and function in pulmonary artery myocytes. Am J Physiol Lung Cell Mol Physiol 280: L801-812.

235. Shimoda LA, Manalo DJ, Sham JS, Semenza GL, Sylvester JT (2001) Partial HIF-1alpha deficiency impairs pulmonary arterial myocyte electrophysiological responses to hypoxia. Am J Physiol Lung Cell Mol Physiol 281: L202-208.

236. Shimoda LA, Sylvester JT, Sham JS (1999) Chronic hypoxia alters effects of endothelin and angiotensin on K+ currents in pulmonary arterial myocytes. Am J Physiol 277: L431-439.

237. Smirnov SV, Robertson TP, Ward JP, Aaronson PI (1994) Chronic hypoxia is associated with reduced delayed rectifier K+ current in rat pulmonary artery muscle cells. Am J Physiol 266: H365-370.

238. Lin MJ, Leung GP, Zhang WM, Yang XR, Yip KP, et al. (2004) Chronic hypoxia-induced upregulation of store-operated and receptor-operated Ca2+ channels in

pulmonary arterial smooth muscle cells: a novel mechanism of hypoxic pulmonary hypertension. Circ Res 95: 496-505.

239. Shimoda LA, Wang J, Sylvester JT (2006) Ca2+ channels and chronic hypoxia. Microcirculation 13: 657-670.

240. Barlow CA, Rose P, Pulver-Kaste RA, Lounsbury KM (2006) Excitation-transcription coupling in smooth muscle. J Physiol 570: 59-64.

241. Wamhoff BR, Bowles DK, Owens GK (2006) Excitation-transcription coupling in arterial smooth muscle. Circ Res 98: 868-878.

242. Rodat L, Savineau JP, Marthan R, Guibert C (2006) Effect of chronic hypoxia on voltage-independent calcium influx activated by 5-HT in rat intrapulmonary arteries. Pflugers Arch.

243. Wang J, Weigand L, Wang W, Sylvester JT, Shimoda LA (2005) Chronic hypoxia inhibits Kv channel gene expression in rat distal pulmonary artery. Am J Physiol Lung Cell Mol Physiol 288: L1049-1058.

244. Weir EK, Olschewski A (2006) Role of ion channels in acute and chronic responses of the pulmonary vasculature to hypoxia. Cardiovasc Res 71: 630-641.

245. Moudgil R, Michelakis ED, Archer SL (2006) The role of k+ channels in determining pulmonary vascular tone, oxygen sensing, cell proliferation, and apoptosis: implications in hypoxic pulmonary vasoconstriction and pulmonary arterial hypertension. Microcirculation 13: 615-632.

246. Bonnet S, Archer SL (2007) Potassium channel diversity in the pulmonary arteries and pulmonary veins: implications for regulation of the pulmonary vasculature in health and during pulmonary hypertension. Pharmacol Ther 115: 56-69.

247. Archer SL, Souil E, Dinh-Xuan AT, Schremmer B, Mercier JC, et al. (1998) Molecular identification of the role of voltage-gated K+ channels, Kv1.5 and Kv2.1, in hypoxic pulmonary vasoconstriction and control of resting membrane potential in rat pulmonary artery myocytes. J Clin Invest 101: 2319-2330.

248. Shimoda LA, Sylvester JT, Booth GM, Shimoda TH, Meeker S, et al. (2001) Inhibition of voltage-gated K(+) currents by endothelin-1 in human pulmonary arterial myocytes. Am J Physiol Lung Cell Mol Physiol 281: L1115-1122.

249. Whitman EM, Pisarcik S, Luke T, Fallon M, Wang J, et al. (2008) Endothelin-1 mediates hypoxia-induced inhibition of voltage-gated K+ channel expression in pulmonary arterial myocytes. Am J Physiol Lung Cell Mol Physiol 294: L309-318.

250. Mauban JR, Remillard CV, Yuan JX (2005) Hypoxic pulmonary vasoconstriction: role of ion channels. J Appl Physiol (1985) 98: 415-420.

251. Post JM, Hume JR, Archer SL, Weir EK (1992) Direct role for potassium channel inhibition in hypoxic pulmonary vasoconstriction. Am J Physiol 262: C882-890.

252. Peng W, Hoidal JR, Karwande SV, Farrukh IS (1997) Effect of chronic hypoxia on K+ channels: regulation in human pulmonary vascular smooth muscle cells. Am J Physiol 272: C1271-1278.

253. Roth M, Rupp M, Hofmann S, Mittal M, Fuchs B, et al. (2009) Heme oxygenase-2 and large-conductance Ca2+-activated K+ channels: lung vascular effects of hypoxia. Am J Respir Crit Care Med 180: 353-364.

254. Shigemori K, Ishizaki T, Matsukawa S, Sakai A, Nakai T, et al. (1996) Adenine nucleotides via activation of ATP-sensitive K+ channels modulate hypoxic response in rat pulmonary artery. Am J Physiol 270: L803-809.

255. Nielsen G, Wandall-Frostholm C, Sadda V, Olivan-Viguera A, Lloyd EE, et al. (2013) Alterations of N-3 polyunsaturated fatty acid-activated K2P channels in hypoxia-induced pulmonary hypertension. Basic Clin Pharmacol Toxicol 113: 250-258.

256. Beech DJ (2005) Emerging functions of 10 types of TRP cationic channel in vascular smooth muscle. Clin Exp Pharmacol Physiol 32: 597-603.

257. Wang J, Weigand L, Lu W, Sylvester JT, Semenza GL, et al. (2006) Hypoxia inducible factor 1 mediates hypoxia-induced TRPC expression and elevated intracellular Ca2+ in pulmonary arterial smooth muscle cells. Circ Res 98: 1528-1537.

258. Kirsch M, Kemp-Harper B, Weissmann N, Grimminger F, Schmidt HH (2008) Sildenafil in hypoxic pulmonary hypertension potentiates a compensatory up-regulation of NO-cGMP signaling. FASEB J 22: 30-40.

259. Guilluy C, Sauzeau V, Rolli-Derkinderen M, Guerin P, Sagan C, et al. (2005) Inhibition of RhoA/Rho kinase pathway is involved in the beneficial effect of sildenafil on pulmonary hypertension. Br J Pharmacol 146: 1010-1018.

260. Lu W, Ran P, Zhang D, Peng G, Li B, et al. (2010) Sildenafil inhibits chronically hypoxic upregulation of canonical transient receptor potential expression in rat pulmonary arterial smooth muscle. Am J Physiol Cell Physiol 298: C114-123.

261. Wang J, Yang K, Xu L, Zhang Y, Lai N, et al. (2013) Sildenafil inhibits hypoxia-induced transient receptor potential canonical protein expression in pulmonary arterial smooth muscle via cGMP-PKG-PPARgamma axis. Am J Respir Cell Mol Biol 49: 231-240.

262. Wang J, Jiang Q, Wan L, Yang K, Zhang Y, et al. (2013) Sodium tanshinone IIA sulfonate inhibits canonical transient receptor potential expression in pulmonary arterial smooth muscle from pulmonary hypertensive rats. Am J Respir Cell Mol Biol 48: 125-134.

263. Weissmann N, Dietrich A, Fuchs B, Kalwa H, Ay M, et al. (2006) Classical transient receptor potential channel 6 (TRPC6) is essential for hypoxic pulmonary vasoconstriction and alveolar gas exchange. Proc Natl Acad Sci U S A 103: 19093-19098.

264. Malczyk M, Veith C, Fuchs B, Hofmann K, Storch U, et al. (2013) Classical Transient Receptor Potential Channel 1 in Hypoxia-induced Pulmonary Hypertension. Am J Respir Crit Care Med.

265. Liu XR, Zhang MF, Yang N, Liu Q, Wang RX, et al. (2012) Enhanced store-operated Ca(2)+ entry and TRPC channel expression in pulmonary arteries of monocrotaline-induced pulmonary hypertensive rats. Am J Physiol Cell Physiol 302: C77-87.

266. Alzoubi A, Almalouf P, Toba M, O'Neill K, Qian X, et al. (2013) TRPC4 Inactivation Confers a Survival Benefit in Severe Pulmonary Arterial Hypertension. Am J Pathol.

267. Martin E, Dahan D, Cardouat G, Gillibert-Duplantier J, Marthan R, et al. (2012) Involvement of TRPV1 and TRPV4 channels in migration of rat pulmonary arterial smooth muscle cells. Pflugers Arch 464: 261-272.

268. Dahan D, Ducret T, Quignard JF, Marthan R, Savineau JP, et al. (2012) Implication of the ryanodine receptor in TRPV4-induced calcium response in pulmonary arterial smooth muscle cells from normoxic and chronically hypoxic rats. Am J Physiol Lung Cell Mol Physiol 303: L824-833.

269. Liu XR, Liu Q, Chen GY, Hu Y, Sham JS, et al. (2013) Down-regulation of TRPM8 in pulmonary arteries of pulmonary hypertensive rats. Cell Physiol Biochem 31: 892-904.

270. Franco-Obregon A, Lopez-Barneo J (1996) Differential oxygen sensitivity of calcium channels in rabbit smooth muscle cells of conduit and resistance pulmonary arteries. J Physiol 491 (Pt 2): 511-518.

271. Platoshyn O, Brevnova EE, Burg ED, Yu Y, Remillard CV, et al. (2006) Acute hypoxia selectively inhibits KCNA5 channels in pulmonary artery smooth muscle cells. Am J Physiol Cell Physiol 290: C907-916.

272. Davidson A, Bossuyt A, Dab I (1989) Acute effects of oxygen, nifedipine, and diltiazem in patients with cystic fibrosis and mild pulmonary hypertension. Pediatr Pulmonol 6: 53-59.

273. Fike CD, Kaplowitz MR (1999) Nifedipine inhibits pulmonary hypertension but does not prevent decreased lung eNOS in hypoxic newborn pigs. Am J Physiol 277: L449-456.

274. Shimoda LA, Sham JS, Shimoda TH, Sylvester JT (2000) L-type Ca(2+) channels, resting [Ca(2+)](i), and ET-1-induced responses in chronically hypoxic pulmonary myocytes. Am J Physiol Lung Cell Mol Physiol 279: L884-894.

275. Kennedy TP, Michael JR, Summer W (1985) Calcium channel blockers in hypoxic pulmonary hypertension. Am J Med 78: 18-26.

276. Hirenallur SD, Haworth ST, Leming JT, Chang J, Hernandez G, et al. (2008) Upregulation of vascular calcium channels in neonatal piglets with hypoxia-induced pulmonary hypertension. Am J Physiol Lung Cell Mol Physiol 295: L915-924.

277. Luke T, Maylor J, Undem C, Sylvester JT, Shimoda LA (2012) Kinase-dependent activation of voltage-gated Ca2+ channels by ET-1 in pulmonary arterial myocytes during chronic hypoxia. Am J Physiol Lung Cell Mol Physiol 302: L1128-1139.

278. Jernigan NL, Paffett ML, Walker BR, Resta TC (2009) ASIC1 contributes to pulmonary vascular smooth muscle store-operated Ca(2+) entry. Am J Physiol Lung Cell Mol Physiol 297: L271-285.

279. Jernigan NL, Herbert LM, Walker BR, Resta TC (2012) Chronic hypoxia upregulates pulmonary arterial ASIC1: a novel mechanism of enhanced store-operated Ca2+ entry and receptor-dependent vasoconstriction. Am J Physiol Cell Physiol 302: C931-940.

280. Nitta CH, Osmond DA, Herbert LM, Beasley BF, Resta TC, et al. (2013) Role of ASIC1 in the development of chronic hypoxia-induced pulmonary hypertension. Am J Physiol Heart Circ Physiol.

281. Bonnet S, Hyvelin JM, Bonnet P, Marthan R, Savineau JP (2001) Chronic hypoxia-induced spontaneous and rhythmic contractions in the rat main pulmonary artery. Am J Physiol Lung Cell Mol Physiol 281: L183-192.

282. Archer SL, Gomberg-Maitland M, Maitland ML, Rich S, Garcia JG, et al. (2008) Mitochondrial metabolism, redox signaling, and fusion: a mitochondria-ROS-HIF-1alpha-Kv1.5 O2-sensing pathway at the intersection of pulmonary hypertension and cancer. Am J Physiol Heart Circ Physiol 294: H570-578.

283. Norton CE, Broughton BR, Jernigan NL, Walker BR, Resta TC (2013) Enhanced depolarization-induced pulmonary vasoconstriction following chronic hypoxia requires EGFR-dependent activation of NAD(P)H oxidase 2. Antioxid Redox Signal 18: 1777-1788.

284. Wang YX, Zheng YM (2010) ROS-dependent signaling mechanisms for hypoxic Ca(2+) responses in pulmonary artery myocytes. Antioxid Redox Signal 12: 611-623.

285. Liao B, Zheng YM, Yadav VR, Korde AS, Wang YX (2011) Hypoxia induces intracellular Ca2+ release by causing reactive oxygen species-mediated dissociation of FK506-binding protein 12.6 from ryanodine receptor 2 in pulmonary artery myocytes. Antioxid Redox Signal 14: 37-47.

286. Morita K, Kitayama T, Kitayama S, Dohi T (2006) Cyclic ADP-ribose requires FK506-binding protein to regulate intracellular Ca2+ dynamics and catecholamine release in acetylcholine-stimulated bovine adrenal chromaffin cells. J Pharmacol Sci 101: 40-51.

287. Lin MJ, Yang XR, Cao YN, Sham JS (2007) Hydrogen peroxide-induced Ca2+ mobilization in pulmonary arterial smooth muscle cells. Am J Physiol Lung Cell Mol Physiol 292: L1598-1608.

288. Cornfield DN, Stevens T, McMurtry IF, Abman SH, Rodman DM (1994) Acute hypoxia causes membrane depolarization and calcium influx in fetal pulmonary artery smooth muscle cells. Am J Physiol 266: L469-475.

289. Jabr RI, Toland H, Gelband CH, Wang XX, Hume JR (1997) Prominent role of intracellular Ca2+ release in hypoxic vasoconstriction of canine pulmonary artery. Br J Pharmacol 122: 21-30.

290. Connolly MJ, Prieto-Lloret J, Becker S, Ward JP, Aaronson PI (2013) Hypoxic pulmonary vasoconstriction in the absence of pretone: essential role for intracellular Ca2+ release. J Physiol 591: 4473-4498.

291. Lee HC (2011) Cyclic ADP-ribose and NAADP: fraternal twin messengers for calcium signaling. Sci China Life Sci 54: 699-711.

292. Graeff R, Liu Q, Kriksunov IA, Kotaka M, Oppenheimer N, et al. (2009) Mechanism of cyclizing NAD to cyclic ADP-ribose by ADP-ribosyl cyclase and CD38. J Biol Chem 284: 27629-27636.

293. Liu Q, Graeff R, Kriksunov IA, Jiang H, Zhang B, et al. (2009) Structural basis for enzymatic evolution from a dedicated ADP-ribosyl cyclase to a multifunctional NAD hydrolase. J Biol Chem 284: 27637-27645.

294. Brailoiu E, Churamani D, Cai X, Schrlau MG, Brailoiu GC, et al. (2009) Essential requirement for two-pore channel 1 in NAADP-mediated calcium signaling. J Cell Biol 186: 201-209.

295. Zong X, Schieder M, Cuny H, Fenske S, Gruner C, et al. (2009) The two-pore channel TPCN2 mediates NAADP-dependent Ca(2+)-release from lysosomal stores. Pflugers Arch 458: 891-899.

296. Lin-Moshier Y, Walseth TF, Churamani D, Davidson SM, Slama JT, et al. (2012) Photoaffinity labeling of nicotinic acid adenine dinucleotide phosphate (NAADP) targets in mammalian cells. J Biol Chem 287: 2296-2307.

297. Kim SY, Gul R, Rah SY, Kim SH, Park SK, et al. (2008) Molecular mechanism of ADP-ribosyl cyclase activation in angiotensin II signaling in murine mesangial cells. Am J Physiol Renal Physiol 294: F982-989.

298. Thai TL, Arendshorst WJ (2008) ADP-ribosyl cyclase and ryanodine receptors mediate endothelin ETA and ETB receptor-induced renal vasoconstriction in vivo. Am J Physiol Renal Physiol 295: F360-368.

299. Haller H, Luft FC (1998) Angiotensin II acts intracellularly in vascular smooth muscle cells. Basic Res Cardiol 93 Suppl 2: 30-36.

300. Alexander RW, Brock TA, Gimbrone MA, Jr., Rittenhouse SE (1985) Angiotensin increases inositol trisphosphate and calcium in vascular smooth muscle. Hypertension 7: 447-451.

301. Rajagopalan S, Kurz S, Munzel T, Tarpey M, Freeman BA, et al. (1996) Angiotensin II-mediated hypertension in the rat increases vascular superoxide production via membrane NADH/NADPH oxidase activation. Contribution to alterations of vasomotor tone. J Clin Invest 97: 1916-1923.

302. Griendling KK, Minieri CA, Ollerenshaw JD, Alexander RW (1994) Angiotensin II stimulates NADH and NADPH oxidase activity in cultured vascular smooth muscle cells. Circ Res 74: 1141-1148.

303. Torrecillas G, Boyano-Adanez MC, Medina J, Parra T, Griera M, et al. (2001) The role of hydrogen peroxide in the contractile response to angiotensin II. Mol Pharmacol 59: 104-112.

304. Grover AK, Samson SE, Fomin VP, Werstiuk ES (1995) Effects of peroxide and superoxide on coronary artery: ANG II response and sarcoplasmic reticulum Ca2+ pump. Am J Physiol 269: C546-553.

305. Fellner SK, Arendshorst WJ (2005) Angiotensin II, reactive oxygen species, and Ca2+ signaling in afferent arterioles. Am J Physiol Renal Physiol 289: F1012-1019.

306. Chose O, Sansilvestri-Morel P, Badier-Commander C, Bernhardt F, Fabiani JN, et al. (2008) Distinct role of nox1, nox2, and p47phox in unstimulated versus angiotensin II-induced NADPH oxidase activity in human venous smooth muscle cells. J Cardiovasc Pharmacol 51: 131-139.

307. Touyz RM, Chen X, Tabet F, Yao G, He G, et al. (2002) Expression of a functionally active gp91phox-containing neutrophil-type NAD(P)H oxidase in smooth muscle cells from human resistance arteries: regulation by angiotensin II. Circ Res 90: 1205-1213.

308. Ge Y, Jiang W, Gan L, Wang L, Sun C, et al. (2010) Mouse embryonic fibroblasts from CD38 knockout mice are resistant to oxidative stresses through inhibition of

reactive oxygen species production and Ca(2+) overload. Biochem Biophys Res Commun 399: 167-172.

309. Kumasaka S, Shoji H, Okabe E (1999) Novel mechanisms involved in superoxide anion radical-triggered Ca2+ release from cardiac sarcoplasmic reticulum linked to cyclic ADP-ribose stimulation. Antioxid Redox Signal 1: 55-69.

310. Xie GH, Rah SY, Yi KS, Han MK, Chae SW, et al. (2003) Increase of intracellular Ca(2+) during ischemia/reperfusion injury of heart is mediated by cyclic ADP-ribose. Biochem Biophys Res Commun 307: 713-718.

311. Umesh A, Paudel O, Cao YN, Myers AC, Sham JS (2011) Alteration of pulmonary artery integrin levels in chronic hypoxia and monocrotaline-induced pulmonary hypertension. J Vasc Res 48: 525-537.

312. Rodgers KE, Xiong S, Steer R, diZerega GS (2000) Effect of angiotensin II on hematopoietic progenitor cell proliferation. Stem Cells 18: 287-294.

313. Crider BP, Xie XS, Stone DK (1994) Bafilomycin inhibits proton flow through the H+ channel of vacuolar proton pumps. J Biol Chem 269: 17379-17381.

314. Christensen KA, Myers JT, Swanson JA (2002) pH-dependent regulation of lysosomal calcium in macrophages. J Cell Sci 115: 599-607.

315. Malavasi F, Deaglio S, Funaro A, Ferrero E, Horenstein AL, et al. (2008) Evolution and function of the ADP ribosyl cyclase/CD38 gene family in physiology and pathology. Physiol Rev 88: 841-886.

316. Thai TL, Arendshorst WJ (2009) Mice lacking the ADP ribosyl cyclase CD38 exhibit attenuated renal vasoconstriction to angiotensin II, endothelin-1, and norepinephrine. Am J Physiol Renal Physiol 297: F169-176.

317. Rao GN, Lassegue B, Alexander RW, Griendling KK (1994) Angiotensin II stimulates phosphorylation of high-molecular-mass cytosolic phospholipase A2 in vascular smooth-muscle cells. Biochem J 299 (Pt 1): 197-201.

318. Zhang DX, Harrison MD, Li PL (2002) Calcium-induced calcium release and cyclic ADP-ribose-mediated signaling in the myocytes from small coronary arteries. Microvasc Res 64: 339-348.

319. Rosen D, Lewis AM, Mizote A, Thomas JM, Aley PK, et al. (2009) Analogues of the nicotinic acid adenine dinucleotide phosphate (NAADP) antagonist Ned-19 indicate two binding sites on the NAADP receptor. J Biol Chem 284: 34930-34934.

320. Gagliardi S, Rees M, Farina C (1999) Chemistry and structure activity relationships of bafilomycin A1, a potent and selective inhibitor of the vacuolar H+-ATPase. Curr Med Chem 6: 1197-1212.

321. Rao GN, Griendling KK, Frederickson RM, Sonenberg N, Alexander RW (1994) Angiotensin II induces phosphorylation of eukaryotic protein synthesis initiation factor 4E in vascular smooth muscle cells. J Biol Chem 269: 7180-7184.

322. Griendling KK, Lassegue B, Murphy TJ, Alexander RW (1994) Angiotensin II receptor pharmacology. Adv Pharmacol 28: 269-306.

323. Garrido AM, Griendling KK (2009) NADPH oxidases and angiotensin II receptor signaling. Mol Cell Endocrinol 302: 148-158.

324. Dipp M, Evans AM (2001) Cyclic ADP-ribose is the primary trigger for hypoxic pulmonary vasoconstriction in the rat lung in situ. Circ Res 89: 77-83.

325. Okabe E, Tsujimoto Y, Kobayashi Y (2000) Calmodulin and cyclic ADP-ribose interaction in Ca2+ signaling related to cardiac sarcoplasmic reticulum: superoxide anion radical-triggered Ca2+ release. Antioxid Redox Signal 2: 47-54.

326. Gul R, Shawl AI, Kim SH, Kim UH (2012) Cooperative interaction between reactive oxygen species and Ca2+ signals contributes to angiotensin II-induced hypertrophy in adult rat cardiomyocytes. Am J Physiol Heart Circ Physiol 302: H901-909.

327. Hordijk PL (2006) Regulation of NADPH oxidases: the role of Rac proteins. Circ Res 98: 453-462.

328. Lassegue B, Sorescu D, Szocs K, Yin Q, Akers M, et al. (2001) Novel gp91(phox) homologues in vascular smooth muscle cells : nox1 mediates angiotensin II-induced superoxide formation and redox-sensitive signaling pathways. Circ Res 88: 888-894.

329. Xu M, Li XX, Ritter JK, Abais JM, Zhang Y, et al. (2013) Contribution of NADPH oxidase to membrane CD38 internalization and activation in coronary arterial myocytes. PLoS One 8: e71212.

330. Gianni D, Taulet N, Zhang H, DerMardirossian C, Kister J, et al. (2010) A novel and specific NADPH oxidase-1 (Nox1) small-molecule inhibitor blocks the formation of functional invadopodia in human colon cancer cells. ACS Chem Biol 5: 981-993.

331. ten Freyhaus H, Huntgeburth M, Wingler K, Schnitker J, Baumer AT, et al. (2006) Novel Nox inhibitor VAS2870 attenuates PDGF-dependent smooth muscle cell chemotaxis, but not proliferation. Cardiovasc Res 71: 331-341.

332. Thai TL, Fellner SK, Arendshorst WJ (2007) ADP-ribosyl cyclase and ryanodine receptor activity contribute to basal renal vasomotor tone and agonist-induced renal vasoconstriction in vivo. Am J Physiol Renal Physiol 293: F1107-1114.

333. Dong M, Si YQ, Sun SY, Pu XP, Yang ZJ, et al. (2011) Design, synthesis and biological characterization of novel inhibitors of CD38. Org Biomol Chem 9: 3246-3257.

334. Escande C, Nin V, Price NL, Capellini V, Gomes AP, et al. (2013) Flavonoid apigenin is an inhibitor of the NAD+ ase CD38: implications for cellular NAD+ metabolism, protein acetylation, and treatment of metabolic syndrome. Diabetes 62: 1084-1093.

335. Voelkel NF, Tuder RM (2000) Hypoxia-induced pulmonary vascular remodeling: a model for what human disease? J Clin Invest 106: 733-738.

336. Stenmark KR, Fagan KA, Frid MG (2006) Hypoxia-induced pulmonary vascular remodeling: cellular and molecular mechanisms. Circ Res 99: 675-691.

337. Laursen BE, Dam MY, Mulvany MJ, Simonsen U (2008) Hypoxia-induced pulmonary vascular remodeling and right ventricular hypertrophy is unaltered by long-term oral L-arginine administration. Vascul Pharmacol 49: 71-76.

338. Vender RL (1994) Chronic hypoxic pulmonary hypertension. Cell biology to pathophysiology. Chest 106: 236-243.

339. Wang J, Juhaszova M, Rubin LJ, Yuan XJ (1997) Hypoxia inhibits gene expression of voltage-gated K+ channel alpha subunits in pulmonary artery smooth muscle cells. J Clin Invest 100: 2347-2353.

340. Tang C, To WK, Meng F, Wang Y, Gu Y (2010) A role for receptor-operated Ca2+ entry in human pulmonary artery smooth muscle cells in response to hypoxia. Physiol Res 59: 909-918.

341. De Flora A, Guida L, Franco L, Zocchi E, Bruzzone S, et al. (1997) CD38 and ADP-ribosyl cyclase catalyze the synthesis of a dimeric ADP-ribose that potentiates the calcium-mobilizing activity of cyclic ADP-ribose. J Biol Chem 272: 12945-12951.

342. Kiselyov KI, Shin DM, Wang Y, Pessah IN, Allen PD, et al. (2000) Gating of store-operated channels by conformational coupling to ryanodine receptors. Mol Cell 6: 421-431.

343. Fellner SK, Arendshorst WJ (2000) Ryanodine receptor and capacitative Ca2+ entry in fresh preglomerular vascular smooth muscle cells. Kidney Int 58: 1686-1694.

344. Xia Y, Entman ML, Wang Y (2013) CCR2 Regulates the Uptake of Bone Marrow-Derived Fibroblasts in Renal Fibrosis. PLoS One 8: e77493.

345. Hartman WR, Pelleymounter LL, Moon I, Kalari K, Liu M, et al. (2010) CD38 expression, function, and gene resequencing in a human lymphoblastoid cell line-based model system. Leuk Lymphoma 51: 1315-1325.

346. Kontani K, Nishina H, Ohoka Y, Takahashi K, Katada T (1993) NAD glycohydrolase specifically induced by retinoic acid in human leukemic HL-60 cells. Identification of the NAD glycohydrolase as leukocyte cell surface antigen CD38. J Biol Chem 268: 16895-16898.

347. White TA, Kannan MS, Walseth TF (2003) Intracellular calcium signaling through the cADPR pathway is agonist specific in porcine airway smooth muscle. FASEB J 17: 482-484.

348. Li Z, Huang W, Jiang ZL, Gregersen H, Fung YC (2004) Tissue remodeling of rat pulmonary arteries in recovery from hypoxic hypertension. Proc Natl Acad Sci U S A 101: 11488-11493.

349. Huang W, Sher YP, Peck K, Fung YC (2001) Correlation of gene expression with physiological functions: Examples of pulmonary blood vessel rheology, hypoxic hypertension, and tissue remodeling. Biorheology 38: 75-87.

350. Fung YC, Liu SQ (1991) Changes of zero-stress state of rat pulmonary arteries in hypoxic hypertension. J Appl Physiol (1985) 70: 2455-2470.

351. Polzonetti V, Pucciarelli S, Vita A, Vincenzetti S, Natalini P (2009) CD38 in bovine lung: A multicatalytic NADase. J Membr Biol 227: 105-110.

352. Camelo Jr JS, Martins AR, Rosa E, Ramos SG, Hehre D, et al. (2012) Angiotensin II type 1 receptor blockade partially attenuates hypoxia-induced pulmonary hypertension in newborn piglets: relationship with the nitrergic system. Braz J Med Biol Res 45: 163-171.

353. Adamy C, Oliviero P, Eddahibi S, Rappaport L, Samuel JL, et al. (2002) Cardiac modulations of ANG II receptor expression in rats with hypoxic pulmonary hypertension. Am J Physiol Heart Circ Physiol 283: H733-740.

354. Chassagne C, Eddahibi S, Adamy C, Rideau D, Marotte F, et al. (2000) Modulation of angiotensin II receptor expression during development and regression of hypoxic pulmonary hypertension. Am J Respir Cell Mol Biol 22: 323-332.

355. Zhao L, al-Tubuly R, Sebkhi A, Owji AA, Nunez DJ, et al. (1996) Angiotensin II receptor expression and inhibition in the chronically hypoxic rat lung. Br J Pharmacol 119: 1217-1222.

356. Semenza GL, Shimoda LA, Prabhakar NR (2006) Regulation of gene expression by HIF-1. Novartis Found Symp 272: 2-8; discussion 8-14, 33-16.

357. Lim CS, Kiriakidis S, Sandison A, Paleolog EM, Davies AH (2013) Hypoxia-inducible factor pathway and diseases of the vascular wall. J Vasc Surg 58: 219-230.

358. Nanduri J, Yuan G, Kumar GK, Semenza GL, Prabhakar NR (2008) Transcriptional responses to intermittent hypoxia. Respir Physiol Neurobiol 164: 277-281.

359. Oh-hora M, Rao A (2009) The calcium/NFAT pathway: role in development and function of regulatory T cells. Microbes Infect 11: 612-619.

360. Gomez MF, Bosc LV, Stevenson AS, Wilkerson MK, Hill-Eubanks DC, et al. (2003) Constitutively elevated nuclear export activity opposes Ca2+-dependent NFATc3 nuclear accumulation in vascular smooth muscle: role of JNK2 and Crm-1. J Biol Chem 278: 46847-46853.

361. Filosa JA, Nelson MT, Gonzalez Bosc LV (2007) Activity-dependent NFATc3 nuclear accumulation in pericytes from cortical parenchymal microvessels. Am J Physiol Cell Physiol 293: C1797-1805.

362. van der Velden JL, Schols AM, Willems J, Kelders MC, Langen RC (2008) Glycogen synthase kinase 3 suppresses myogenic differentiation through negative regulation of NFATc3. J Biol Chem 283: 358-366.

363. Hou X, Chen J, Luo Y, Liu F, Xu G, et al. (2013) Silencing of STIM1 attenuates hypoxia-induced PASMCs proliferation via inhibition of the SOC/Ca2+/NFAT pathway. Respir Res 14: 2.

364. Amberg GC, Rossow CF, Navedo MF, Santana LF (2004) NFATc3 regulates Kv2.1 expression in arterial smooth muscle. J Biol Chem 279: 47326-47334.

365. Gomez MF, Stevenson AS, Bonev AD, Hill-Eubanks DC, Nelson MT (2002) Opposing actions of inositol 1,4,5-trisphosphate and ryanodine receptors on nuclear factor of activated T-cells regulation in smooth muscle. J Biol Chem 277: 37756-37764.

366. de Frutos S, Spangler R, Alo D, Bosc LV (2007) NFATc3 mediates chronic hypoxia-induced pulmonary arterial remodeling with alpha-actin up-regulation. J Biol Chem 282: 15081-15089.

367. Malczyk M, Veith C, Fuchs B, Hofmann K, Storch U, et al. (2013) Classical Transient Receptor Potential Channel 1 in Hypoxia-induced Pulmonary Hypertension. Am J Respir Crit Care Med 188: 1451-1459.

368. Undem C, Rios EJ, Maylor J, Shimoda LA (2012) Endothelin-1 augments Na(+)/H(+) exchange activity in murine pulmonary arterial smooth muscle cells via Rho kinase. PLoS One 7: e46303.

Suengwon Lee, PhD candidates

Department of Environmental Health Sciences, Bloomberg School of Public Health
Johns Hopkins University

5501 Hopkins Bayview Circle, Room 4A.8
Baltimore, MD, 21224
(410)550-5208
slee@jhsph.edu / suengwon@gmail.com

EDUCATION:

PhD candidate, expected acquisition of degree in March 2014

Program in Respiratory Biology and Lung Disease, Department of Environmental Health Sciences, Bloomberg School of Public Health, Johns Hopkins University
Dissertation: Alteration of intracellular Ca^{2+} release mediated by CD38 under chronic hypoxia in pulmonary arterial smooth muscle cell
Dissertations Advisor: James S.K. Sham, PhD

M.Sc., May 2007

Program in Human Nutrition, Department of Environmental Health Sciences, School of Public Health, University of Michigan, Ann Arbor
Master's Thesis: The association between childhood obesity and asthma

B.Ag., February 2003

Department of Applied Animal Sciences, College of Natural Resources, Korea University

EXPERIMENTAL SKILLS:

- Basic techniques for biochemistry & molecular biology: Western Blot analysis, immunocytochemistry, RNA extraction, conventional reverse transcription PCR, quantitative real-time PCR, primer design, electrophoresis and gel extraction.
- Ca^{2+} imaging: measurement of intracellular Ca^{2+} level with Ca^{2+}-sensitive fluorescent dye
- Measurement of isometric contractile force: organ-bath experiment for arteries
- Primary cell culture: isolation of intralobal pulmonary arterial smooth muscle cell
- Animal surgery: mouse left pulmonary artery ligation surgery
- Techniques for cell mechanics measurement: optical magnetic twisting cytometry and fourier transform traction cytometry

AWARDS:

2011	"Hanmi" Travel Award in Baltimore/Washington Metropolitan Area Life Scientists Poster Symposium hosted by Baltimore Life Science & NIH Korean Scientist Association, Baltimore, MD
	The 3rd place for poster presentation in Baltimore/Washington Metropolitan Area Life Scientists Poster Symposium hosted by Baltimore Life Science & NIH Korean Scientist Association, Baltimore, MD
2001–2002	Honored Scholarship and Honored Award, Korea University, Seoul, South Korea

RESEARCH/TEACHING EXPERIENCE:

- Johns Hopkins University, Baltimore, MD, USA
  PhD student, 2007–2014
  - Research:
    i. Dr. James S.K. Sham Lab (2010–2014): Ca^{2+} physiology in pulmonary arterial smooth muscle cell (thesis project)
    ii. Dr. Elizabeth Wagner Lab (2009–2010): Ischemia-induced lung angiogenesis (rotation)
    iii. Dr. Steven An Lab (2008–2009): Cell mechanics in airway smooth muscle cell (rotation)
    iv. Global Tobacco Control (2007–2009): Research assistant
  - Teaching:
    Teaching assistant & grader (2009): Class of fundamental of human physiology, Bloomberg School of Public Health

- Korea University, Seoul, South Korea
  Undergraduate, 1996–2003
  Lab of Food and Microbiology (2000–2003): Research student

ABSTRACT/POSTER PRESENTATION:

Lee S, Jiang YL, Paudel O, and Sham JS. Chronic hypoxia-induced alterations in the CD38-dependent pathways in rat pulmonary arterial smooth muscle. American Thoracic Society. 2013 (Poster Discussion)

Lee S, Jiang YL, Paudel O, and Sham JS. Alteration in Intracellular Ca^{2+} Release via CD38-dependent Pathways in Pulmonary Arterial Smooth Muscle of Rat by Chronic Hypoxia. Experimental Biology. 2012

Lee S, Jiang YL, and Sham JS. Alteration of CD38 and two-pore channels expression by hypoxia exposure in pulmonary arterial smooth muscle. Baltimore/Washington Metropolitan Area Life Scientists Poster Symposium. 2011

Jiang YL, **Lee S**, and Sham JS. Differential expression of CD38 and two-pore channels in rat pulmonary arterial smooth muscles. Experimental Biology. 2011

PUBLICATION:

Jiang YL, Lin AH, Xia Y, **Lee S**, Paudel O, Sun H, Yang XR, Ran P, and Sham JS. Nicotinic acid adenine dinucleotide phosphate (NAADP) activates global and heterogeneous local Ca^{2+} signals from NAADP- and ryanodine receptor-gated Ca^{2+} stores in pulmonary arterial myocytes. 2013. J Biol Chem. 288(15):10381-94.

Ahn EH, Kim Y, Kshitiz, An SS, Afzal J, **Lee S**, Kwak M, Suh KY, Kim DH and Levchenko A. Spatial control of adult stem cell fate using nanotopographic cues. 2014. Biomaterials. 35(8):2401-10.

‹In process for publication›

Lee S, Jiang YL, Paudel O, Xia Y, Yang XR and Sham JS. CD38 mediates angiotensin II-indueced intracellular Calcium release in rat pulmonary arterial smooth muscle cell.

Lee S, Subedi KP, Paudel O, Chung SY, and Sham JS. Chronic hypoxia regulates the expression and activity of CD38 in rat pulmonary arterial smooth muscle cell.

REFERENCES

James S.K. Sham, PhD
Associate Professor
Department of Medicine, School of Medicine
Johns Hopkins University
5501 Hopkins Bayview Circle, Room 4B.43
410-550-7751
jsks@jhmi.edu
Relationship: PhD advisor

Bradley Undem, PhD
Professor
Department of Medicine, School of Medicine
Johns Hopkins University
5501 Hopkins Bayview Circle, Room 3A.44
Baltimore, MD, 21224
410-550-2160
bundem@jhmi.edu
Relationship: PhD thesis advisory committee

Steven S. An, PhD
Associate Professor
Department of Environmental Health Sciences, School of Public Health
Johns Hopkins University
615 N. Wolfe Street, Room E7616
Baltimore, MD, 21205a
410-502-5085
san@jhsph.edu
Relationship: PhD thesis advisory committee